University of Tennessee, Knoxville

TRACE: Tennessee Research and Creative Exchange

Doctoral Dissertations

Graduate School

5-2017

All Acrylic Based Thermoplastic Elastomers: Design and Synthesis for Improved Mechanical Performance

Wei Lu
University of Tennessee, Knoxville, wlu14@vols.utk.edu

Follow this and additional works at: https://trace.tennessee.edu/utk_graddiss

Part of the Materials Chemistry Commons, Organic Chemistry Commons, Polymer and Organic Materials Commons, Polymer Chemistry Commons, and the Polymer Science Commons

Recommended Citation

Lu, Wei, "All Acrylic Based Thermoplastic Elastomers: Design and Synthesis for Improved Mechanical Performance. " PhD diss., University of Tennessee, 2017.
https://trace.tennessee.edu/utk_graddiss/4411

This Dissertation is brought to you for free and open access by the Graduate School at TRACE: Tennessee Research and Creative Exchange. It has been accepted for inclusion in Doctoral Dissertations by an authorized administrator of TRACE: Tennessee Research and Creative Exchange. For more information, please contact trace@utk.edu.

To the Graduate Council:

I am submitting herewith a dissertation written by Wei Lu entitled "All Acrylic Based Thermoplastic Elastomers: Design and Synthesis for Improved Mechanical Performance." I have examined the final electronic copy of this dissertation for form and content and recommend that it be accepted in partial fulfillment of the requirements for the degree of Doctor of Philosophy, with a major in Chemistry.

Jimmy W. Mays, Major Professor

We have read this dissertation and recommend its acceptance:

Alexei P. Sokolov, Michael D. Best, Thomas A. Zawodzinski

Accepted for the Council:

Dixie L. Thompson

Vice Provost and Dean of the Graduate School

(Original signatures are on file with official student records.)

All Acrylic Based Thermoplastic Elastomers: Design and Synthesis for Improved Mechanical Performance

A Dissertation Presented for the

Doctor of Philosophy

Degree

The University of Tennessee, Knoxville

Wei Lu

May 2017

Copyright © 2017 by Wei Lu

All rights reserved.

ACKNOWLEDGEMENTS

It would not be possible to complete either the work in this thesis and all my PhD work and life without the kindness and support from numerous people.

First and foremost, I would like to thank Professor Jimmy Mays for his guidance, supervision, instructions, encouragement and full support of every aspect from research to life. His generous and patient help and various opportunities provided have made me acquainted with the panorama of polymer not only in academia but also in industrial applications. His passion, wisdom, and spirit of collaboration have greatly influenced my attitude toward my future career and life.

I would like to thank my doctoral committee members: Dr. Alexei Sokolov for kind interpretations and suggestions on the theories and physics behind and beyond polymer chemistry, Dr. Michael Best for his valuable time and advising on synthetic chemistry, Dr. Thomas Zawodzinski for his explanations on the mechanism and engineering aspects of membrane applications. It is my great honor to have all these collaboration and support.

I sincerely thank Dr. Nam-Goo Kang, and Dr. Kunlun Hong (ORNL) for all-sided help and sharing their knowledge, experience and insightful perspective, not only as friends but also as mentors through many difficult times.

Throughout these five years' graduate research and studies, it is my great fortune to have worked with and learned from many smart, kind, helpful, and

selfless polymer scientists and engineers including: From ORNL: Dr. Panchao Yin for guidance on DLS, SAXS, self-assembly and solution characterizations; Dr. Yangyang Wang and Dr. Shiwang Cheng for mechanical tests, rheology and polymer physics; Dr. Jiahua Zhu for SAXS and TEM. From UT: Dr. Carlos Steren for guidance on theories and experiments of NMR; Dr. John Dunlap for AFM; Dr. Weiyu Wang for kind suggestions, experimental skills, and DMA; Tom Malmgren for GPC, Ms. Ting Wu from Dr. Binhu's lab for spin coating techniques. I would also like to thank Dr. Mi Zhou (Zhejiang University of Technology, China) and Dr. Chunhui Bao (Solvay USA Inc) for their guidance on living radical polymerization; Dr. Xiaojun Wang (Novus International) for his sharing with rich research experience.

I am also lucky to work with many lively and aspirant current and ex- group members in Mays' group including: Dr. Kostas Mischronis, Dr. Beomgoo Kang, Dr. Priyank Shah, Dr. Andrew Goodwin, Dr. Sachin Bobade, Dr. Vikram Srivastava, Dr. Christopher Hurley, Hongbo Feng, Xinyi Lu, Huiqun Wang, and Benjamin Ripy.

Finally, I want to express my great love and appreciation to my family: Thank my wife Yuecheng Fang for tireless support and encouragement, thank you for constituting a happy family with me and bringing me a cute baby! Thank my parents, Zhonghai Lu and Jinmei Huang, and parents in law, Xuehong fang and Xiaoping Tian for your trust and great concern, thank you for taking care of my baby and making the strong back for me! Finally, thank my little baby, Daniel

Muyang Lu to give me the chance to be your father, thank you for all the laugh and precious moments you have brought to my life! Thus I exclusively dedicate this dissertation to my family, especially my little baby!

ABSTRACT

Thermoplastic elastomers (TPEs) have been widely studied because of their recyclability, good processability, low production cost and distinct performance. Compared to the widely-used styrenic TPEs, acrylate based TPEs have potential advantages including exceptional chemical, heat, oxygen and UV resistance, optical transparence, and oil resistance. However, their high entanglement molecular weight lead to “disappointing” mechanical performance as compared to styrenic TPEs. The work described in this dissertation is aimed at employing various approaches to develop the all acrylic based thermoplastic elastomers with improved mechanical performance.

The first part of this work focuses on the introduction of acrylic polymers with high glass transition temperatures. Poly(1-adamantyl acrylate) (PAdA) was studied including the anionic polymerization, molecular information, thermal properties, unperturbed chain dimensions and chain flexibility. The homopolymers exhibit a high glass transition temperature (133 ^{o}C) and decomposition temperature (376 ^{o}C). The polymer chain exhibits a comparable persistence length, diameter per bead, and characteristic ratio to those of poly(methyl methacrylate) and polystyrene. The outstanding properties of PAdA were utilized by the cooperation with poly(tetrahydrofurfuryl acrylate) (PTHFA) to make the PAdA-b-PTHF-b-PAdA (ATA) triblock copolymers. The resulting polymer showed distinct microphase separation behaviors and an upper service temperature at 123

^{o}C, which is higher than that of both conventional styrenic TPEs and acrylic TPEs. The ATA triblock copolymers exhibited mechanical strength and elongation higher than those of commercial all acrylic TPEs.

The second part involves the synthesis of poly(butyl acrylate)-g-poly(methyl methacrylate) (PBA-g-PMMA) graft copolymers. Secondary-butyl lithium/N-isopropyl-4-vinylbenzylamine (*sec*-BuLi/PVBA) initiation system was used to synthesize the PMMA macromonomer by anionic polymerization. By the combination of enhanced molecular weight and complex architecture, the resulting polymer showed exceptional microphase separation behavior, extraordinary mechanical strength and superelastomer characteristics with greatly improved elongation and exceptional recovery behavior.

In the final chapter, other approaches to improve the mechanical properties of all acrylic based TPEs are discussed and prospected, including the introduction of extra driving forces, and the possible combination routes of all the approaches attempted. In addition, the great potential of PVBA to build complex architectures is proposed, including triarm stars, multigraft copolymers with tetrafuntional branch points, four arm stars and H-shaped copolymers.

TABLE OF CONTENTS

Chapter 1 Introduction to All Acrylic Based Thermoplastic Elastomers.....1

1.1 Thermoplastic Elastomers.....2

1.1.1 Advantages and Disadvantages of TPEs.....2

1.1.2 Classification of TPEs.....3

1.2 Styrenic Block Copolymers (SBCs) Thermoplastic Elastomers.....5

1.2.1 Mechanism of Function of TPEs.....5

1.2.2 Styrenic Thermoplastic Elastomers (SBCs).....8

1.3 All Acrylic Based TPEs.....9

1.3.1 Industrial Applications of Acrylic based TPEs.....11

1.3.2 Entanglement Molecular Weight (M_e).....12

1.3.3 Synthesis and Properties of PMMA-b-PBA-b-PMMA Triblock Copolymer TPEs.....18

1.4 Approaches to Improve the Performance of TPEs.....24

1.4.1 Compounding.....24

1.4.2 Glass Transition Temperature.....26

1.4.3 Complex Architectures.....30

1.4.4 Introducing Other Driving Forces.....47

1.5 Characterization Methods for TPE.....50

1.5.1 Thermal Characterization.....50

1.5.2 Phase Separation Behavior 55
1.5.3 Stress-Strain Behavior 65
1.6 The Scope of this Thesis 73
References 77
Chapter 2 Poly(1-Adamantyl Acrylate) - Good Candidate For TPE With Distinct Thermal Properties 96
Abstract 97
2.1 Poly(1-adamantyl acrylate): Living Anionic Polymerization, Block Copolymerization, and thermal properties 99
2.1.1 Introduction 99
2.1.2 Experimental Part 104
2.1.3 Result and Discussion 111
2.1.4 Conclusion 131
2.2 Solution Properties, Unperturbed Dimensions and Chain Flexibility of Poly(1-Adamantyl Acrylate) 132
2.2.1 Introduction 132
2.2.2 Experimental Part 133
2.2.3 Result and Discussion 135
2.2.4 Conclusion 148
References 150

Chapter 3 All Acrylic-based Thermoplastic Elastomers with High Service Temperature and Distinct Mechanical Strength 163
Abstract 164
3.1 Introduction 165
3.2 Experimental Part 166
3.3 Results and Discussion 170
3.3.1 Molecular Characterization of Homopolymers and Triblock Copolymers of PAdA and PTHFA. 170
3.3.2 Thermal Properties of ATA Triblock Copolymers 170
3.3.3 Microphase Separation Behaviors of ATA Triblock Copolymers 174
3.3.4 Mechanical Properties of ATA Triblock Copolymers 177
3.4 Conclusion 182
References 183
Chapter 4 All Acrylic Multigraft Copolymer Superelastomer 186
Abstract 187
4.1 Introduction 188
4.2 Experimental Part 190
4.3 Results and Discussion 195
4.3.1 Synthesis PVBA-PMMA Macromonomer 195
4.3.2 Synthesis of PBA-g-PMMA Graft Copolymers 199
4.3.3 Thermal Properties of PBA-g-PMMA Graft Copolymers 204

4.3.4 Microphase Separation Behaviors of PBA-g-PMMA Graft Copolymers 204
4.3.5 Mechanical Properties of PBA-g-PMMA Graft Copolymers 207
4.4 Conclusion.....214
References.....215
Chapter 5 Conclusions, Future Work, and Perspective 219
5.1 Conclusions.....220
5.2 Future Work and Perspectives 222
5.2.1 Driving Forces-- Extensive Influence on the Improvement of the Performance of TPEs 223
5.2.2 The Combination of High Upper Service Temperature and Complex Architecture.....230
5.2.3 PVBA-Powerful Tool to Build Complex Architectures 232
References.....239
Vita.....241

LIST OF TABLES

Table 1-1. Average chain entanglement molecular weight (M_e) for polymers[27] ..17

Table 2-1. Anionic Polymerization of AdA Using Various Initiators[a].....114

Table 2-2. Diblock Copolymerization of AdA with MMA in THF at -78 ^oC[a].....125

Table 2-3. Molecular Characteristics of Poly(1-adamantyl acrylate)[a].....134

Table 2-4. Values of K_θ and C_∞ of Poly(meth)acrylates 144

Table 2-5. The Values of A_2 and R_g for PAdA in Different Solvents at 30 ^oC. ...147

Table 3-1. Molecular Characteristics of ATA Triblock Copolymers 172

Table 3-2. Mechanical Property Parameters of ATA Triblock Copolymers 180

Table 4-1. Synthesis of PMMA macromonomer by living anionic polymerization [a] 201

Table 4-2. Sample Information of PBA-g-PMMA Graft Copolymers.....203

Table 4-3. Mechanical Property Parameters of PBA-g-PMMA Graft Copolymers 210

Table 5-1. Sample Information of PBA-g-PtBMA Graft Copolymer.....225

LIST OF FIGURES

Figure 1-1. (a) Approximate ranges of performance vs. cost for commercial TPEs.[2] (b) Percent break-up by market segments in revenue in 2000. (Courtesy of Frost & Sullivan Market Insight) 4

Figure 1-2. (a) Equilibrium morphologies of diblock or triblock copolymers in bulk. S and S'= spheres, C and C'= cylinders, G and G'= gyroids, and L = lamellae. (b) Theoretical phase diagram of diblock and triblock copolymers predicted by the self- consistent mean-field theory, depending on volume fraction (f) of the blocks and the segregation parameter, χ N, where χ is the Flory–Huggins segment–segment interaction energy and N is the degree of polymerization. [4,5].....7

Figure 1-3. (a) Stress-strain curves of SBS and SEBS; (b) Dynamic hysteresis as a function of butylene concentration in partially hydrogenated SBS. The concentration of butylene is proportional to the hydrogenation degree. [11].....10

Figure 1-4. Examples for acrylic TPE in automotive application.[22].....13

Figure 1-5. Schematic representation of relaxation function G(t) for an amorphous 14

Figure 1-6. Ultimate tensile strength as a function of 1/ M_e. Where M: PMMA; I: Poly(isooctyl acrylate); nB: poly(n-butyl acrylate); nP: poly(n-propyl

acrylate); E: poly(ethyl acrylate); S: PS; IB: poly(isobutylene); IP: polyisoprene.[28] 17

Figure 1-7. SEC curve for "Kurarity™" acrylic triblock coplymers.[17] 23

Figure 1-8. Mechanical properties of PMMA-b-PBA-b-PMMA triblock copolymers: (a) Storage modulus as a function of temperature; (b) stress-strain curves.[43] 23

Figure 1-9. Young's modulus of (a) microsilica (□) and nanosilica (●) composites; (b) unmodified (○) and modified (●), wt% of silica composites virsus silica content. 25

Figure 1-10. Transmission electron micrograph of (a) neat SEBS copolymer; (b) SEBS gel with $\boldsymbol{\omega oil}$ 0.70. (9.3 wt% styrene).[44] 27

Figure 1-11. The change of storage modulus of thermoplastic elastomers at various temperatures.[3] 29

Figure 1-12. TEM images of PI_2PS sample having 0.44 vol fraction PS and forming hexagonally packed cylinders (confirmed by SAXS). (a) A slice perpendicular to the cylinders and, (b) a slice parallel to the cylinders. 31

Figure 1-13. Mechanical properties of PI-g-PS multigraft copolymers. (a) Influence of functionality on stress-strain behavior. (b) Comparison of tetrafunctional multigraft copolymers (MG) with commercial SIS-block copolymer (Kraton®) and star copolymer (Styroflex®). (c) Influence of

number of branchpoints on the tensile strength. (d) Hysteresis curve of a tetrafunctional multigraft copolymer.[83] 46

Figure 1-14. Temperature variations of specific volume at T_g and T_m.[45] 52

Figure 1-15. Features of different DSC curves. 52

Figure 1-16. Illustration of the typical TMA curve.[99] 54

Figure 1-17. Modulus values changes with temperature and transitions in materials.[97] 54

Figure 1-18. The values of T_g and shapes of DSC thermograms for different pressure change-temperature change sequences.[100] 56

Figure 1-19. Stress-strain curves for SIS triblock copolymers. Sphere: wt% of PS 0.18, molecular weight 10-89-10. Cylinders: wt% of PS 0.30, molecular weight 14-66-14. Lamellae: wt% of PS 0.45, molecular weight 22-29-22.[102] 57

Figure 1-20. Schematic operation of AFM.[103] 59

Figure 1-21. The components of a SAXS instrument.[110] 62

Figure 1-22. Contrast mechanisms of TEM: a) for polymers with crystallinity or heavy element; b) for amorphous soft materials with small variations in density. [111] 63

Figure 1-23. Illustration of stress-strain plots for (a) typical Hookean and non-Hookean materials, [112] and (b) TPEs like SBS.[6] 67

Figure 1-24 Schemes illustrating development of the tensile growth stress and strain hardening behavior with different strain rates. Arrows show the direction of increasing strain rates. 70

Figure 1-25. Stress-strain curves for Kraton 101 and Thermolastic 226 at -40, 0, 40 ^{o}C.[116] 71

Figure 1-26. Schematic representation of the dependence of stress-strain curves on strain rate and temperature. 72

Figure 2-1. ^{1}H NMR spectra of PAdA. 108

Figure 2-2. ^{13}C NMR spectra of PAdA. 108

Figure 2-3. SEC profiles of PtBA by RAFT polymerization. 110

Figure 2-4. SEC profiles of PMA by ATRP. 112

Figure 2-5. SEC profiles of PAdA synthesized by anionic polymerization with a) initiation system with different cations, results shown as Run 01, 02 and 06 in Table 2-1; b) different amount of Et_2Zn added, results shown as Run 04, 05 and 06 in Table 2-1; c) different reaction time, results shown as Run 06 to Run 09 in Table 2-1; d) wide molecular range, results shown as Run 08 and 10 in Table 2-1. 118

Figure 2-6. SEC profiles of PAdA synthesized by NaphNa/DPE/Et2Zn via anionic polymerization with 40-fold excess of Et2Zn (Run 03 in Table 2-1). 119

Figure 2-7. ^{13}C NMR spectra of the carbonyl carbons of the PAdA with Mn 71.8 kg/mol (Run 10 in Table 2-1) measured in $CDCl_3$. 123

Figure 2-8. SEC profiles from a) PMMA homopolymer to PMMA-b-PAdA block copolymer, and b) PAdA homopolymer to PAdA-b-PMMA block copolymer. 126

Figure 2-9. The thermal properties of polymers including PAdA with Mn 71.8 kg/mol, PtBA 54.2 kg/mol, and PMA 110.4 kg/mol. a) DSC thermogram of polymers under nitrogen at a heating rate of 10 $^{o}C\ min^{-1}$; b) TGA thermograms of polymers under nitrogen at a heating rate of 10 $^{o}C\ min^{-1}$. 130

Figure 2-10. ^{13}C NMR spectra of the carbonyl carbons of the PAdA with M_n 8.3 kg/mol (PAdA-B in Table 1) measured in $CDCl_3$. 136

Figure 2-11. SEC chromatograph tracings for the polymer mixture of PAdA-N and PAdA-B (weight ratio around 50/50). 138

Figure 2-12. Relationships between log [η] and log M_w of PAdA in THF at 40 ^{o}C. 140

Figure 2-13. Burchard-Stockmayer-Fixman relation for PAdA in THF at 40 ^{o}C. 143

Figure 2-14. Zimm plot for PAdA in toluene at 30 ^{o}C. 146

Figure 3-1. SEC profile of ATA-26.2-53.0 from Table 3-1. 173

Figure 3-2. DSC thermograph of ATA-26.2-33.5 from Table 3-1 and its normalized first derivative. 173

Figure 3-3. AFM images of ATA-16.2-25.4 in Table 3-1: (left) height image; (right) phase image. 175

Figure 3-4. SAXS profiles of ATA-28.6-14.3, ATA-16.2-25.4, ATA-28.6-60.6 in Table 3-1. 176

Figure 3-5. Storage modulus (black), loss modulus (red), and tan δ (blue) for ATA-26.2-33.5. 178

Figure 3-6 Stress-strain curves of ATA triblock copolymers. 181

Figure 4-1. Reaction solutions on the synthesis of PMMA macromonomer: (a) activation of PVBA by sec-BuLi upon mixing; (b) the completion of the activation of PVBA by sec-BuLi; (c) formation of a complex between LiCl and nitrogen anion; (d) Solutions of living PMMA. 198

Figure 4-2. ^{1}H NMR spectrum of PMMA macromonomer (PMMA-18 in Table 4-1). 200

Figure 4-3. ^{1}H NMR spectrum of PBA-g-PMMA(MG-18.1-2.8-18.4 in Table 4-2) 202

Figure 4-4. SEC profiles of PBA-g-PMMA (MG-18.1-2.8-18.4 in Table 4-2) and PMMA macromonomer (PMMA-18 in Table 4-1).....202

Figure 4-5 DSC thermograph of MG-18.1-2.8-18.4 and its normalized first derivative. Two transitions correspond to each of the acrylic domains were observed. The difference of the intensity of each transition is

caused by the proportion diversity between PMMA and PBA components. 205

Figure 4-6. AFM height images (left) and phase images (mid), and SAXS profiles (right) of PBA-g-PMMA. From top to bottom correspond to: (a) MG-8.4-3.3-8.6; (b) MG-18.1-2.8-18.4; (c) MG-29.3-3.0-33.8 206

Figure 4-7. Storage modulus, loss modulus, and tan δ of MG-18.1-2.8-18.4.... 208

Figure 4-8. Stress-strain behaviors of PBA-g-PMMA graft copolymers 211

Figure 4-9 Photographs on the hysteresis test of MG-29.3-1.5-9.3. From top to bottom are: Initial sample with the cross head length of 16 mm; sample stretched to 200 mm with around 1200% strain; recovered sample with the cross head length of around 18 mm. 213

Figure 5-1. ^{1}H NMR spectra of PBA-g-PtBMA graft copolymer..... 226

Figure 5-2. SEC profiles of PBA-g-PtBMA and PtBMA macronomer. 226

Figure 5-3. AFM height images (left) and phase images (right) of PBA-g-PtBMA with the hydrolysis degress of (a) 0%; (b) 42%; (c) 54%. 227

Figure 5-5. (a) Illustrate scheme on the synthesis of PS-PMMA-PMMA miktoarm star; (b) photographs of the reaction solutions..... 233

Figure 5-6. SEC traces of PS, PS-PMMA, and PS-PMMA-PMMA miktoarm star. 235

LIST OF SCHEMES

Scheme 1-1. Illustration of thermoplastic elastomers structures. 6

Scheme 1-2. Initiators for the synthesis of PMMA-b-PBA-b-PMMA triblock copolymers via NMP. (a) SG-1; (b) SG1- based difunctional alkoxyamine (DIAMA). 19

Scheme 1-3. Anionic polymerization of PMMA-b-PtBA-b-PMMA 21

Scheme 1-4. Illustration of polymer structures with different architectures 33

Scheme 1-5. Methodologies for the synthesis of graft copolymers: (a) graft from; (b) graft onto; (c) graft through. 37

Scheme 1-6. Example on the chain conformation of multigraft copolymers with microphase-separation state.[72] 39

Scheme 1-7. Graft from methodology to make graft copolymer TPEs based on cellulose matrix through (a) ATRP;[59] (b) ring opening polymerization.[73] 41

Scheme 1-8. Methodologies for the synthesis of styrenic graft copolymers by anionic polymerization: (a) graft from; (b) graft onto; (c) graft through. 43

Scheme 1-9. Anionic polymerization of multigraft copolymer architectures with trifunctional (comb), tetrafunctional (centipede) and hexafunctional (barbwire) branch points.[75,76] 44

Scheme 2-1. (a) Synthesis of 1-adamantyl acrylate (AdA)[38] and anionic polymerization of AdA initiated by DPMK or DPHLi in the presence of Et_2Zn or LiCl. Denote: TEA: triethylamine, DPMK: diphenylmethyl potassium, Et_2Zn: diethyl zinc, DPHLi: diphenylhexyl lithium, and LiCl: lithium chloride. M is Li or K metal.(b) Anionic polymerization of AdAA using NaphNa/DPE initiator in the presence of Et_2Zn in THF at -78 ^oC. 113

Scheme 3-1. Synthesis of PAdA-b-PTHFA-b-PAdA triblock copolymers.....171

Scheme 4-1. Synthesis of PBA-g-PMMA graft copolymer. 197

Scheme 5-1. Proposed on the approach to enhance the mechanical property of ATA triblock copolymers. 231

Scheme 5-2. Illustration on the approach to make multigraft copolymer superelastomers with tetrafunctional branch points. 236

Scheme 5-3. Illustration of the approach for the synthesis of (a) PS_2PMMA_2 star; (b)$PSPMMA_2P_2VP_2$ H-shape copolymer.....238

CHAPTER 1 INTRODUCTION TO ALL ACRYLIC BASED THERMOPLASTIC ELASTOMERS

1.1 Thermoplastic Elastomers

Thermoplastic elastomers (TPEs), first announced by the Shell Chemical Company (USA) in 1965, have been widely used in industry with the market size 4.19 million tons in 2015 and may observe gains at over 4.4% up to 2023.[1] They refer to polymer materials with both thermoplastic and elastomeric properties. When stretched, their relatively long and flexible polymer chains allow for high deformation. Meanwhile, these chains are linked together to form a network that can retain the toughness of the material and allow for reversible deformation. Compared to conventional chemically crosslinked rubbers (normally known as vulcanized rubbers), the crosslink junctions are physically formed and are reversible through processes such as change in temperature and or dissolution in a certain solvent.

1.1.1 Advantages and Disadvantages of TPEs

As compared to the vulcanized rubbers, the physical crosslinking behavior means that changes in behavior may be reversed by heating or external force. The non-phase separated material may then be re-processed. Thus, TPEs have various merits including recyclability, ease of processability, and low cost (with no requirement of vulcanization process). Less energy is required to achieve control of product quality.[2]

Meanwhile, the reversible melt-to-solid transition also leads to the sacrifices of some properties, like compression set, solvent resistance and resistance to

deformation at high temperature, for which conventional thermoset rubbers normally have better performance.

Based on these pros and cons, TPEs are greatly used in the fields including automotive applications, footwear, wire insulation, adhesives, polymer blending and food packaging.[3]

1.1.2 Classification of TPEs

Different types of thermoplastic elastomers have been developed, including: (1) styrenic block copolymers (SBCs), (2) polymer blends by dynamic vulcanization (TPVs), (3) polyolefin based thermoplastic elastomers (TPOs), (4) halogen-containing polyolefins, (5) thermoplastic polyurethane elastomers (TPUs), (6) polyamide based thermoplastic elastomers (COPA), (7) polyether ester elastomers (COPE), (8) ionomeric thermoplastic elastomers, etc.[2] The comparison of performance, cost and market share of different TPEs is shown in **Figure 1-1.**

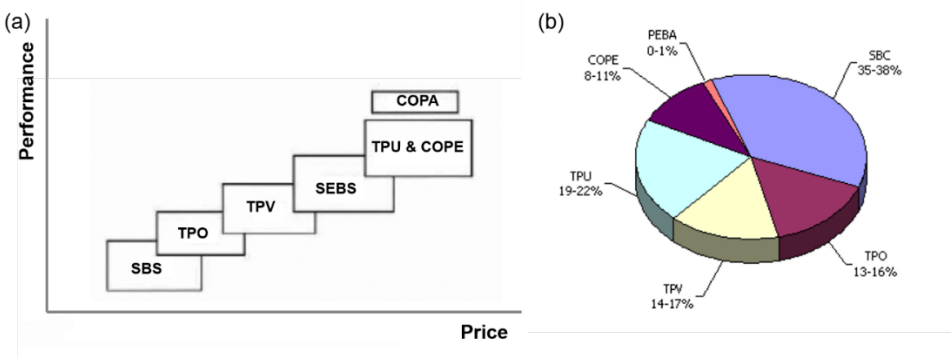

Figure 1-1. (a) Approximate ranges of performance vs. cost for commercial TPEs.[2] (b) Percent break-up by market segments in revenue in 2000. (Courtesy of Frost & Sullivan Market Insight)

1.2 Styrenic Block Copolymers (SBCs) Thermoplastic Elastomers

1.2.1 Mechanism of Function of TPEs

Block copolymers or polymer blends are good candidates to make TPEs, where the physically crosslinked network structure in TPEs is normally composed of two different domains: with elastomeric chains forming the matrix and plastic domains serving as the junctions, as illustrated in **Scheme 1-1**. The driving force for this behavior is thermodynamic incompatibility of the different blocks.[4]

The phase separation into the soft matrix and dispersed hard domains is driven by the Flory-Huggins interaction parameter χ and the degree of polymerization *N*. As shown in **Figure 1-2**, for AB diblock and ABA symmetric triblock copolymers, with either the increase of χ or *N*, more distinct microphase separation behavior can be observed.[4,5] For the former parameter, the combination of components with chemically different structures and the introduction of additional forces like ionic charge and hydrogen bonding can contribute to the large χ; the role of the latter parameter indicates that segment with high molecular weight can lead to better phase separation behavior of TPEs.

One of the most traditional types of block copolymer TPEs is ABA triblock block copolymers, where A consists of glassy domains and B consists of elastomeric domains. In contrast, other types of structures, such as AB diblock copolymers and BAB triblock (with elastomeric domain as the endblocks) copolymers do not show the characteristic behavior of TPEs. It has been

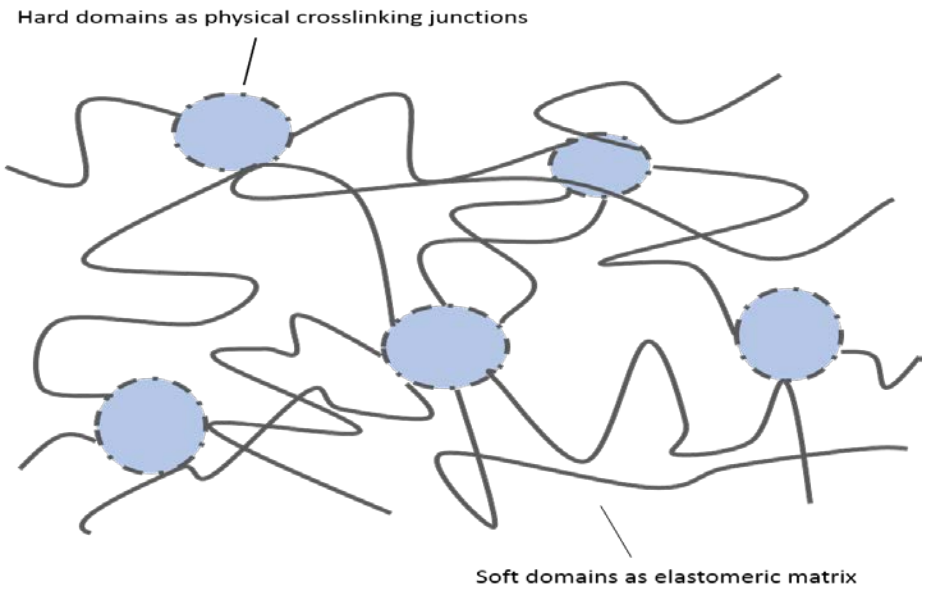

Scheme 1-1. Illustration of thermoplastic elastomers structures.

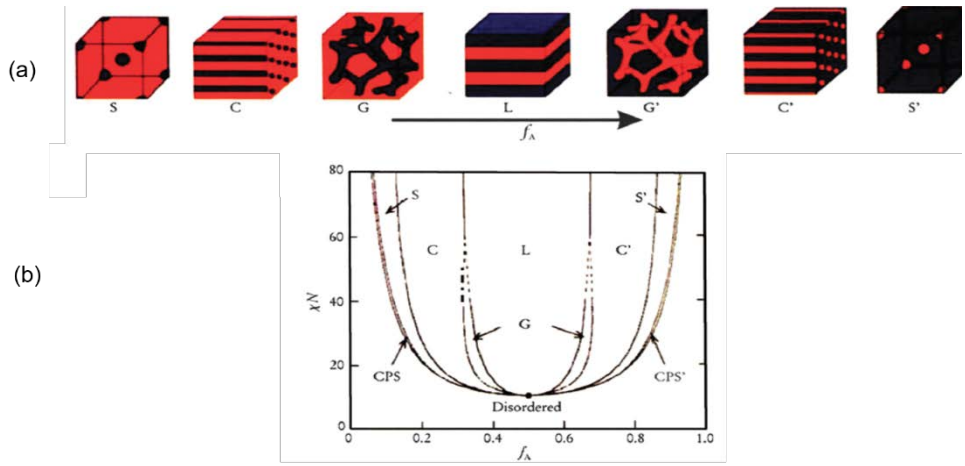

Figure 1-2. (a) Equilibrium morphologies of diblock or triblock copolymers in bulk. S and S'= spheres, C and C'= cylinders, G and G'= gyroids, and L = lamellae. (b) Theoretical phase diagram of diblock and triblock copolymers predicted by the self-consistent mean-field theory, depending on volume fraction (f) of the blocks and the segregation parameter, χ N, where χ is the Flory–Huggins segment–segment interaction energy and N is the degree of polymerization. [4,5]

demonstrated that both ends of the elastomer segment must be linked with the non-elastomeric domains, in order to ensure the formation of the physical crosslinking junctions to reinforce the mechanical strength of the materials.[6] Otherwise, both the final stress and the reversible elongation of the resulting materials are limited.

1.2.2 Styrenic Thermoplastic Elastomers (SBCs)

The market size of SBCs is dominant among TPEs and generated over $6 billion in revenue in 2015.[1,7] They are typically based on the ABA triblock copolymers where A is polystyrene (PS) (T_g ~ 100 ^oC) and its derivatives as the hard domain, and B is a polydiene like polybutadiene (PB) (T_g ~ -90 ^oC) or polyisoprene (PI) (T_g ~ -56 ^oC) as the elastomeric domain.[2]

The spherical morphology is typically formed from microphase separation and is preferred in order to to get good mechanical properties.[8] SBCs exhibit similar performance as vulcanized rubber at ambient temperature, with tensile strengths in excess of 28 MPa, and elongation at break over 800%.[9]

The most conventional and classic SBCs are polystyrene-block-polybutadiene-block-polystyrene (SBS) and polystyrene-block-polyisoprene-block-polystyrene (SIS) triblock copolymers. However, the polydiene used as the soft domains contains unsaturated bonds that are vulnerable to oxidation and UV degradation. Thus, the lifetime and stability of the material are limited.

One solution to overcome the vulnerability of the unsaturated bonds is to convert the middle block into saturated polymer chains. This can be achieved by hydrogenation of PB or PI into poly(ethylene/butylene) (PEB) or poly(ethylene/propylene) (PEP), and the final SBCs are thus SEBS or SEPS.[10] The modification not only increases the material's resistance to the attack of oxygen, ozone, and UV, but also improves the processability and mechanical strength, as shown in **Figure 1-3 (a)**.[11] Meanwhile, the hydrogenation can induce crystallinity, which affects the mechanical properties and dynamic hysteresis of the material. **(Figure 1-3 (b))** Thus the hydrogenation degree needs to be considered during this modification. Another approach is to introduce a saturated non-crystalline polyolefin as a replacement of polydiene, such as polyisobutylene (PIB). The resulting triblock copolymer SIBS can be directly synthesized by living cationic polymerization.[12]

1.3 All Acrylic Based TPEs

Acrylic based block copolymers offer a promising alternative to SBCs. Highly syndiotactic poly(methyl methacrylate) (sPMMA) was used to replace PS to improve the upper service temperature of the material.[13] Poly(*n*-butyl acrylate) (PBA) (T_g ~ -54 ^{o}C, similar to PI) was demonstrated to be a good candidate as the soft domain to improve the chemical stability with the elimination of the unsaturated backbone.[14] Moreover, as a large family of polymers with various pendent groups, a series of different poly(alkyl (meth)acrylate)s with different T_gs provide a tool box

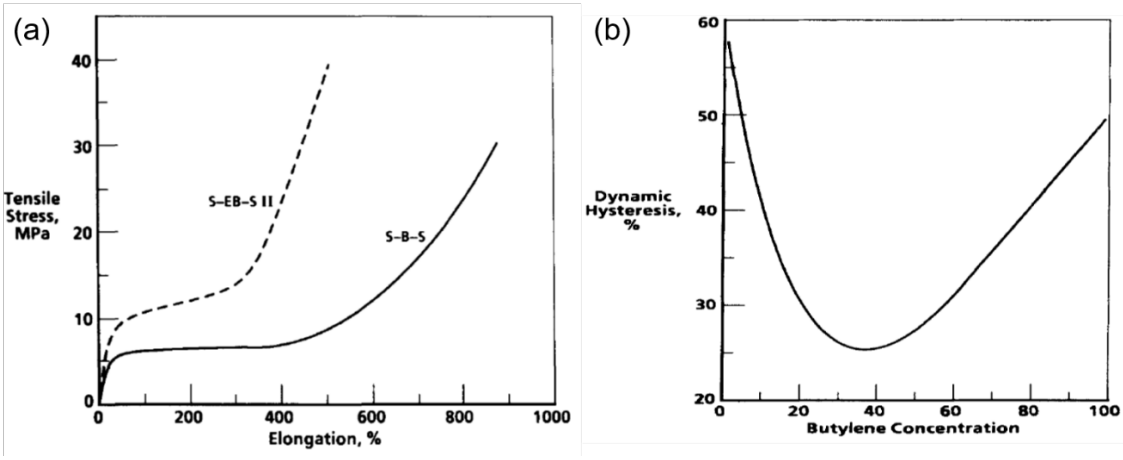

Figure 1-3. (a) Stress-strain curves of SBS and SEBS; (b) Dynamic hysteresis as a function of butylene concentration in partially hydrogenated SBS. The concentration of butylene is proportional to the hydrogenation degree. [11]

that can meet various mechanical and thermal requirements for various applications. For example, an ultra-high temperature all acrylic TPE might be comprised of poly(isobornyl methacrylate) (T_g ~ 200 ^oC) as the glassy segment, and poly(2-ethylhexyl acrylate) (T_g ~ -65 ^oC)[15] or poly(isoctyl acrylate) (T_g ~ -50 ^oC)[16] as the elastomeric segment.

1.3.1 Industrial Applications of Acrylic based TPEs.

Besides the flexible options and chemical stability of the resulting materials, all acrylic based TPEs have advantages over SBCs including optical transparency, versatility of adhesion, weatherability, oil resistance, printability, compatibility with fillers, abrasion resistance and low viscosity.[17,18]

The introduction of polymethacrylates extends the application range of SBCs, such as the toughener in various fields.[7] PS-b-PB-b-PMMA has been effectively used as the toughener for both thermoplastic and thermosetting systems, such as poly(phenylene oxide), poly(vinylidene fluoride), and poly(vinyl chloride), due to the polarity of PMMA that can increase the blend compatibility.[7] For the epoxy systems, the triblock copolymer also shows the ability to improve the toughness of the epoxy network by the formation of “spheres on spheres” morphology.[19]

Acrylic polymer is one of the most commonly used class of adhesives, and it is ideal for UV-curable materials that can be used in 3D printing.[20] Acrylic adhesives can also improve aesthetics, bonding to plastics and metals, and even

bonding between oily or contaminated surfaces, which make them also popularly applied in automobile and furniture industries.[21] For acrylic TPEs, the potential uses in automotive applications include instrument panel, dashboard skins, inner door grips, parking levers shift grips, steering wheel covers, assist grips, switches, etc.(**Figure 1-4**)[22]

Their thermoplastic properties make acrylic TPEs good candidate for pressure sensitive adhesive applications. The low-temperature adhesiveness, good die-cut properties, and great holding power make it ideal as the removable and reusable adhesive. Moreover, with certain amounts of tackifiers such as PBA oligomer, the tack properties can even be adjusted as needed.[23]

1.3.2 Entanglement Molecular Weight (M_e)

The mechanical performance of all acrylic TPEs as compared to SBCs is always “disappointing”, especially with much lower elongation at break.[24] The much higher entanglement molecular weight (M_e) can help to shed light on their poor mechanical properties. It is defined as the molecular weight between adjacent temporary entanglement points and is controlled by the molecular architecture of the polymers. Based on the equation below, M_e can be estimated by dynamic oscillatory measurements using rheometers, as shown in **Figure 1-5**.[25]

$$M_e = K\frac{\rho RT}{G_N^0} \qquad (1)$$

Figure 1-4. Examples for acrylic TPE in automotive application.[22]

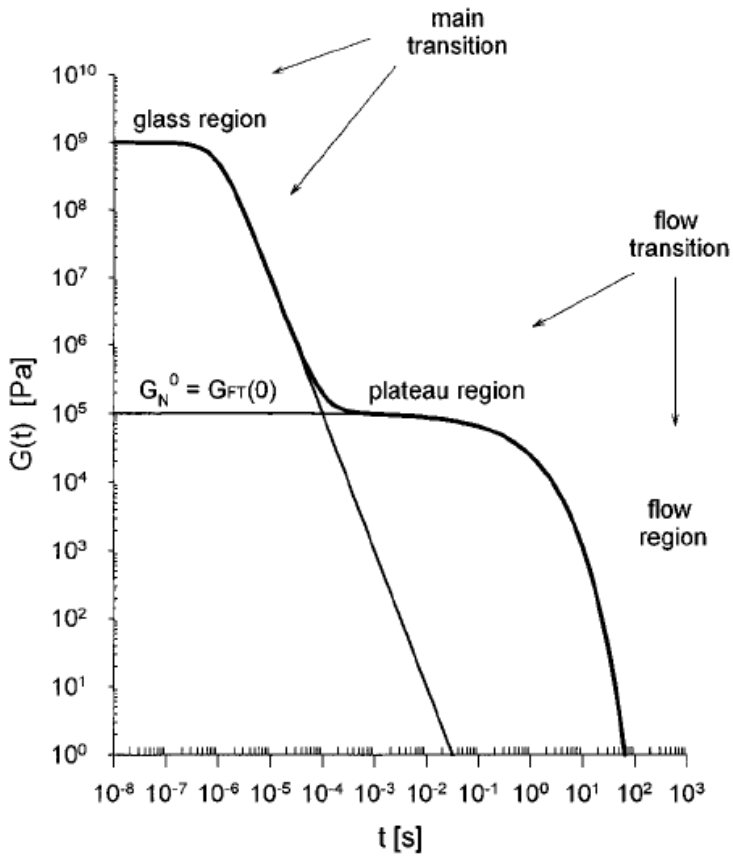

Figure 1-5. Schematic representation of relaxation function G(t) for an amorphous polymer. The plateau modulus G_N^0 can be used for the calculation of M_e.[25]

in which K is a constant with a value of 1 or 4/5, R is the universal gas constant, T is the temperature, and ρ is the polymer melt density.[26]

The entanglement molecular weight is related by the power law to the packing length of the polymer species:

$$M_e = n_t^2 N_a \rho p^3 \quad (2)$$

In which N_a is the Avogadro number, and p is the packing length.

The packing length p is analogous to the molecular diameter of the repeat unit in the polymer chain. As shown in Equation (3), if the polymer chain is regarded to be composed of freely jointed rods, p is proportional to the ratio of the cross-sectional area to the length of each rod.

$$\mathrm{p} \sim \frac{h^2}{[C_\infty l_0]} \quad (3)$$

In which the product $C_\infty l_0$ is the Kuhn step length and h is the diameter. Thus, the smaller h is the 'skinnier' the chain and the smaller p.[26]

Compared to polydienes, the large side groups impart poly(meth)acrylates a large diameter. Thus the packing lengths are normally larger for acrylic polymers. As a result, the entanglement molecular weights of poly(meth)acrylates are large as compared to polydienes. Moreover, with the increase of the length of pendent groups, the increase of packing lengths leads to the further increase of M_e, as shown in **Table 1-1**.[27]

The M_es of the soft blocks determine the elastomeric properties, while the M_e of the hard blocks is reported to have an effect on the rheological behavior.[16]

Larger M_e can lead to fewer entanglements in the polymer networks. Therefore, the mechanical strength and strain at break will be lower.

The M_e influence on tensile strength may be expressed by the equation below:[28]

$$F = A + kf_e/M_e \tag{4}$$

in which A is a constant related to the composition, k is a constant at a certain copolymer composition, f_e is the force shared by the slippage of one chain entanglement, and F is the ultimate tensile strength of the triblock copolymer.

As shown in **Figure 1-6**, with the decrease of M_e, higher mechanical strength can be attained.[28]

The M_e's influence on elongation can be reflected by the comparison between different TPEs composed of PS, PMMA, PB and poly(n-butyl acrylate) (PBA). The classic SBS can normally reach around 1000% elongation at break.[9] When the outer block is changed to PMMA, the elongation at break can also reach 1000%.[13] Meanwhile, the switch of the soft domain from PB to PBA distinctly decreased the elongation at break. PS-b-PBA-b-PS exhibited the elongation less than 600% with similar molecular weight to SBS.[14] PMMA-b-PBA-b-PMMA normally gives elongation at break around 500%.[27]

Table 1-1. Average chain entanglement molecular weight (M_e) for polymers[27]

Polymer	$M_e \times 10^{-3}$ (g/mol)
Polyisoprene	6.1
Polybutadiene	1.7
Poly(ethylacryate)	11
Poly(n-propylacrylate)	16
Poly(n-butylacrylate)	28
Poly(isooctylacrylate)	59

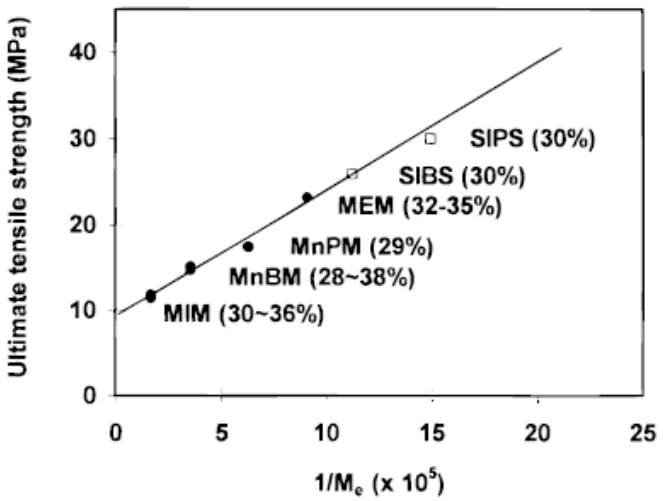

Figure 1-6. Ultimate tensile strength as a function of 1/ M_e. Where M: PMMA; I: Poly(isooctyl acrylate); nB: poly(*n*-butyl acrylate); nP: poly(*n*-propyl acrylate); E: poly(ethyl acrylate); S: PS; IB: poly(isobutylene); IP: polyisoprene.[28]

1.3.3 Synthesis and Properties of PMMA-b-PBA-b-PMMA Triblock Copolymer TPEs

Conventional TPEs are based on ABA triblock copolymers, with the outer block as the hard domains and medium block as the soft domains. Similar to SBCs, all acrylic based TPEs follow the same principle. Various products of PMMA-b-PBA-b-PMMA triblock copolymers have been developed and commercialized, such as Nanostrength® from Arkema, and Kurarity® from Kuraray. For the synthesis of well-defined block copolymers, controlled polymerization is essential to keep the living property of polymer chain ends and sequentially grow the other blocks.[29]

Different methods of controlled radical polymerization have been utilized for the synthesis of PMMA-b-PBA-b-PMMA triblock copolymer TPEs. Controlled radical polymerization does not have the ability to achieve the highly desirable 100% conversion with fully intact living properties. Thus, the normal approach to synthesize block copolymers via controlled radical polymerizations is to quench the reaction at certain conversion. After precipitation and purification, the resulting polymer with functional group— either as initiator or chain transfer agent— is used for synthesis of the second block.[30] It is thus difficult to guarantee the same chain length of the outer two blocks through the sequential, three-step polymerization. As a solution, the difunctional initiator or chain transfer agent is used so that the two hard blocks can grow simultaneously. For instance, atom transfer radical

polymerization (ATRP) has been utilized for the production of PMMA-b-PBA-b-PMMA, with the difunctional initiators attempted including 1,2-bis(bromoisobutyryloxy) ethane (bBr-iBE)[15] and diethyl meso-2,5-dibromoadipate (DEMDBA).[31]

The exception is Arkema's Nanostrength®,which is reported to be synthesized through nitroxide-mediated polymerization (NMP) using BlocBuilder® alkoxyamine (SG-1) as the monofunctional initiator, the structure of which is shown in **Scheme 1-2 (a).**[32] This initiator has advantages including excellent control on the polymerization of acrylates and methacrylates, fast reaction and no metal residue left in the product. However, the more efficient and promising initiator to build symmetric triblock copolymers by NMP is the modified difunctional initiator from SG-1, structure as shown in **Scheme 1-2 (b).**[33]

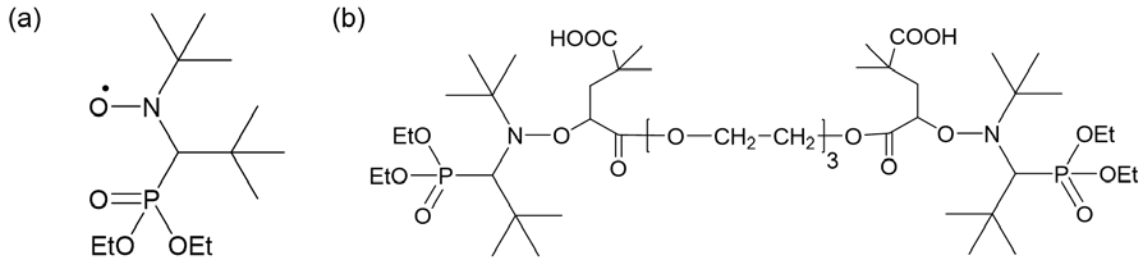

Scheme 1-2. Initiators for the synthesis of PMMA-b-PBA-b-PMMA triblock copolymers via NMP. (a) SG-1; (b) SG1- based difunctional alkoxyamine (DIAMA).

A better method to synthesize the ABA triblock copolymers is living anionic polymerization by virtue of its predictable molecular weights with narrow polydispersities (PDI), 100% conversion and superior living properties.[34,35] Both sequential three-step reactions and polymerization initiated by difunctional initiators can produce triblock copolymers with symmetric composition.

Meanwhile, the living anionic polymerization of acrylates is challenging due to intrinsic side reactions including backbiting reactions of propagating enolate anions and aggregations of active chain ends.[36] Although many attempts have been tried, few acrylate monomers have been successfully polymerized anionically with low PDI and predicted molecular weights, and the successful ones contain bulky pendent groups to prevent the side reactions.[37-39] Although PBA was also successfully synthesized with PDI of 1.30 by using tetrabutylammonium dimethyl malonate as the initiator, the living character of the anions is still limited.[40]

Transalcoholysis reactions offer the solution to the difficulties in the direct anionic polymerization of n-butyl acrylate by the synthesis of poly(tert-butyl acrylate) (PtBA) first. Tong, et al. reported the synthesis of PMMA-b-PtBA-b-PMMA by sequential anionic polymerization using the sec-butyllithium/diphenylethylene/lithium chloride (sec-BuLi/DPE/LiCl) initiator system. The polymerization was performed in THF at -78 ^{o}C, as shown in **Scheme 1-3**. Thereafter, the transalcoholysis was performed by adding excess of n-butanol in the presence of p-toluenesulfonic acid (PTSA).[41]

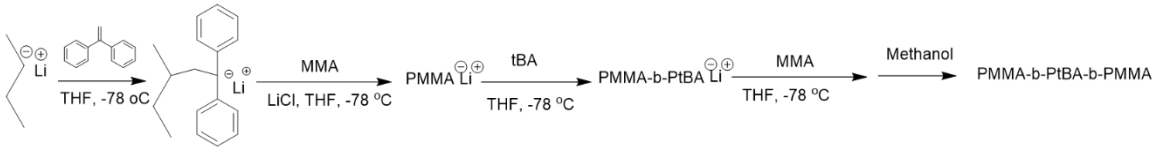

Scheme 1-3. Anionic polymerization of PMMA-b-PtBA-b-PMMA

The obstacle for the industrialization of the anionic polymerization approaches are the complex post-modification operations and the critical conditions required—THF solution at -78 ^{o}C. Surprisingly, Kuraray Co. Ltd has developed a new anionic polymerization system using compounds composed of a Lewis base and di-phenoxyalkyl almuminum. (LA system). With this system, living polymerization of acrylates can be performed at roughly -10 ^{o}C, and at roughly 50 ^{o}C for methacrylates with no sacrifice of living properties, even for the direct polymerization of nBA. Therefore, the PMMA-b-PBA-b-PMMA triblock copolymers can be synthesized directly with sequential addition of MMA, nBA, MMA monomers(GPC curves as shown in **Figure 1-7**).The mild temperature greatly decrease the energy consumption.[17,42]

Although the same composition can be made through both living radical polymerization and living anionic polymerization, the performances of the resulting materials can be different. Tong et al. synthesized the triblock copolymers by ATRP and anionic polymerization that gave the same molecular characteristics except for the PDI of PMMA blocks (broader for the ATRP samples). Similar separation behaviors were observed. However, part of the chains from ATRP did not participate in the network formation and lead to the low storage modulus and poor tensile properties, as shown in **Figure 1-8**. Hence, the low PDIs and well-defined structures make living anionic polymerization an ideal method for the synthesis of acrylic based TPEs.[43]

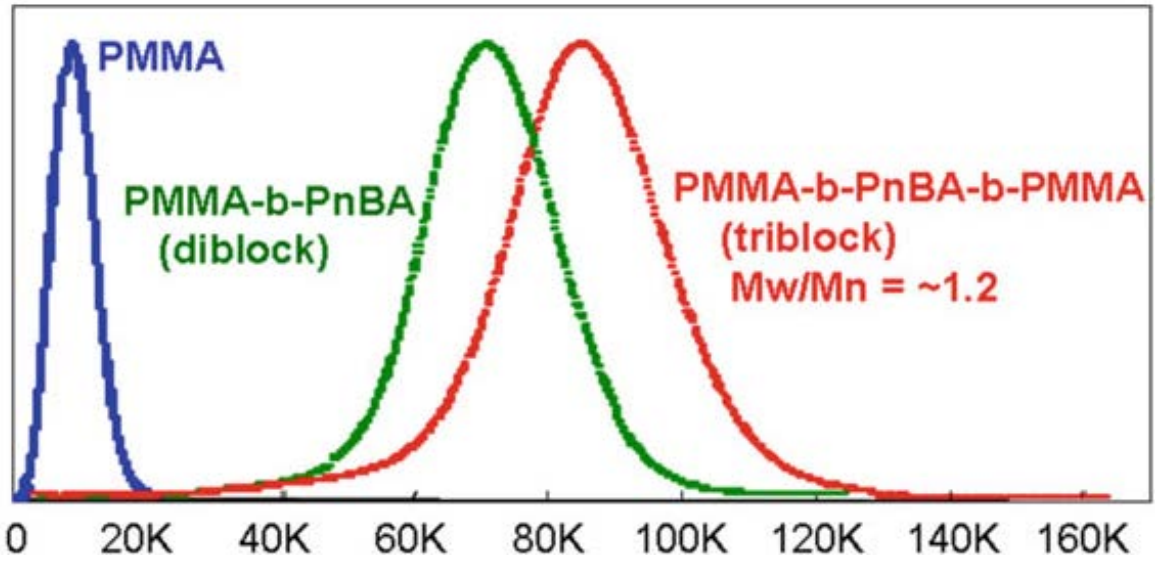

Figure 1-7. SEC curve for "Kurarity™" acrylic triblock coplymers.[17]

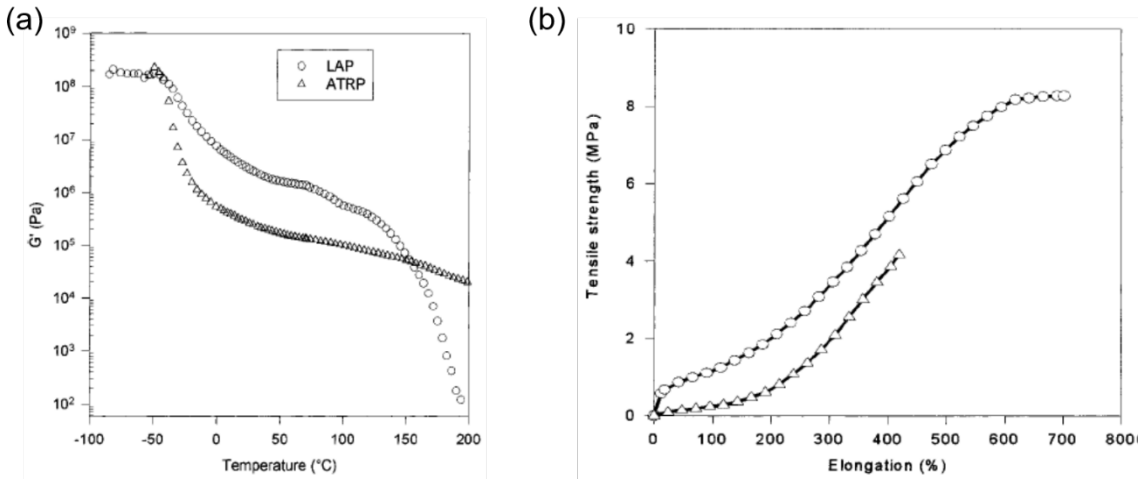

Figure 1-8. Mechanical properties of PMMA-b-PBA-b-PMMA triblock copolymers: (a) Storage modulus as a function of temperature; (b) stress-strain curves.[43]

1.4 Approaches to Improve the Performance of TPEs

1.4.1 Compounding

Theoretically, the thermoplastic elastomers can be used without any additives. However, many additives have been used in industry to fulfill different performance and processing needs, including fillers, oils, plasticizers, resins, etc.[2] In principle, if the appropriated additive accumulates in the hard phase, the physically crosslinked junctions are reinforced so that the mechanical strength can be improved. For additives made of polymeric materials, their glass transition temperatures should be higher than that of hard segments composing TPEs. If the appropriate additive accumulates in the elastomeric matrix, the resulting material can be softer and more flexible. In addition, different forces between the additives and the TPE components can lead to the enhancement of phase separation behavior, so that the mechanical performance can be greatly improved.

Nanofillers have been studied for their effect on the mechanical properties of TPEs. The addition of fumed silica (SiO_2) to polyether ester elastomer has been shown to be effective to improve the modulus, elongation at break and creep resistance. To achieve such results, it is critical that the size and distribution of the silica need to be selected. For incorporation of unmodified silica, the elongation can even be reduced. The influence of microsilica is more distinct than that of nanosilica filler, as shown in **Figure 1-9**.

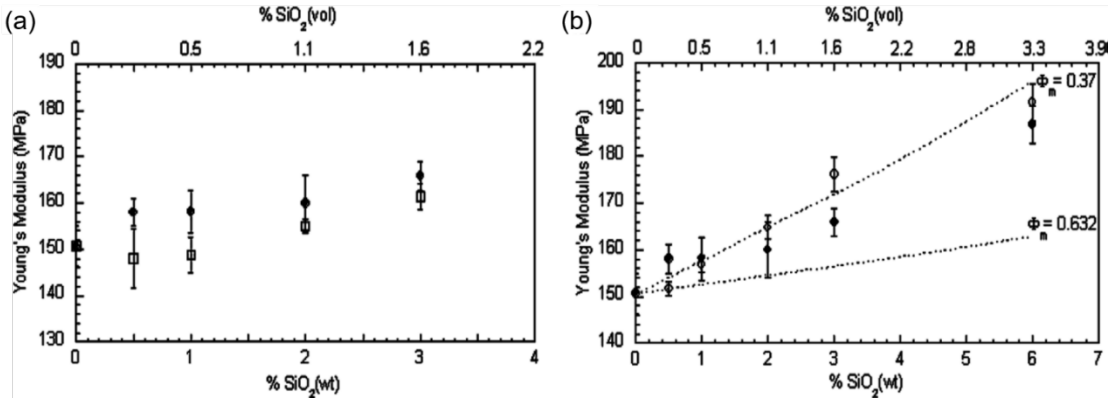

Figure 1-9. Young's modulus of (a) microsilica (□) and nanosilica (●) composites; (b) unmodified (○) and modified (●), wt% of silica composites virsus silica content.

In the case of acrylic based TPEs, the addition of PBA oligomer as the tackifier helps to improve the tack properties of PMMA-b-PBA-b-PMMA triblock copolymers. The addition does not change the T_g or modulus at low temperature, since the additive has the same structure as the soft domain. However, its accumulation in the soft regime makes the material more elastic, and the cohesive strength is improved.[23]

The phase separation behavior can also be adjusted by incorporating certain additives. With a low-volatility, midblock-compatible mineral oil added, the thermoplastic elastomer gel composed of SEBS was reported to undergo a major change in morphology, as shown in **Figure 1-10**. It is speculated that the self-association of the styrene endblocks due to thermodynamic incompatibility with the oil-rich matrix leads to the formation of spheroidal micelles.[44]

1.4.2 Glass Transition Temperature

SBCs, halogen containing polyolefins are normally based on the great differences in glass transition temperatures (T_g). The value of T_g can be influenced by many different factors, including flexibility of the main chain, the functionality of side groups and end groups, the polymer tacticity, the chain microstructure, etc.[45] The great difference in T_g provides the driving force for the thermodynamic incompatibility of different components that comprise the TPEs. With the increase of this difference, the strength of phase separation can normally be enhanced. Moreover, the upper service temperature (UST) is closely related with the T_g of the

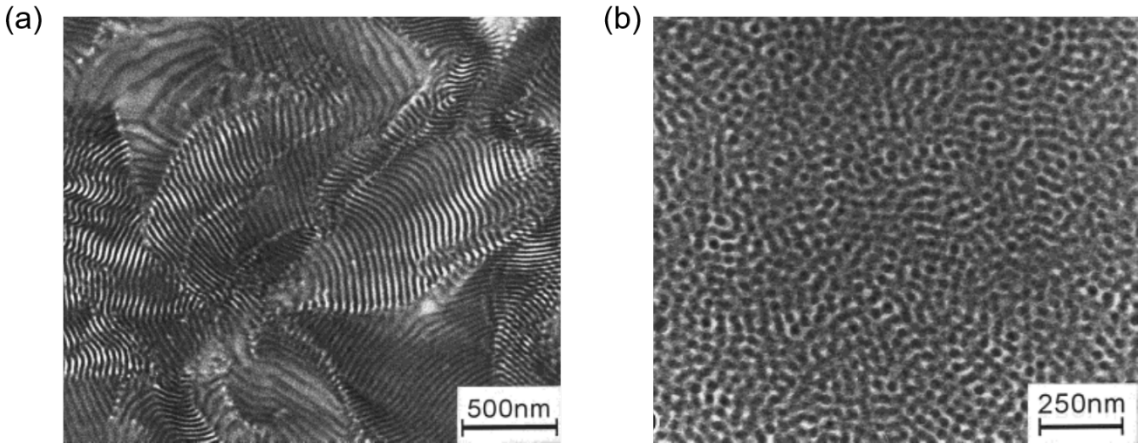

Figure 1-10. Transmission electron micrograph of (a) neat SEBS copolymer; (b) SEBS gel with $\boldsymbol{\omega_{oil}}$ 0.70. (9.3 wt% styrene).[44]

hard segments. As shown in **Figure 1-11**, when the temperature is between the T_gs of different segments, the modulus stays relatively constant and in a region defined as the "rubbery plateau." When it is further increased to higher than the T_g of the hard segment, the modulus drops dramatically and the TPE becomes fluid.[3] Thus to increase the UST of the material, the selection of hard segment with higher T_g is essential.

The typical T_g of PS is around 100 ^oC. However, SBS shows the upper service temperature (UST) limited to 60-70 ^oC due to the partial miscibility of the styrene and butadiene blocks.[46]

Based on the current SBS material, one approach to improve the UST is to fully hydrogenate the unsaturated bonds including the transition from polystyrene to poly(cyclohexylethylene), for which the T_g is around 145 ^oC.[47,48] Moreover, the crystallinity of poly(cyclohexylethylene) also counts for the enhancement of the UST. The resulting TPE gives the order-disorder transition temperature at around 170 ^oC.

Several polystyrene derivatives with higher T_gs have been applied and exhibited great effect on the improvement of UST, such as poly(p-tert-butylstyrene) (T_g: ~130 ^oC),[49] poly(α-methylstyrene) (T_g: ~173 ^oC),[50] and poly(1-adamantylstyrene) (T_g: ~203 ^oC).[51] Polymers with similar structures but higher T_g were also reported, such as polybenzofulvene (T_g: ~190 ^oC).[52]

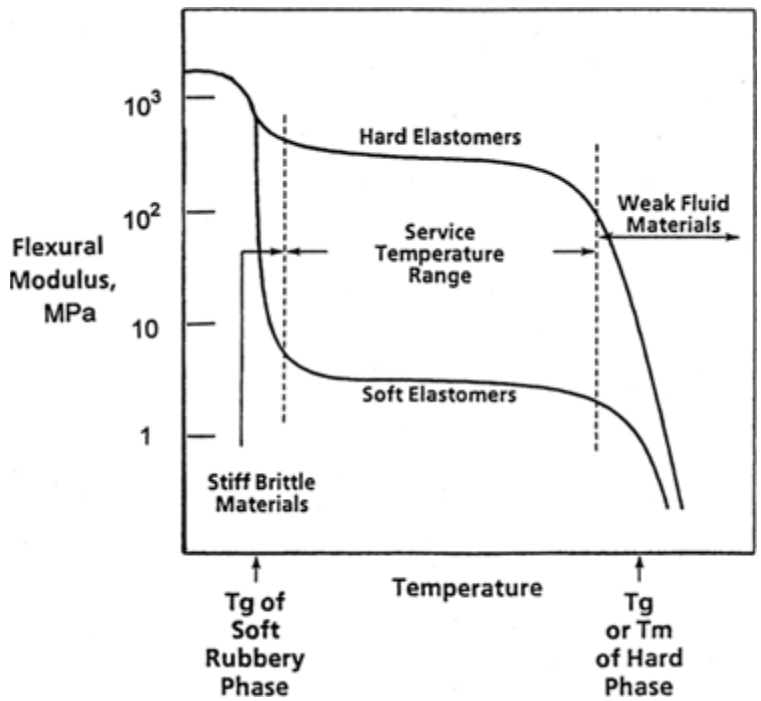

Figure 1-11. The change of storage modulus of thermoplastic elastomers at various temperatures.[3]

As another approach, alkyl (meth)acrylates are also promising candidates to increase the UST. Yu et at. reported the replacement of PS into syndiotactic PMMA (T_g: ~125 ^oC) that distinctly increases the UST of SBS into 125 ^oC[53]. More interestingly, if highly isotactic PMMA (T_g: ~127 ^oC) was used, they reported the resulting PMMA-b-PEB-b-PMMA with a soft point as high as 173 ^oC, which is even much higher the T_g of PMMA. The formation of semi-crystalline stereocomplexes caused by the isotactic PMMA, which reinforces the aggregation of hard segments, accounted for this surprisingly high service temperature.

1.4.3 Complex Architectures

Compared to linear block copolymers, polymers with complex architectures have more advantages of 1) smaller hydrodynamic radii, 2) potentially lower melt viscosity and lower solution viscosities, 3) lower glass transition temperature, 4) lower crystallinity, and 5) higher solubility, which will endow them with improved rheological behavior (such as strain and hardening) and processability.[54] Furthermore, block copolymers with miktoarm star architectures and graft/multigraft architectures allow additional capacity to tune morphology and long range order.[55] It is reported that for PI_2PS miktoarm star copolymers the long range order in cylindrical morphologies could be exceptionally good (**Figure 1-12**) or very poor, depending on whether PI or PS constitutes the continuous phase [55].

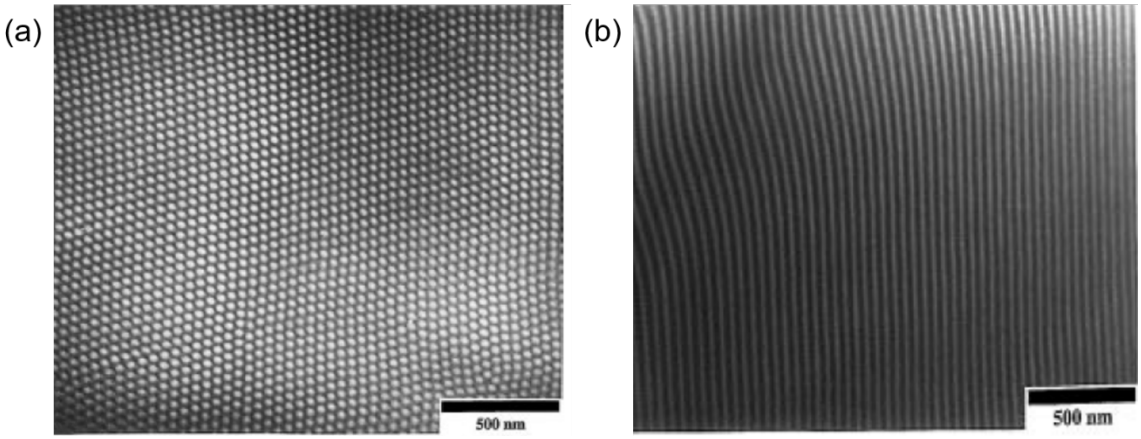

Figure 1-12. TEM images of PI_2PS sample having 0.44 vol fraction PS and forming hexagonally packed cylinders (confirmed by SAXS). (a) A slice perpendicular to the cylinders and, (b) a slice parallel to the cylinders.

Various polymer architectures (also termed as topologies) have been synthesized and studied, including linear, cyclic, star, graft (comb), multigraft, hyperbranched (dendrimer), network type structures (**Scheme 1-4**). Similar to that for block copolymer, “living”/controlled polymerizations provide powerful and ideal approaches to build complex architectures, such as living radical polymerization,[56] living anionic polymerization,[54] and living cationic polymerization.[57]

For the application of TPEs, in addition to its better ability to tune the phase separation behavior, the complex architecture can increase the density of hard segments that form the outer blocks the polymer structure, so that more entanglements between the soft domains can be formed. This improvement of entanglements can further enhance the physical crosslinking behavior of the material. As a result, the mechanical strength of TPEs with complex architectures are usually increased.

There are three common methodologies to build the star architecture: “graft from” the multifunctional initiators,[58,59] “graft to” through coupling reactions with the functional cores, “linking reactions” by the use of linking agents.[54] The star shaped TPEs are usually composed of the soft domains as the inner block and hard domains as the outer block. The entanglements of hard segments are usually dramatically enhanced, even when compared to other architectures. The materials synthesized usually have great toughness, while the elongation can be either

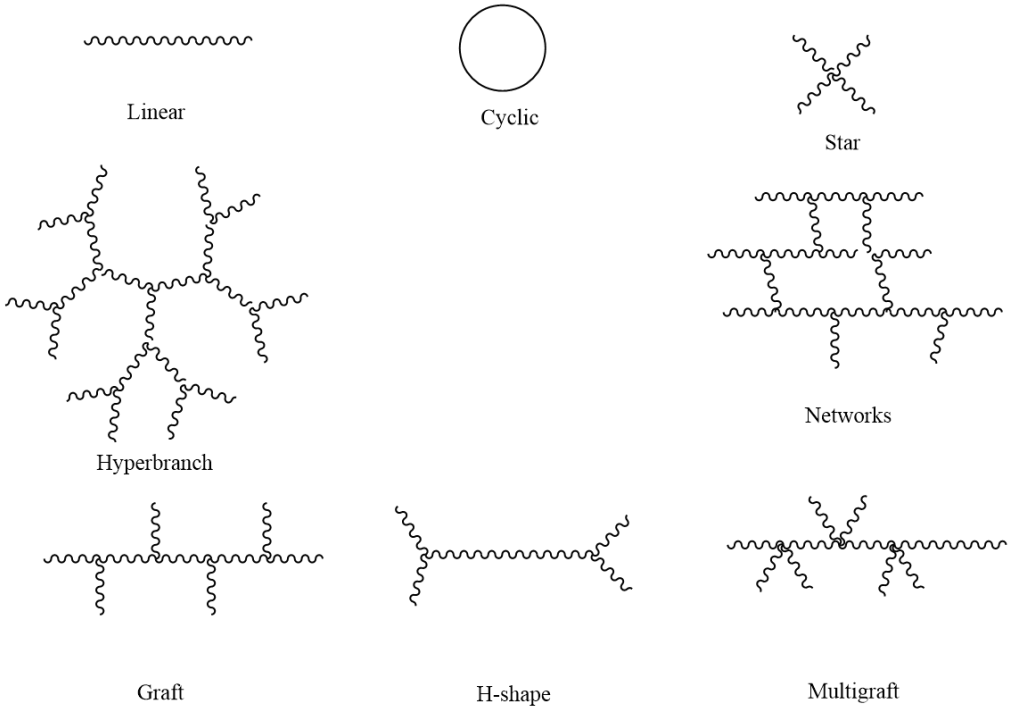

Scheme 1-4. Illustration of polymer structures with different architectures

increased or sacrificed. Thus, the resulting materials are ideal for the use as the tougher to enhance the mechanical strength of conventional linear type TPEs.[60]

Analogous to the linear SBCs, the star copolymers composed of PS and PB or PI have been greatly studied. Dair et al. reported the formation of double gyroid morphology with the PI-b-PS star copolymers.[61] As compared to the common morphologies formed in linear SBCs, such as spheres, cylinders, and lamella structures, this 3-dimensionally interpenetrating periodic structure may have superior properties to prevent the sliding of the junctions while the material is stretched. Thus, the resulting polymer exhibited considerably higher stresses for yield than classical SBCs. However, the strain was only 350% to 400%, which is much lower than the conventional SIS TPEs. In addition, asymmetric miktoarm PS-b-PI copolymers were also reported. Taking advantages of the star architecture, much less content of soft domains is necessary for the material. In other words, the resulting material can possess very high mechanical strength, but still have elastomeric property instead of being too rigid.[62,63]

More distinct comparisons between linear type TPEs and star type TPEs can be found from Imaeda and co-workers' work on poly(2-adamantyl vinyl ether)-b-poly(n-butyl vinyl ether) block copolymers. Both linear type and star type were synthesized through living cationic polymerization. Both the tensile strength and elongation values for star type copolymers were greatly higher than those for linear copolymers at similar composition.[64] Similar improvement of both stress and

elongation was also reported by Juhari and co-workers on the study of poly(n-butyl acrylate)-b-poly(α-methylene-γ-butyrolactone) block copolymers.[65] Another key factor that influences the mechanical performance is the number of arms. By the comparison of poly (p-chlorostyrene)-b-poly(isobutylene) star block copolymers composed of tri-arms and octa-arms, it was demonstrated that the increase of the arm numbers can help to increase the tensile strengths and moduli, although the elongation was decreased.[66]

Accompanying the increase of mechanical strength, many attempts were also performed to improve the upper service temperature at the same time, such as using polyacrylonitrile (PAN, UST of resulting PBA-b-PAN star copolymer higher than 300 ^{o}C).[67] The study on all acrylic star block copolymers was also reported. By using functionalized lignin as the ATRP initiator, the pentarm star of lignin-g-P(MMA-co-BA) exhibited greatly enhanced mechanical strength, where MMA and nBA were randomly copolymerized as the soft segments, and lignin was used as the hard segment.[58] However, another work producing triarm star composed of PBA-g-PMMA diblock copolymers found only comparable mechanical performance as compared to the PMMA-b-PBA-b-PMMA triblock copolymers.[68] It is supposed that the introduction of lignin as the hard segment contributed to the superior stress in the former case.

Similar to the star architecture, hyperbranched copolymers were also attempted. He and coworkers reported the one step production of random

hyperbranched linear polyethylene, taking advantage of an α-diiminonickel complex precatalyst. The resulting polymer exhibited good elastomeric properties. Moreover, the elastomeric properties changed dramatically with the change of temperatures, due to the formation of crystallinities.[69] Hyperbranched PMMA-b-PB and PS-PI block copolymers were also reported. The macromonomers of PMMA-b-PB and PS-b-PI were synthesized through anionic polymerization first, followed by the Williamson etherification reactions to build the final hyperbranched architectures. The resulting materials exhibited higher mechanical strength but poorer elongation than that of linear TPEs. However, when used as additives in the conventional linear TPEs like Kraton® SIS liner block copolymer, they can considerably increase the strength and even elongation behavior of the materials.[70] Thus, hyperbranched TPEs are also good candidates for use as toughener to the conventional linear type TPEs, similar to star-shaped TPEs.

The graft type architecture is more promising to be used as TPEs, with both improvements in mechanical strength and elongation. Three common methodologies can be performed to build the graft architecture, including “graft onto” by the linking reactions, “graft from” by synthesized the main chain with initiation sites, and “graft through” by the copolymerization of the monomer with macromonomers, as shown in **Scheme 1-5**.

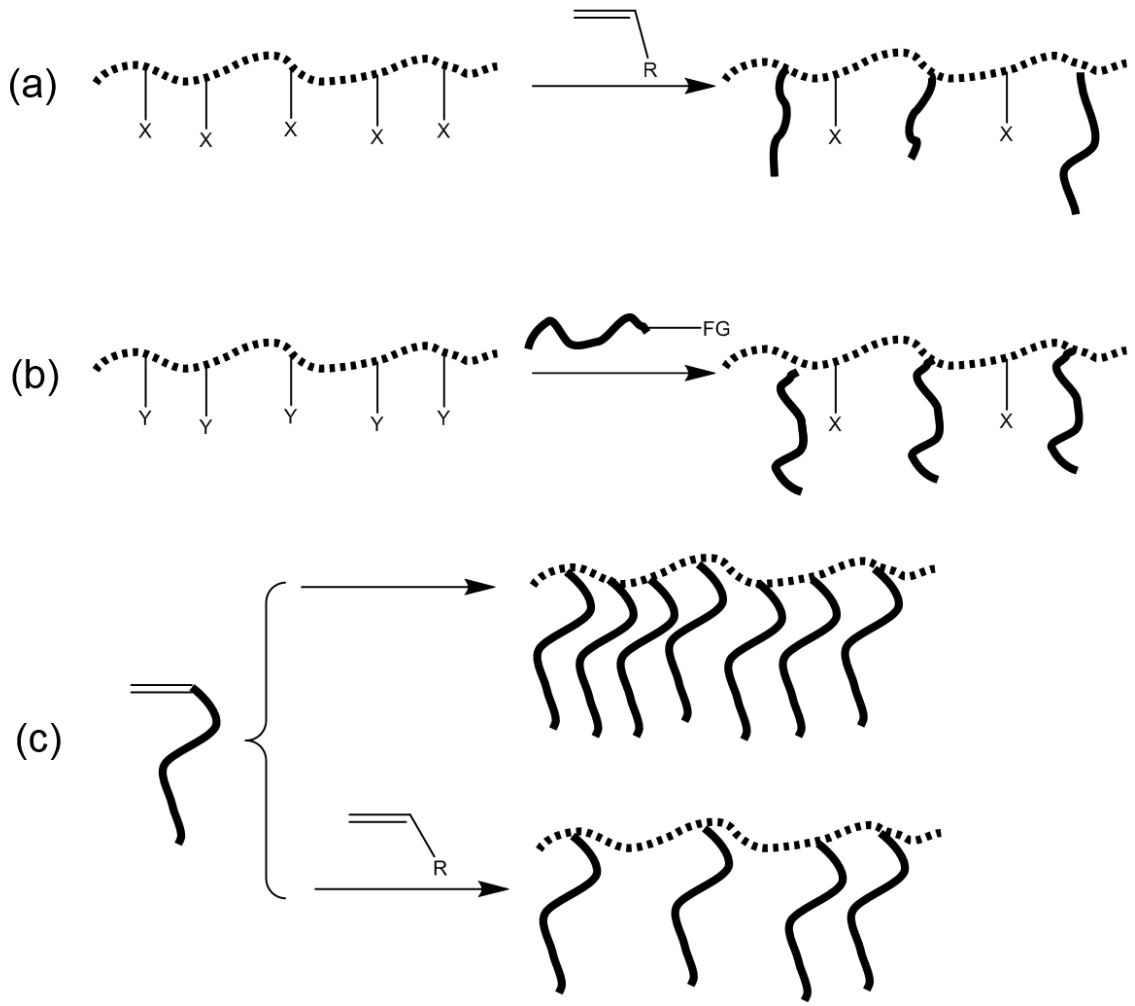

Scheme 1-5. Methodologies for the synthesis of graft copolymers: (a) graft from; (b) graft onto; (c) graft through.

For the use of TPEs, the graft copolymers are usually composed of the soft segment as the main chain and hard segment as the side chains. Similar to the principle of star copolymers, the building of graft architecture can bring more entanglement between the hard segments. Thus the physical crosslinking behavior can be reinforced. (**Scheme 1-6**) Meanwhile, the soft segments can still have entanglements with each other rather than isolated by the outer block as the star architecture. The enhancement of physical crosslinking behavior also makes it possible to reduce the content of the hard segments without sacrificing on the mechanical strength. This increase of the soft segments ratio and their entanglements can help to improve the elongation of the resulting materials. As a result, the building of graft architecture offers an ideal method to improve both mechanical strength and elongation of TPEs.

Suksawad, Patjaree and coworkers reported the introduction of graft architecture into nature rubber.[71] After deproteinization, some of the double bonds in natural rubber (DPNR) were attacked by tert-butyl hydroperoxide/tetraethylenepentamine to create the initiation sites so that styrene monomer can be polymerized therein. Through this approach, the grafting efficiency can be more than 90 mol%. The resulting DPNR-g-PS exhibited a stress 4 times higher and strain twice to that of unmodified nature rubber, which was similar to that for the crosslinked nature rubber.

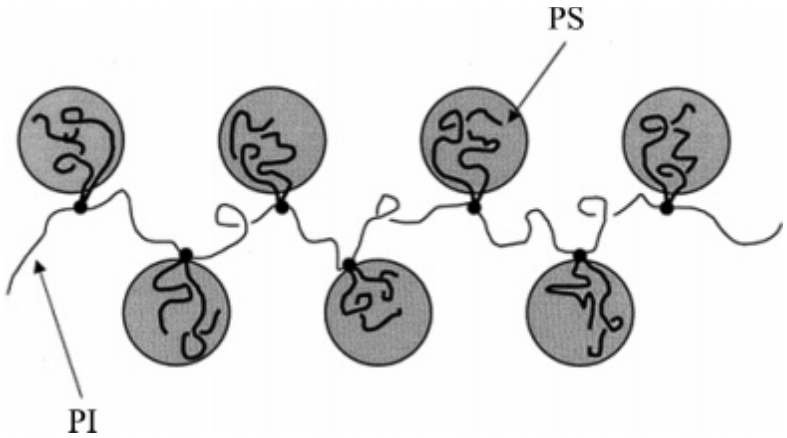

Scheme 1-6. Example on the chain conformation of multigraft copolymers with microphase-separation state.[72]

Like the work above, the graft from methodology was also used for the development of many materials through living radical polymerization, living cationic polymerization or ring opening polymerization. Some natural polymers are “born” with the potential to build graft copolymer architectures, such as cellulose which contains many hydroxyl groups along the polymer chain. Jiang and co-workers modified the hydroxyl groups with 2-bromoisobutyryl bromide so that many initiator sites were formed for the ATRP of MMA/nBA mixtures. (**Scheme 1-7(a)**).[59] Zhang, and Hillmyer’s approach was more straightforward. The hydroxyl group in hydroxypropyl methylcellulose (HPMC) was directly used as the initiation site for the ring opening polymerization of poly(β-methyl-δ-valerolactone)-b-poly(L-lactide) (PMVL-b-PLLA) (**Scheme 1-7(b)**).[73] Both approaches successfully use the cellulose as the matrix to build the graft copolymer TPEs.

As one of the most classic TPEs, graft SBCs have been extensively studied. The graft from methodology was also attempted. Fonagy, Tamas and co-workers reported the synthesis of PIB-g-PS by ATRP. To introduce the initiation sites along the polymer main chain, isobutylene was polymerized by a combination of a trace amount of 4-bromomethylstyrene, after which styrene was polymerized by ATRP using the bromomethyl group along the polymer main chain as the initiator.[74]

Inspired by the traditional method to produce SIS triblock copolymer in industry, anionic polymerization has also been one of the most powerful

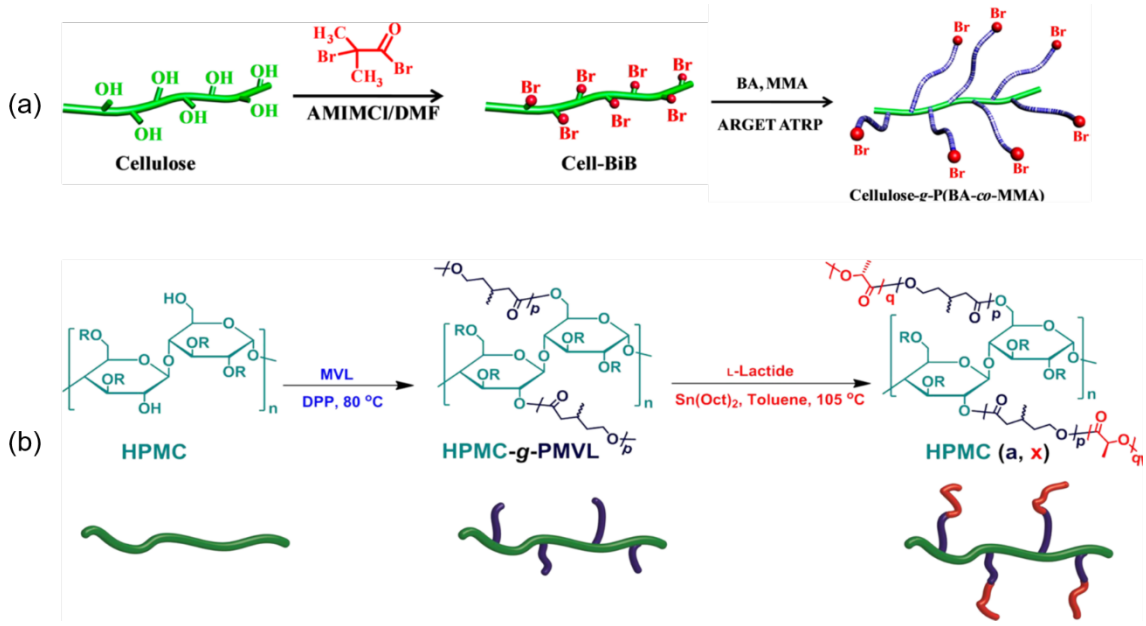

Scheme 1-7. Graft from methodology to make graft copolymer TPEs based on cellulose matrix through (a) ATRP;[59] (b) ring opening polymerization. [73]

approaches to make graft copolymers with well-defined structures, both for practical application and for their theoretical study. All three methodologies can be used to synthesize graft copolymers by anionic polymerization. As shown in **Scheme 1-8**, anionic sites can be created through metalation of the PI main chain, where styrene monomers can be polymerized anionically through graft from methodology (**Scheme 1-8 (a)**). PB can be chlorosilytated through hydrosilation chemistry, where the living PS chain can be graft onto the main chain by the coupling reaction (**Scheme 1-8 (b)**). The graft through methodology can be attained by the synthesis of PS macromonomer first, followed by the copolymerization with isoprene or butadiene monomers. (**Scheme 1-8 (c)**).[75]

Moreover, Mays, et al. reported a unique methodology to synthesize the graft copolymers by combining anionic polymerization, and what is called polycondensation polymerizations.[75-78] With this novel approach, not only the graft copolymers with trifunctional (comb), tetrafunctional (centipede), and hexafunctional (barbwire) branch points can be produced, the resulting polymers also possess strictly well-defined structures, with both same length of side chains and soft segments between the junction points. (**Scheme 1-9**)

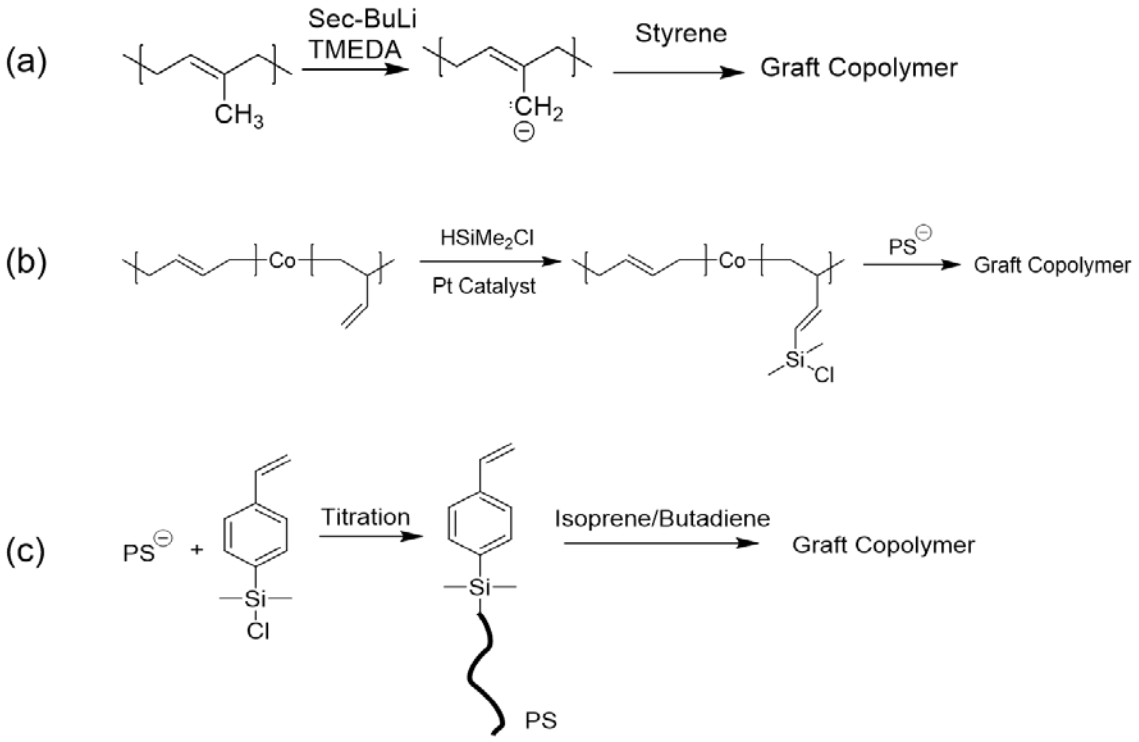

Scheme 1-8. Methodologies for the synthesis of styrenic graft copolymers by anionic polymerization: (a) graft from; (b) graft onto; (c) graft through.

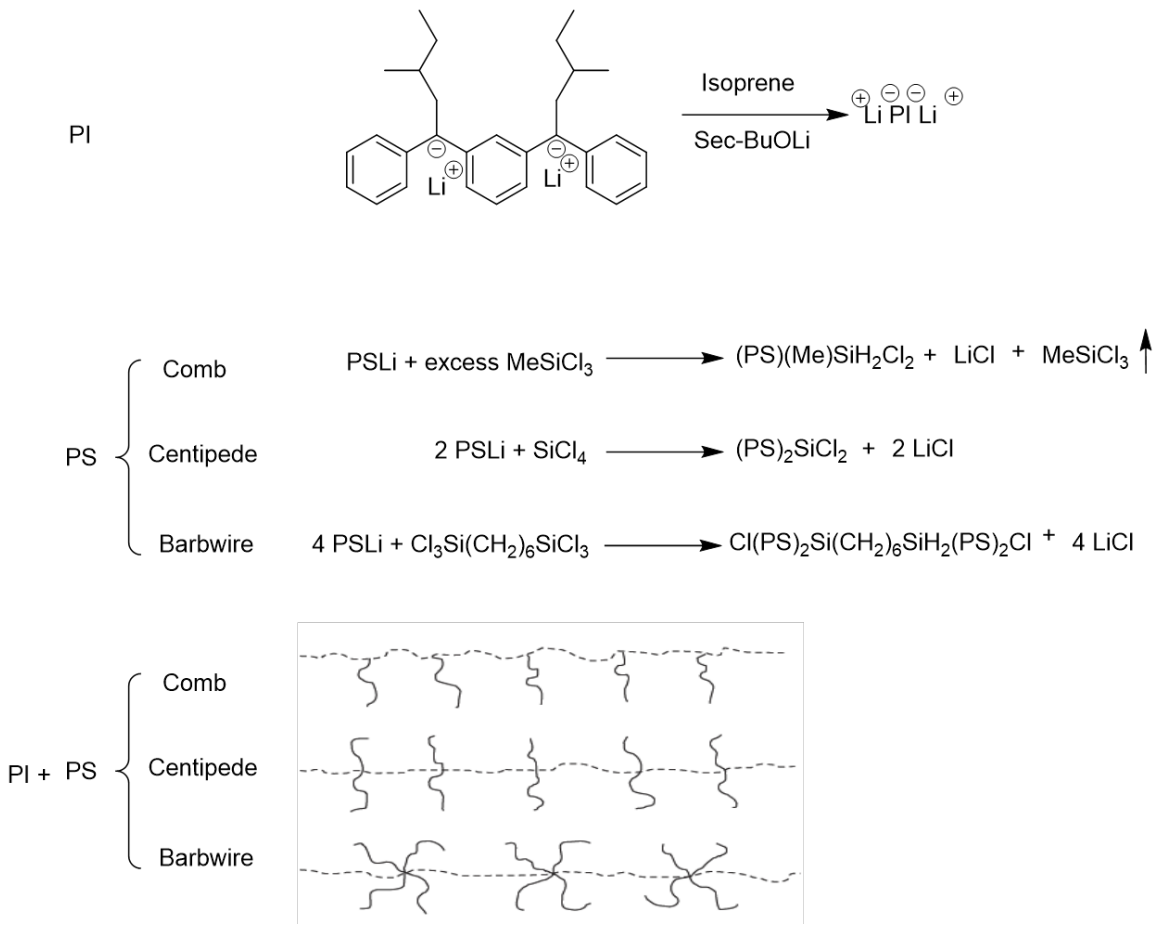

Scheme 1-9. Anionic polymerization of multigraft copolymer architectures with trifunctional (comb), tetrafunctional (centipede) and hexafunctional (barbwire) branch points.[75,76]

With these well-defined graft copolymers, different characterization was performed on this type of architecture, including rheology,[79] morphology,[72] deformation behavior,[80,81] stress softening,[82] mechanical properties, and hysteresis.[83] The performance of the material can be influenced by various factors as discussed below:

(1) Functionality. With the increase of functionality, the morphology changes from sphere (trifunctional) to cylinder (tetrafunctional) and lamellae (hexafunctional). Thus the mechanical properties also change.[72] Among them, the tetrafunctional multigraft copolymers exhibit the best combination of high mechanical strength and elongation.[83] (**Figure 1-13 (a)**)

(2) The tetrafunctional multgraft copolymer shows a surprisingly high strain at break of about 1550%, which is far exceeding the values for commercial TPEs (Styroflex®: 620% due to the the star architecture; Kraton®: 1050%).[83] (**Figure 1-13(b)**) In this way, they name the material as “superelatomer” that can better identify it superior elongation property.[84]

(3) Branch points. With the increase of branch points, more entanglements can be acquired. Thus the mechanical strength can be increased.[83] (**Figure 1-13 (c)**)

(4) Hysteresis. The tetrafunctional multigraft copolymer can be deformed until 1400% and reveals a residual strain of only 40%. (**Figure 1-13 (d)**) This recovery behavior is also distinct as compared to commercial products.

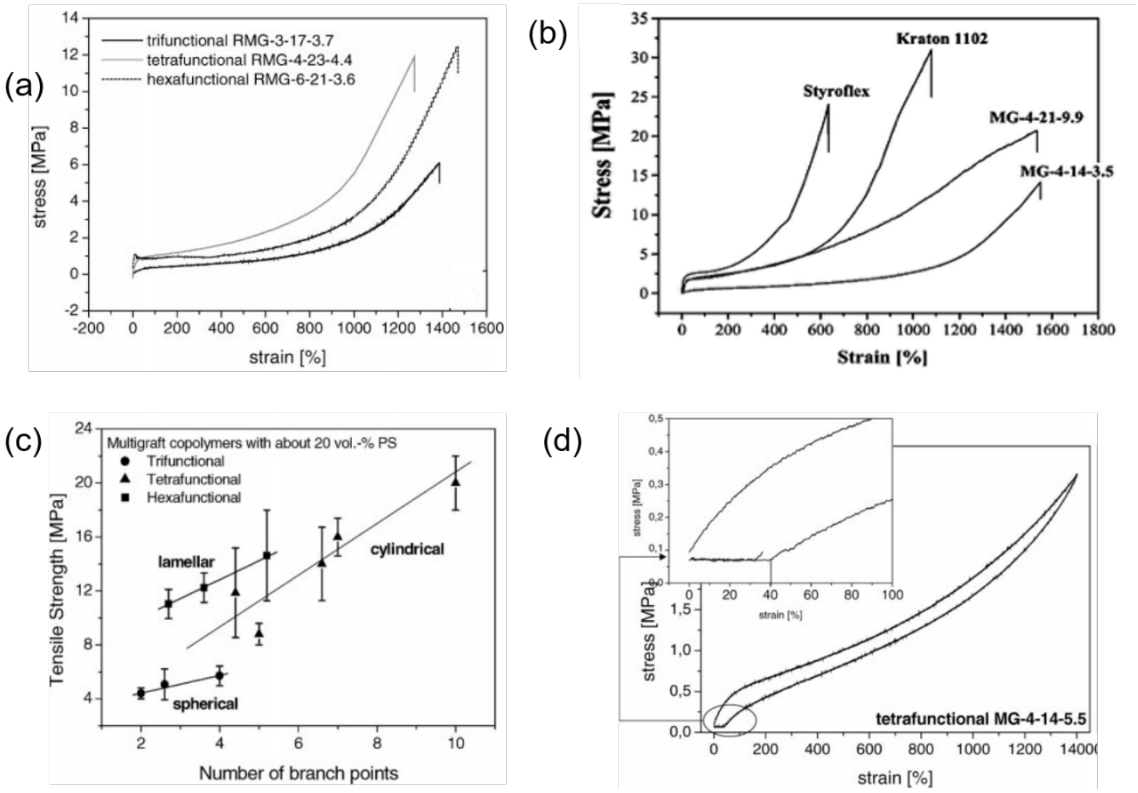

Figure 1-13. Mechanical properties of PI-g-PS multigraft copolymers. (a) Influence of functionality on stress-strain behavior. (b) Comparison of tetrafunctional multigraft copolymers (MG) with commercial SIS-block copolymer (Kraton®) and star copolymer (Styroflex®). (c) Influence of number of branchpoints on the tensile strength. (d) Hysteresis curve of a tetrafunctional multigraft copolymer.[83]

If not restricted to one polymerization method, the graft through methodology can give more versatile options on the synthesis of graft copolymers. Anionic polymerization can be used to make the macromonomers, followed by the copolymerization with the second monomer to build the final structure. Following this strategy, Schulz, et al. synthesized the PBA-g-PS graft copolymer as early as 1982.[85] The PS macromonomer was synthesized through anionic polymerization, endcapped by ethylene oxide and coupled with methacryloyl chloride. Then the macromonomer was copolymerized with nBA monomer by free radical polymerization. Similarly, PBA-b-PS,[86] PI-g-PS,[87] PBA-g-PMMA[88] were synthesized by anionic polymerization to make the macromomers and emulsion polymerization was used to make final copolymers.

In the case of all acrylic TPEs, the PMMA macromonomer can be synthesized by group-transfer polymerization,[89] anionic polymerization,[90] or free radical polymerization.[91] The resulting graft copolymers exhibited comparable mechanical properties to the linear all acrylic TPEs.[90]

1.4.4 Introducing Other Driving Forces

Thermoplastic elastomers were born with the mission to imitate and improve the behavior of vulcanized rubbers. The physical crosslinking behavior is critical to the final mechanical properties of the TPEs. Therefore, the introduction of other driving forces for the association of hard domains can help to increase the

microphase separation and physical crosslinking behavior, which can improve the mechanical properties of TPEs.

As mentioned in section 1.3.2, when isotactic PMMA is introduced, the crystallinity of the hard segment can contribute to the enhancement of the association force inside the hard segments, which in return, can greatly increase the UST, making it even much higher than the T_g of the hard segments.[53]

Analogous to the ionomeric thermoplastic elastomer, when an ionic bond is added to the existing TPEs, the mechanical performance can be modified. Barra and co-workers modified the commercial SEBS by partial sulfonation of the PS domain.[92] Unfortunately, with the increase of sulfonation degree, the mechanical properties were diminished rather than improved. With the sulfonation degree at 8.4%, the tensile stress did not show great change, but the elongation decreased from 800.9% to 720.1%. The further increase of sulfonation degree made the material more brittle, so that less tensile stress and elongation at break was observed. On one hand, the strong ionic bonds exist inside the polymer; on the other hand, the modification greatly increases the glass transition temperature of the hard segment. The strong effect of these two forces dramatically changes the stiffness of the material. It is obvious that the modification increases the mechanical strength at the same strain, but the brittleness of the material makes it impossible to observe the stress at the same degree of elongation at break due to the loss of elastomeric properties.

Hydrogen bonding is another potential force for the modification of TPEs. The study of hydrogen bonding mainly focuses on polymers like polyureas, polyurethanes, etc., which have very strong intermolecular interactions. Söntjens et al. reported poly(propylene adipate) with a 2-ureido-4-[1H]-pyrimidinone (UPy) in the middle of the chain. Even only one unit of UPy can be an efficient hard segment that is physically crosslinked by the strongly dimerizing, for which the hydrogen bonds exist between the UPys.[93] Chen et al. reported the synthesis of PS-g-polyacrylate amide, for which the amide group can form the hydrogen bonding. Although the resulting polymer cannot be strictly defined as a TPE due to the lack of soft domains, it also exhibited the improvement of toughness caused by the hydrogen bonding formation.[94] In addition, this work gives the hint that a simple modification of the hard segment with the functional groups can help to tune the performance.

The use of (meth)acrylate acid can take advantage of both forces mentioned above. In the acidic or neutral condition, the hydrogen bonding can form between the carboxyl groups. While in the basic condition, the ionic bonds can form to improve the physical crosslinking between the polymer chains. With this principle, the carboxylic rubber composed of polybutadiene and poly(methacrylic acid) was reported.[95] With the treatment of NaOH, the tensile strength was increased from around 700 KPa to 12 MPa, while with the treatment of ZnO, the strength was even increased to 41 MPa, reflecting the strong coordination between

the carboxyl group with Zn. However, the elongation was sacrificed in this modification from 1600% to 900% (NaOH treatment), and 400% (ZnO treatment). In addition, the power of metal ligand interaction can be observed in this work.

In conclusion, many intermolecular interactions can be considered for the modification of TPEs. The rather strong interactions can normally dramatically increase the mechanical strength, but the elongation is normally decreased. Prudent consideration of the driving force selection and modification degree is essential to get the optimized performance. On the other hand, the strong interactions also potentially impart self-healing properties to the materials, due to their reversible characteristics.[94]

1.5 Characterization Methods for TPE

1.5.1 Thermal Characterization

As the root cause of TPE's mechanism, it is always critical to characterize the thermodynamic mismatch of different segments, no matter if it is from the difference of glass transition temperature or the existence of crystallinity. The thermal characterization offers a great approach to identify the mismatch. In addition, the evaluation of service temperatures is also essential through the thermal characterization. Herein, we will focus on the TPEs based on T_g difference, and briefly introduce three frequently used thermal characterization methods,

including differential scanning calorimetry (DSC), thermomechanical analysis (TMA), and dynamic mechanical analysis (DMA).

In definition, glass transition is a transition from a liquid state to a solid state. It points out the sharp changes of the temperature dependence of many properties, including volume, entropy, elastic constants, etc. However, another transition termed as melting point, which is commonly observed in a crystalline polymer, is quite different to the glass transition. If a polymer has both amorphous and crystalline domains, both the glass transition temperature (T_g) and melting point (T_m) can be observed. As shown in **Figure 1-14**, when a sample is heated, the change of specific volume at T_g is slow rather than a sharp change of slope at T_m.[45]

As a simple and yet powerful thermal analytical technique, DSC is widely used in various fields to identify the physical and chemical properties. As the sample is heated or cooled, the absorbed or released energy of the material is monitored, by the comparison with the standard. In this way, different DSC curves can be observed depending on different transition types, as shown in **Figure 1-15**. The value of T_g is normally noted as the middle of the incline in the curve.

TMA is a measurement that studies free volume change of a material under a constant load as a function of temperature. The phase change of the sample with an applied force, whether expansion or contraction, is monitored by the function of time or temperature. The plot of this change versus temperature can be obtained and give the information of the sample, such as T_g, the coefficient of thermal

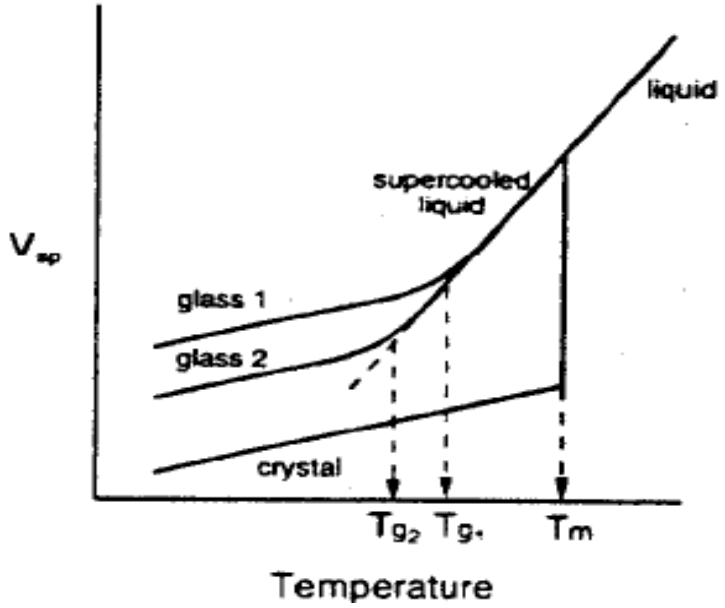

Figure 1-14. Temperature variations of specific volume at T_g and T_m.[45]

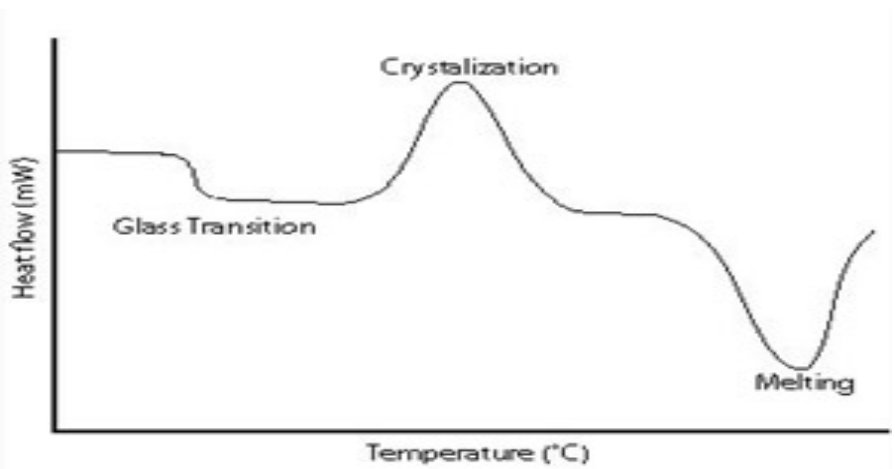

Figure 1-15. Features of different DSC curves.

expansion, service temperature and Young's modulus.[96]

The typical TMA curve is shown in **Figure 1-16**. The T_g corresponds to the expansion of the free volume allowing the great chain mobility above the transition. Similar to that in DSC, this transition is normally a slow change of the slope instead of the sharp curve. Thus the middle of the incline is also used as the value.

DMA, also referred to as dynamic mechanical thermal analysis (DMTA), is a powerful technique that can be used to characterize the mechanical properties as a function of temperature, time, frequency, stress, atmosphere, etc. It measures the material's response to a small deformation applied in a cyclic manner. Instead of the constant static force applied to the material in TMA, an oscillatory at a set frequency is normally used and many more parameters, such as stiffness a damping, can be reported.

In the case of temperature, the change of storage modulus (G') can be illustrated in **Figure 1-17**.[97] At Deformation C, the glass transition happens, where the modulus of the material experiences a sharp drop from glassy state to the rubbery state.

Different characterization methods normally give different but similar T_g values. Meanwhile, the result can also be affected by many factors. First, it was reported that the heating and cooling rate $|q|$ can influence T_g following the relation below:[98] In other words, higher rate of temperature change can lead to the increase of T_g.

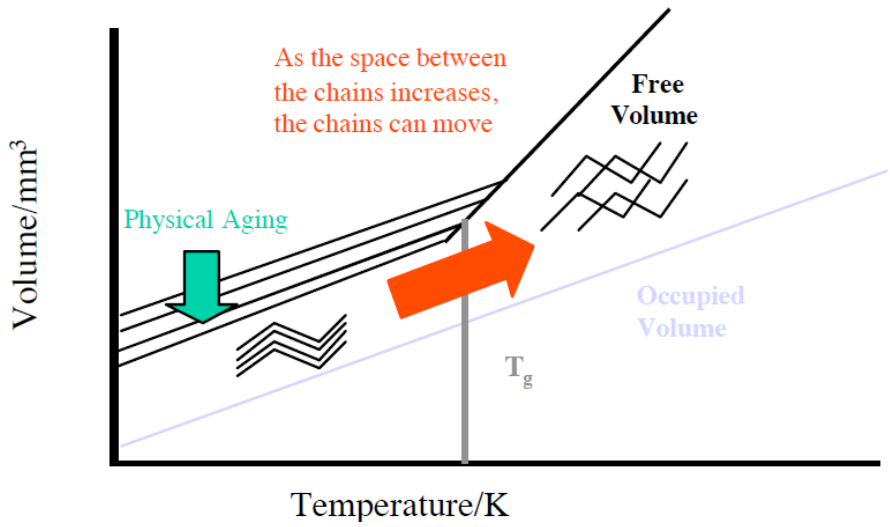

Figure 1-16. Illustration of the typical TMA curve.[99]

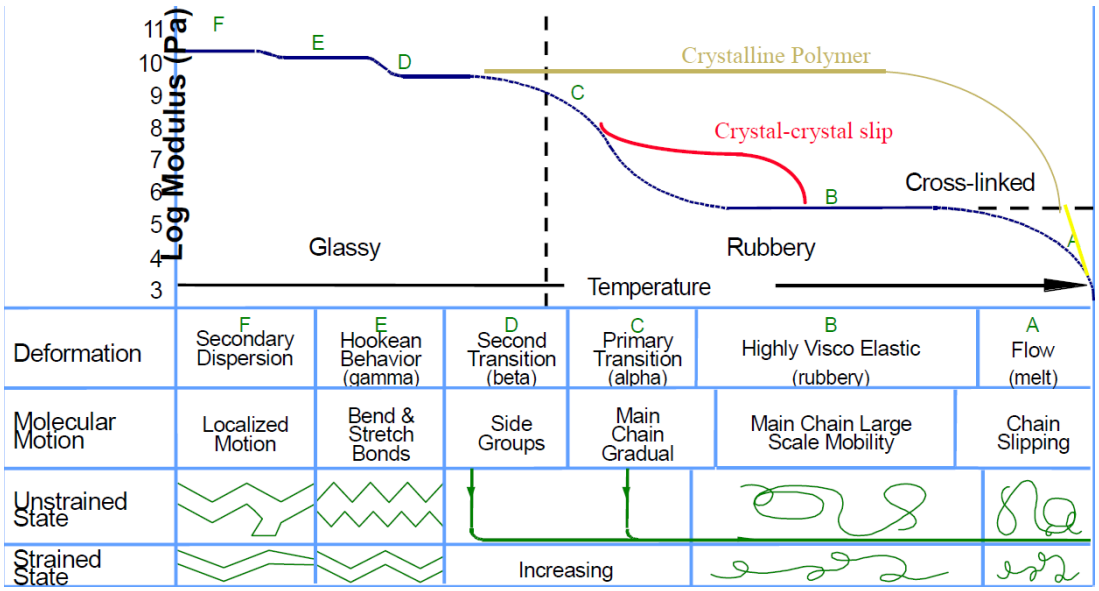

Figure 1-17. Modulus values changes with temperature and transitions in materials.[97]

$$\frac{d\ ln|q|}{d(^1/_{T_g})} = -\Delta h^*/R \quad (5)$$

The increase of pressure can also increase the T_g of the polymer, as shown in **Figure 1-18**.[100]

The use of thermal characterization gives the circumstantial evaluation on the microphase separation behavior. With phase separated materials, two different transitions can be observed,[101] while the phase blending materials give only one T_g. When compared to those of homopolymers, the shift of T_gs can be used to qualitatively evaluate the miscibility of two domains. The larger the T_gs are shifted compared to those in homopolymers, the more th domains are miscible with each other.

1.5.2 Phase Separation Behavior

As discussed in Section 1.1.1, the visualization of the morphology from microphase separation can help to understand the relationship between physical crosslinking behavior and its influence on the mechanical property.

The morphology effect on the mechanical properties cannot be isolated from the ratio of the glassy domain, since these two factors are always related. With different ratios of the glassy domains, different morphologies can be exhibited, and the mechanical properties can also be affected. For instance, with similar total molecular weight, the lamellae morphology shows much better stress and strain behavior as compared to cylindrical and spherical morphologies (**Figure 1-19**).[102]

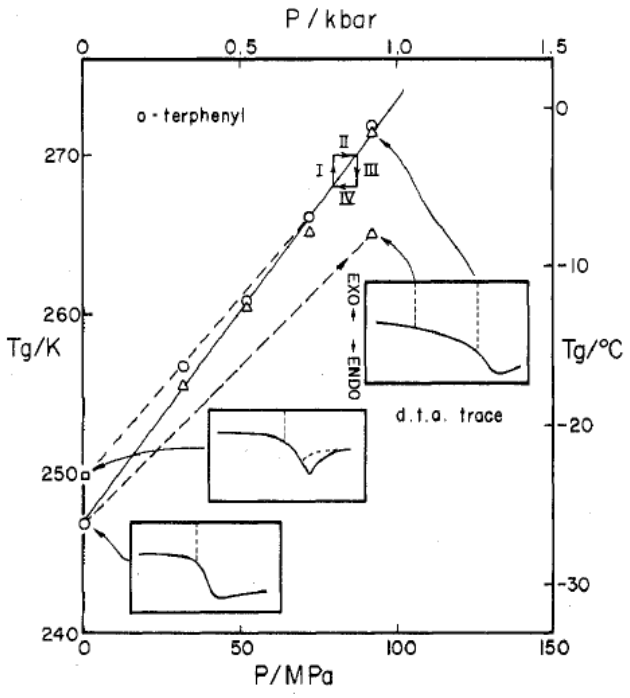

Figure 1-18. The values of T_g and shapes of DSC thermograms for different pressure change-temperature change sequences.[100]

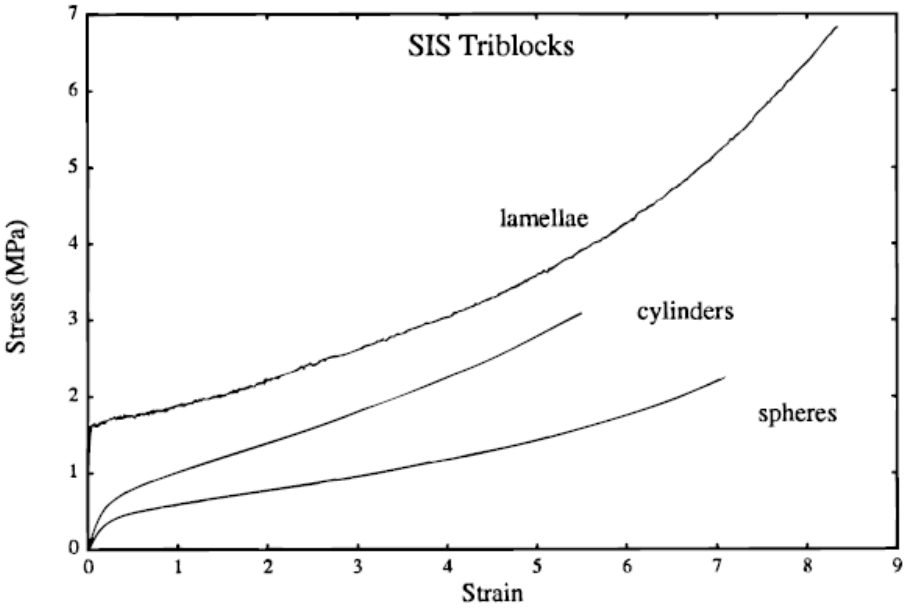

Figure 1-19. Stress-strain curves for SIS triblock copolymers. Sphere: wt% of PS 0.18, molecular weight 10-89-10. Cylinders: wt% of PS 0.30, molecular weight 14-66-14. Lamellae: wt% of PS 0.45, molecular weight 22-29-22.[102]

Among these, the cylinder morphology is most commonly seen in commercial products. (wt% of PS: 20 – 30).

Various techniques can be used to investigate the morphology of TPEs, including atomic force microscopy (AFM), small angle X-ray scattering (SAXS), and transmission electron microscopy (TEM).

Initially invented to observe surface structures at the atomic scale, atomic force microscopy (AFM) has been a multifunctional technique suitable for characterization of topography, adhesion, mechanical, and other properties on scales from hundreds of microns to nanometers.[103] The schematic operation of AFM is illustrated in **Figure 1-20**. There are two common modes for AFM: contact mode and tapping mode. For the former mode, the tip apex is in continuous contact with the surface when imaging is performed; for the latter case, the tip is in intermittent contact with the sample, and the probe is driven into an oscillation at its resonant frequency by a small piezoelectric element. Although the contact mode can give higher resolution and more quantitative characterization, high tip-to-sample forces, especially the presence of lateral forces often cause mechanical deformation of the surface, which makes it not suitable for soft materials like polymers and biological samples. The tapping mode, on the other hand, has been widely used for these applications.[104,105]

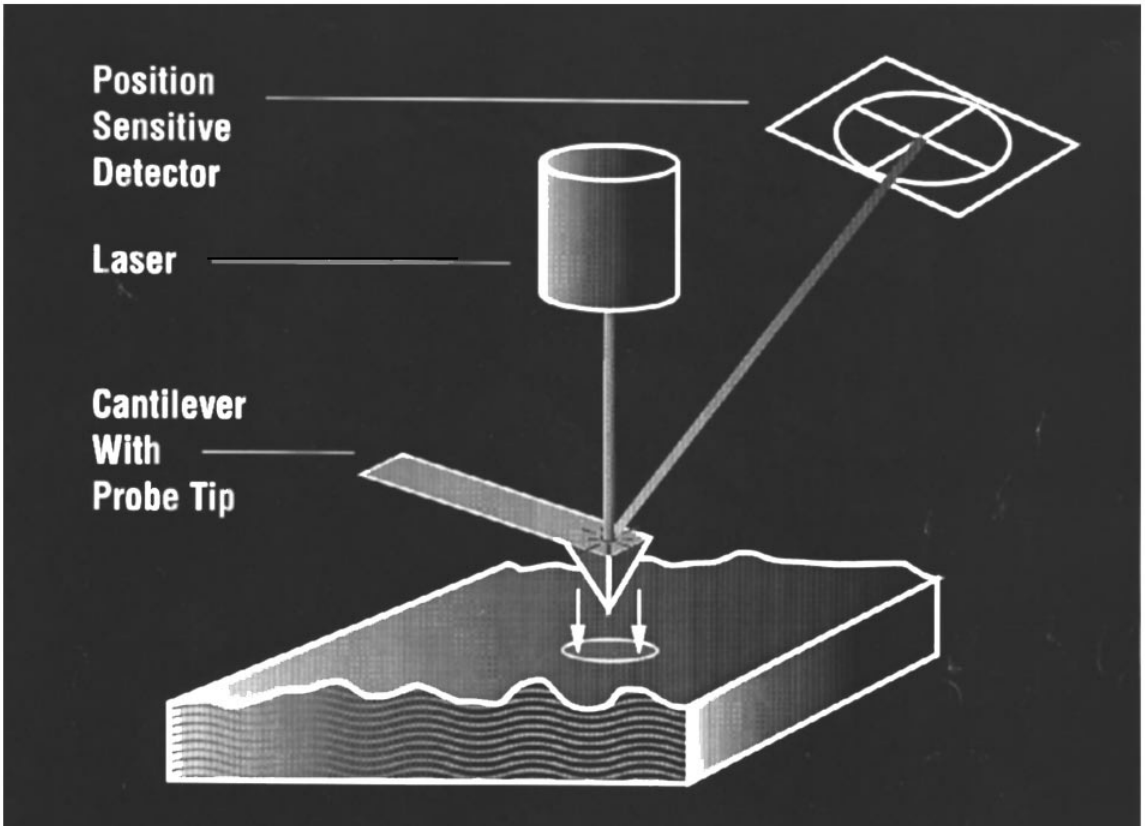

Figure 1-20. Schematic operation of AFM.[103]

Different images can be acquired from the tapping mode AFM, for which the mainly used are height images and phase images. The conventional height images are not necessarily reflecting the surface topography of the sample due to the large influence of tip-sample interactions. The roughness of the surface can usually produce “artifact phantom”.[106] Meanwhile, although this effect also exists in phase images, they are more sensitive to the viscoelasticity of the sample, which can be used for the differentiation of different regimes of the material. The quantitative study on the elasticity and viscoelasticity of the polymer sample using tapping mode AFM has also been reported. With different stiffness of the polymer, the sharpness of the tip should be considered for accurate observation.[107] For the micro-phase separated sample, the stiffness of the sample can cause the change in the phase angle of the probe oscillation: with the increase of the surface stiffness, the phase angle increases. In other words, the bright regions of the phase image represent the stiff domains, while the dark regions represent the soft domains.[108]

Small-angle X-ray scattering (SAXS) is another technique that is commonly used to study the phase separation behavior of the block copolymer systems either in the solid state or in solutions. Its resolution, ranging of 1-100 nm, is ideally fit for the domain size of the morphology formed.[109] Different information on the polymer samples, including radius of gyration, surface per volume, molecular weight, particle structure, polydispersity, morphology formed, and particle interactions can be acquired.[110]

The prototype of a SAXS instrument can be illustrated as shown in **Figure 1-21**. Multiple SAXS peaks can be observed depending on the microdomain structure formed in block copolymers. By the calculation of specific spatical relationships, the type of the morphology can be determined. For instance, for lamellae, the ratio of the q values is 1, 2, 3, 4,…; for cylinders, it will be $1, \sqrt{3}, \sqrt{4}, \sqrt{7}, \ldots$; for spheres in a body-centered cubic array, the ratio will be $1, \sqrt{2}, \sqrt{3}, \sqrt{4}, \ldots$. [109] The lattice spacing of the microdomain can be calculated based on the equation below:

$$d = \frac{2\pi}{q_{min}} \quad \textbf{(6)}$$

where q_{min} is normally the q value of the first peak.

The transmission electron microscope (TEM) has been an essential and vital tool to study the morphology of polymers for decades. Two contrast mechanisms exist that produce the final image. For a polymer with high crystallinity, the contrast is caused by crystal orientation, or density due to the presence of heavy elements. Bragg diffraction and Rutherford scattering can be induced, which can cause the relatively high angle scattering of incident electrons, so that the crystallinity or heavy regions will be dark in a final image. (**Figure 1-22 a**) More commonly, in the case of amorphous materials, the rich valence electron structure can introduce spatial modulations in the phase or energy of incident electrons. (**Figure 1-22 b**). [111]

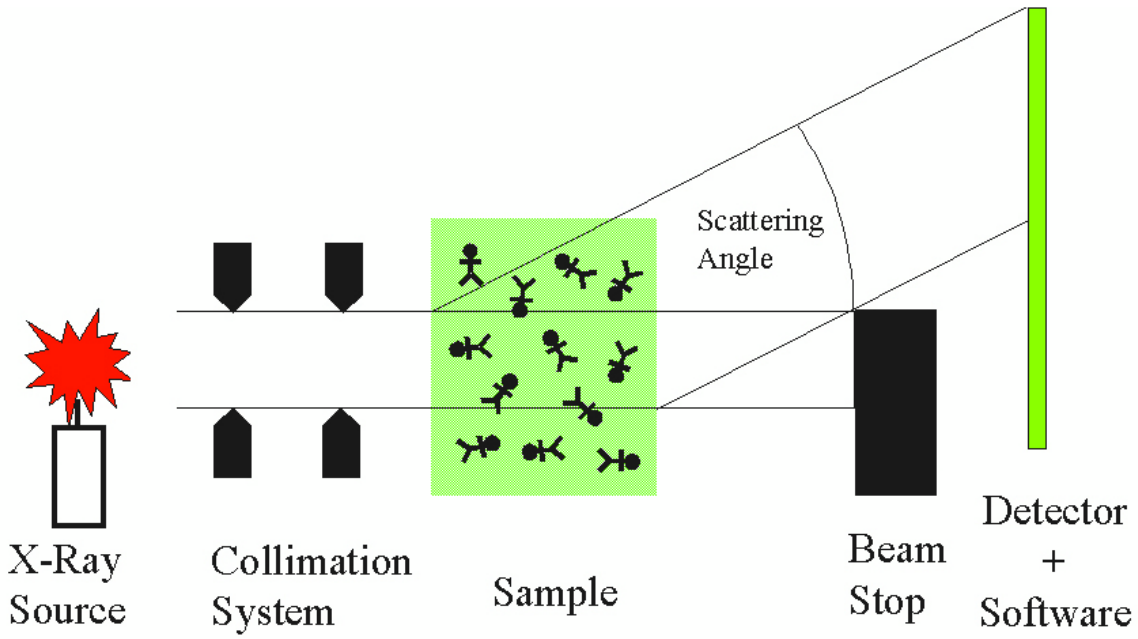

Figure 1-21. The components of a SAXS instrument.[110]

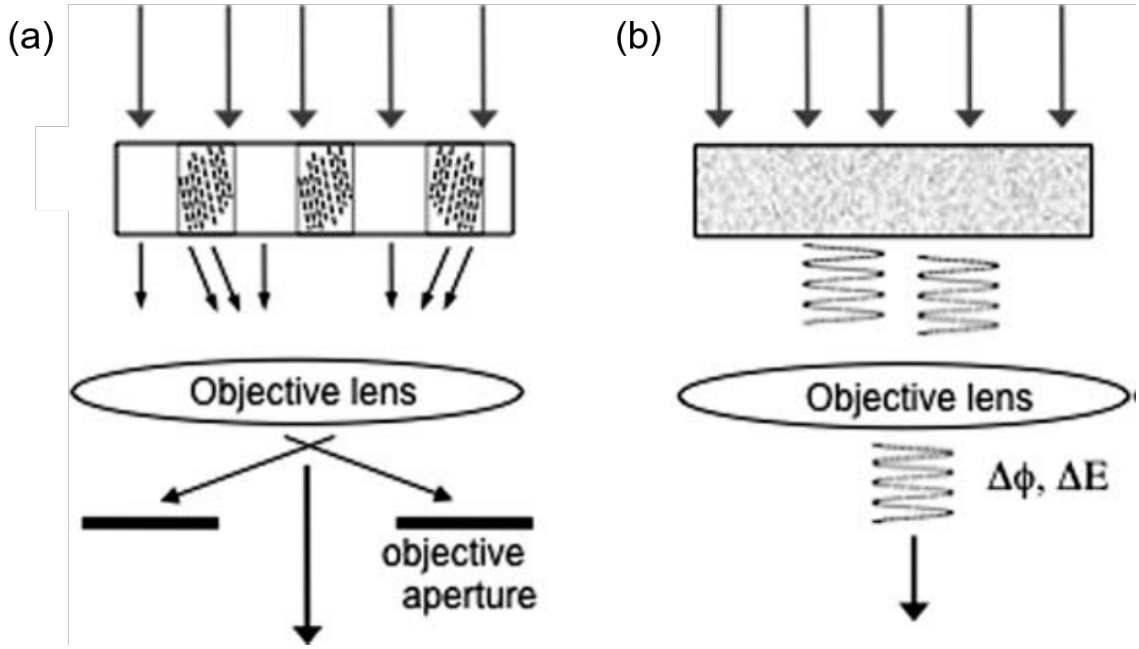

Figure 1-22. Contrast mechanisms of TEM: a) for polymers with crystallinity or heavy element; b) for amorphous soft materials with small variations in density. [111]

TEM is one of the most commonly used techniques to investigate phase separation behavior, with high resolution and direct observation on the formed morphology. However, to form the image with good contrast, complex sample preparation procedures are inevitable, like the microtoming of the sample to produce very thin films and heavy element staining to induce contrast. Moreover, the strong incident ionizing radiation may also damage to the specimen, particularly in unstained materials.

Similarly, AFM can also offer a direct observation of morphology. No expensive and complex sample preparation is needed. More complete information can be obtained from the cross-sectional samples, rather than the two-dimensional profiles in TEM. The other side of the coin of AFM is the limited size of the image, with only about 150×150 micrometers, as compared to square millimeters for TEM. Besides, the scanning speed of an AFM is also much slower. The hysteresis of the piezoelectric materials and the interactions between the cantilever and the sample surface can also cause possible artifacts, which require the filtration and flattening of the image.

SAXS, on the other hand, provides the indirect study on the phase separation behavior. Compared to TEM and AFM which normally study the local surface and details, SAXS can study global parameters and distribution. In situ transitions can be studied during the measurement, and no destructive/artifacts are caused.

In summary, different characterization methods have their merits and drawbacks, which are complementary to carry out a thorough study on the phase separation behavior. SAXS is necessary to obtain significant sampling and make quantitative statements, while TEM or AFM can give the direct observation of the morphologies.

1.5.3 Stress-Strain Behavior

One of the most commonly used and important standards on the performance of a TPE material is the stress-strain curve, which can be measured by the uniaxial tensile test of the sample in specific shape like a dog-bone. The comprehensive illustration on the stress-strain plot of the polymer materials is shown in **Figure 1-23**. For plastic materials that behave elastically and recover to their original dimensions with the applied force, Hook's law of elasticity is followed as $F = -kx$, where F is the restoring force, and x is the displacement of the material. This type of Hookean materials shows the stress-strain behavior like that in **Figure 1-23 (a)**. However, the curve only applies for very stiff materials like steels. For polymers, especially when they are elastomeric, the non-Hookean curve in **Figure 1-23 (a)** is more representative, where the relationship between stress and strain is not linear.[112] As the thermoplastic elastomers have both stiff and elastomeric components, stress-strain curves such as that in **Figure 1-23 (b)** are more common, taking SBS as an example.[6] With low strain, the sample is stretched and behaves like a plastic. The deformation is reversible and

proportional to the stress, the tensile modulus at this linear region is called Young's modulus (E), and can be expressed by $E = \frac{\sigma}{\varepsilon}$, where σ is the stress and ε is the strain. A rubbery plateau can be observed afterward, where the stress increases slightly or even keeps constant with the increase of stain until a certain degree. When a certain strain is reached, the crosslink junctions start to respond to the stress. Thus strain hardening behavior makes the stress increase extensively until the breaking point of the material.[8]

The stiffness/elongation of the TPEs can be easily tuned by the composition between hard and soft segments. When the content of the hard segments is large enough, the elongation of the material can be greatly affected. The yield point can be observed, beyond which the deformation of the material cannot return to its original shape and the recovery ability is permanently damaged. (**Figure 1-23 (b)**, with styrene content as 80%, 65% and 53%). On the other hand, the strain hardening behavior cannot be observed if the content of the hard segments is too small. Thus, the mechanical strength of the material is limited. (**Figure 1-23 (b)**, with styrene content as 13%).

Experimentally, the stress-strain curve can be influenced by measuring conditions and sample preparation methods. The thermal history can influence the tensile strength of the sample, especially for polymers with high ratio of hard segments. Instead of the annealing process, the fast cooling rate will lead to the inhomogeneous distribution of the material in the mold, and even bring micro-

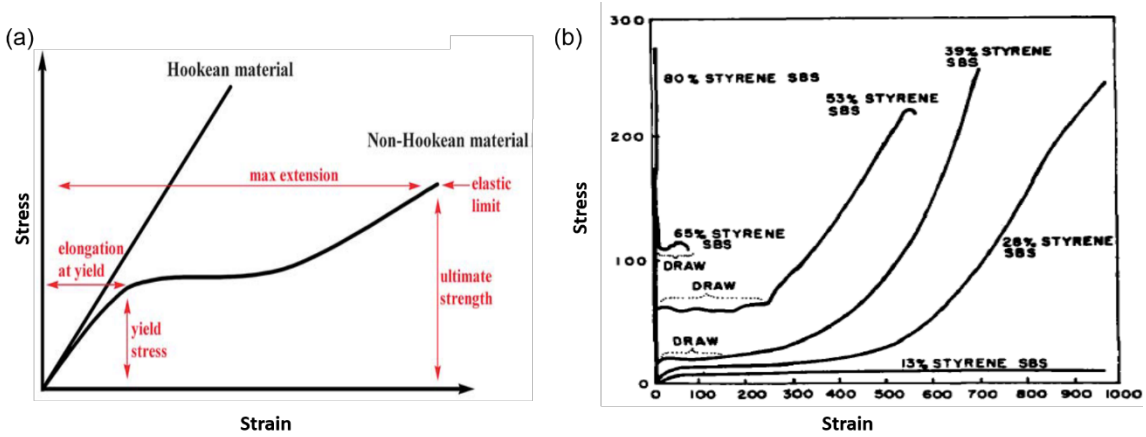

Figure 1-23. Illustration of stress-strain plots for (a) typical Hookean and non-Hookean materials, [112] and (b) TPEs like SBS.[6]

ruptures, which can be observed by viewing the polymer film with polarized light.[113] As a result, the final stress and strain can be limited. On the contrary, this effect is not so distinct for the TPEs with low hard segment content. The soft matrix can easily flow and flexible that makes the resulting film homogenous. In addition, the size of the specimens tested can also affect the stress-strain behaviors. It was observed that the strength increased as the specimen size decreased. It is speculated that the smaller specimens have a lower probability of having large flaws.[114] In summary, other than inherent flaws that are inevitable and homogeneously distributed, the mild and homogenous preparation of the measured samples, such as the annealing process and making specimens with no apparent flaws, can contribute to the premized and reliable stress-strain curves. It also needs to be noticed from the influence of thermal history and specimen size that measured stress-strain curves should always be accompanied by the detailed preparation methods. Various independent tests should be performed to get reliable and consistent results.

In the case of measuring conditions, the stress-strain curve can be greatly influenced by both the temperature and strain rate. As illustrated in **Figure 1-24(a)**, the strain hardening cannot be observed in monodisperse polymer melts. However, as the polymer composed of different segments, this phenomenon is quite common, as discussed previously. Different types of strain hardening exist, including stress growth ending with the breakup of a sample (**Figure 1-24(b)**),

growth for which a second plateau is observed (**Figure 1-24(c)**), and behavior with a maximum in the tensile growth coefficient (**Figure 1-24(d)**).[115] For any of these cases, with the low deformation rates, the viscous deformation prevail and very large stains are possible, even without showing the strain hardening behavior. When the deformation rates are increased, the competition between viscous flow and elastic deformation occurs and the final stresses are increased, with the loss of elongations.

The temperature influences the stress-strain curve in a similar manner. As shown in **Figure 1-25**, two SBCS, Kraton 101 and Thermolastic 226 were tested at different temperatures. With lower temperature, higher stress was observed, with the less elongation.[116] It is easy to understand that the lower temperature can normally make the polymer stiffer. Thus, the elongation of the sample is sacrificed, but the mechanical strength is reinforced. On the other hand, as discussed in Section 1.3, the rubbery plateau can be observed from DMA, where the storage modulus of TPEs does not have apparent change. When the measuring temperatures fall in the range of the rubbery plateau, Young's modulus observed will not change, and the influence of the temperature on the final mechanical property is also limited.

The similarity of the influences of strain rates and temperature have been summarized as the illustration in **Figure 1-26**.[117] In brief, both the increase of strain rate and the decrease of temperature can lead to higher stress and lower strain.

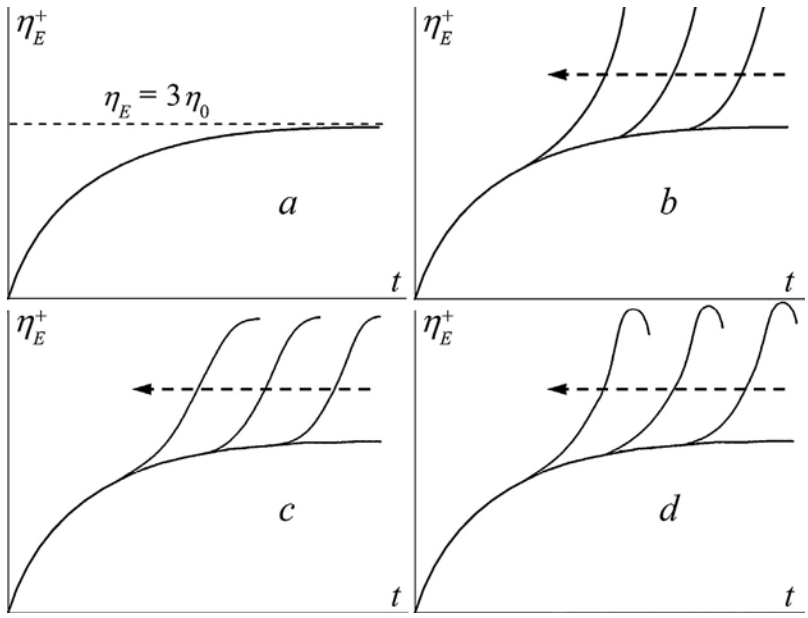

Figure 1-24 Schemes illustrating development of the tensile growth stress and strain hardening behavior with different strain rates. Arrows show the direction of increasing strain rates.

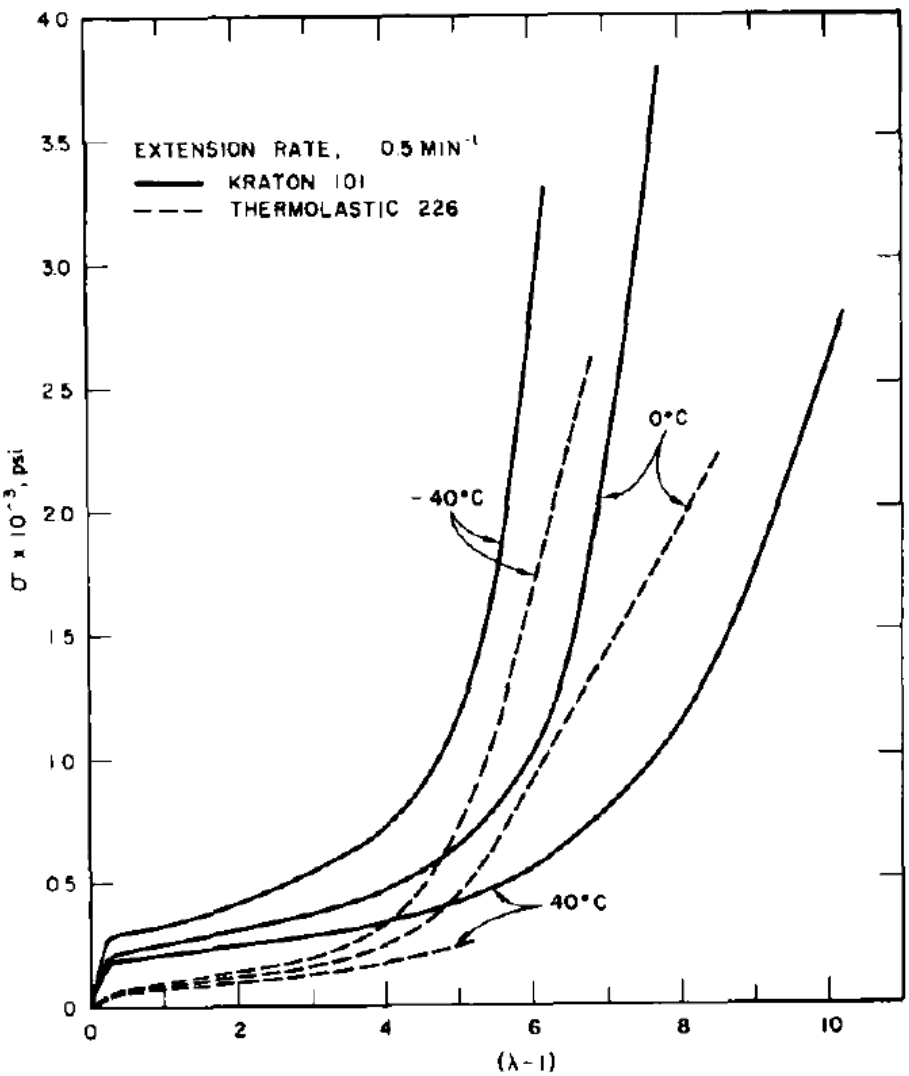

Figure 1-25. Stress-strain curves for Kraton 101 and Thermolastic 226 at -40, 0, 40 °C.[116]

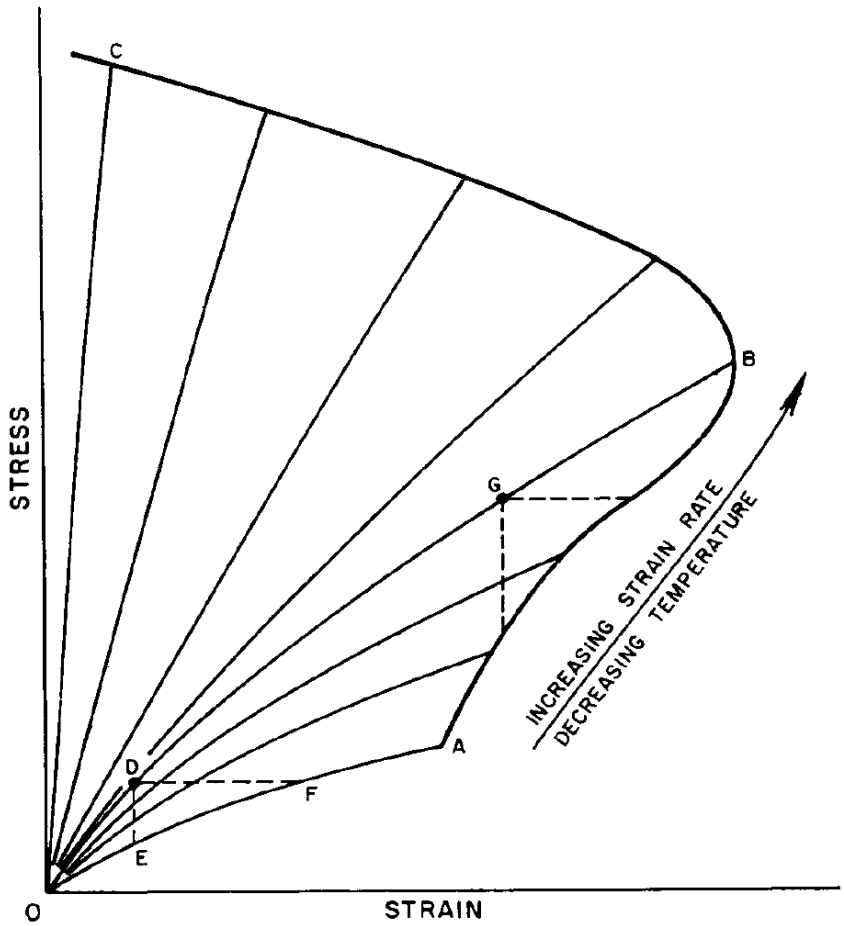

Figure 1-26. Schematic representation of the dependence of stress-strain curves on strain rate and temperature.

This is a perfect example to reflect the time-temperature superposition, which is commonly used for analysis of viscoelastic properties of polymers. It can be illustrated by the Williams-Landel-Ferry (WLF) equation:[118]

$$\log a_T = \log\left(\frac{\omega_1}{\omega_2}\right) = \frac{C_1(T-T_S)}{C_2+(T-T_S)} \quad \textbf{(7)}$$

where $\boldsymbol{a_T}$ is the shift factor. $\boldsymbol{\omega}$ is the relaxation rate (time related), and T is the temperature.

1.6 The Scope of this Thesis

With many advantages over the traditional styrenic based thermoplastic elastomers including chemical stability, optical transparency, versatility of adhesion, weatherability, oil resistance, printability, compatibility with fillers, abrasion resistance and low viscosity,[17,18] all acrylic based thermoplastic elastomers (TPEs) are recognized as the promising candidate for the next generation of TPEs with advanced properties and performances. The work on this thesis will focus on the synthesis and characterization of different types of all acrylic based TPEs. Based on the discussion in Chapter 1, different methodologies will be applied to explore their influences on the mechanical performance of the materials synthesized, including the selection of monomers, the design of complex architectures and the introduction of extra driving forces.

Chapter 2 introduces the synthesis, characterization and solution properties of poly(1-adamantyl acrylate) (PAdA)—a kind of polyacrylate with high glass transition temperature and extraordinary thermal stability. In this chapter, the anionic polymerization of adamantyl acrylate monomer was investigated and it resulted in polymer products with predicted molecular weights, narrow PDIs, quantitative yields and distinct living property. The PAdAA homopolymers exhibit a very high glass transition temperature (132.8 ^{o}C) and outstanding thermal stability (Td: 376 ^{o}C) as compared to other acrylic polymers such as poly(tert-butyl acrylate) and poly(methyl acrylate). Furthermore, the study on the solution properties of PAdA provides further understanding of the chain rigidity and the unperturbed dimensions of the polymer. The solubility of PAdA in different solvents was also evaluated to explore the theta condition of the polymer solutions.

The distinct thermal properties and chain rigidity make PAdAA a promising candidate for acrylic based thermoplastic elastomers with high upper service temperature and enhanced mechanical strength. The investigation on this application is reported in Chapter 3. This all acrylic based triblock copolymer is compsed of PAdA as the hard segment and poly(tetrahydrofurfuryl acrylate) as the soft segment. The influence of molecular weight, ratios of each segment, phase separation behaviors on the final performance of the resulting TPEs are discussed in this chapter. After the optimization, the combination of these two acrylic based

segments leads to the material with higher upper service temperature and better mechanical strength than the current commercial products.

In Chapter 4, the other useful strategy to improve the performance of TPEs is carried out, that is the design of complex structures. By using n-isopropyl-4-vinylbenzylamine (PVBA) as the initiator, the poly(methyl methacrylate) (PMMA) macromonomer is synthesized through living anionic polymerization. As compared to conventional approaches, the macromonomer is synthesized in one batch with 100% conversion, short reaction time and much simpler operations. Thereafter, the graft copolymer of poly(n-butyl acrylate)-graft-poly(methyl methacrylate) (PBA-g-PMMA) is synthesized using graft through methodology by RAFT copolymerization of n-butyl acrylate monomer with the PMMA macromonomer. By the combination of large molecular weight beyond the entanglement molecular weight and improved phase separation behaviors, the resulting TPE exhibited exceptional mechanical properties, especially with the elongation at break higher than 1500%. This makes the material much superior to the current commercial acrylic based TPEs and even comparable to styrenic based multigraft copolymers.

In Chapter 5, other potential modifications of these kind of materials are discussed. Further driving forces are introduced to the graft copolymers of poly(n-butyl acrylate)-g-poly(tert-butyl methacrylate) (PBA-g-PtBMA), including hydrogen bonding, ionic bonds, and coordination interactions.

In addition, as a powerful initiator, the further possible uses of PVBA to build complex architectures have also been discussed and predicted.

References

(1) Thermoplastic Elastomers (TPE) Market Size By Product (Thermoplastic Polyurethanes [TPU], Styrenic Block Copolymers [SIS, SBS, SBC, HSBC], Thermoplastic Vulcanizates [TPV], Copolyester Elastomers [COPE], Thermoplastic Polyolefins [TPO]), By Application (Footwear, Automotive, Medical, Construction, Industrial, Advanced Materials, Electronics), Industry Analysis Report, Regional Outlook (U.S., Germany, UK, France, Italy, China, India, Japan, Brazil), Application Potential, Price Trend, Competitive Market Share & Forecast, 2016 - 2023. *Global Market Insights* **2016**, 230.

(2) Drobny, J. G.: *Handbook of thermoplastic elastomers*; Elsevier, 2014.

(3) Holden, G.: Thermoplastic Elastomers. In *Kirk-Othmer Encyclopedia of Chemical Technology*; John Wiley & Sons, Inc., 2000.

(4) Bates, F. S.; Fredrickson, G. Block copolymers-designer soft materials. *Physics today* **2000**.

(5) Matsen, M. W.; Thompson, R. Equilibrium behavior of symmetric ABA triblock copolymer melts. *The Journal of chemical physics* **1999**, *111*, 7139-7146.

(6) Holden, G.; Bishop, E. T.; Legge, N. R. Thermoplastic elastomers. *Journal of Polymer Science Part C: Polymer Symposia* **1969**, *26*, 37-57.

(7) Handlin, D. L.; Trenor, S.; Wright, K.: Applications of Thermoplastic Elastomers Based on Styrenic Block Copolymers. In *Macromolecular Engineering*; Wiley-VCH Verlag GmbH & Co. KGaA, 2007; pp 2001-2031.

(8) Aoyagi, T.; Honda, T.; Doi, M. Microstructural study of mechanical properties of the ABA triblock copolymer using self-consistent field and molecular dynamics. *The Journal of Chemical Physics* **2002**, *117*, 8153-8161.

(9) Bailey, J.; Bishop, E.; WR, H.; Holden, G.; Legge, N. Thermoplastic Elastomers-Physical Properties and Applications. *Rubber Age* **1966**, *98*, 69-&.

(10) Séguéla, R.; Prud'homme, J. Effects of Casting Solvents on Mechanical and Structural Properties of Polydiene-Hydrogenated Polystyrene-Polyisoprene-Polystyrene and Polystyrene-Polybutadiene-Polystyrene Block Copolymers. *Macromolecules* **1978**, *11*, 1007-1016.

(11) Legge, N. R. Thermoplastic Elastomers. *Rubber Chemistry and Technology* **1987**, *60*, 83-117.

(12) Kaszas, G.; Puskas, J. E.; Kennedy, J. P.; Hager, W. G. Polyisobutylene-containing block polymers by sequential monomer addition. II. Polystyrene–polyisobutylene–polystyrene triblock polymers: Synthesis, characterization, and physical properties. *Journal of Polymer Science Part A: Polymer Chemistry* **1991**, *29*, 427-435.

(13) Yu, Y.; Dubois, P.; Teyssié, P.; Jérôme, R. Difunctional Initiator Based on 1,3-Diisopropenylbenzene. 6. Synthesis of Methyl

Methacrylate−Butadiene−Methyl Methacrylate Triblock Copolymers. *Macromolecules* **1997**, *30*, 4254-4261.

(14) Luo, Y.; Wang, X.; Zhu, Y.; Li, B.-G.; Zhu, S. Polystyrene-block-poly(n-butyl acrylate)-block-polystyrene Triblock Copolymer Thermoplastic Elastomer Synthesized via RAFT Emulsion Polymerization. *Macromolecules* **2010**, *43*, 7472-7481.

(15) Haloi, D. J.; Ata, S.; Singha, N. K.; Jehnichen, D.; Voit, B. Acrylic AB and ABA Block Copolymers Based on Poly(2-ethylhexyl acrylate) (PEHA) and Poly(methyl methacrylate) (PMMA) via ATRP. *ACS Applied Materials & Interfaces* **2012**, *4*, 4200-4207.

(16) Tong, J.-D.; Leclère, P.; Rasmont, A.; Brédas, J.-L.; Lazzaroni, R.; Jérôme, R. Morphology and rheology of poly (methyl methacrylate)-block-poly (isooctyl acrylate)-block-poly (methyl methacrylate) triblock copolymers, and potential as thermoplastic elastomers. *Macromolecular Chemistry and Physics* **2000**, *201*, 1250-1258.

(17) Oshita, S.; Chapman, B.; Hirata, K. Acrylic Block Copolymer for Adhesive Application. *PSTC Tape Summit 2012* **2012**.

(18) MORISHITA, Y. Applications of Acrylic Thermoplastic Elastomer. *Nippon Gomu Kyokaishi* **2013**, *86*, 321-326.

(19) Ritzenthaler, S.; Court, F.; Girard-Reydet, E.; Leibler, L.; Pascault, J. P. ABC Triblock Copolymers/Epoxy−Diamine Blends. 2. Parameters Controlling the Morphologies and Properties. *Macromolecules* **2003**, *36*, 118-126.

(20) Masson, F.; Decker, C.; Andre, S.; Andrieu, X. UV-curable formulations for UV-transparent optical fiber coatings: I. Acrylic resins. *Progress in Organic Coatings* **2004**, *49*, 1-12.

(21) Mori, T.; Hatori, Y.; Nodera, T.; Kawai, H.: Soft blends of polyurethane and acrylic polymer; automobile interiors, furniture. Google Patents, 2005.

(22) Oertel, J.; Kishii, S.; Kilian, D.; Hamada, K.; Morishita, Y.; Kurihara, T.; Ito, T. Acrylic TPE approaching automotive.

(23) Nakamura, Y.; Adachi, M.; Tachibana, Y.; Sakai, Y.; Nakano, S.; Fujii, S.; Sasaki, M.; Urahama, Y. Tack and viscoelastic properties of an acrylic block copolymer/tackifier system. *International Journal of Adhesion and Adhesives* **2009**, *29*, 806-811.

(24) Yu, J. M.; Jérôme, R.; Overbergh, N.; Hammond, P. Triblock copolymer based thermoplastic elastomeric gels of a large service temperature range: preparation and characterization. *Macromolecular Chemistry and Physics* **1997**, *198*, 3719-3735.

(25) Eckstein, A.; Suhm, J.; Friedrich, C.; Maier, R. D.; Sassmannshausen, J.; Bochmann, M.; Mülhaupt, R. Determination of Plateau

Moduli and Entanglement Molecular Weights of Isotactic, Syndiotactic, and Atactic Polypropylenes Synthesized with Metallocene Catalysts. *Macromolecules* **1998**, *31*, 1335-1340.

(26) Fetters, L. J.; Lohse, D. J.; Graessley, W. W. Chain Dimensions and Entanglement Spacings in Dense Macromolecular Systems. *Journal of Polymer Science Part B: Polymer Physics* **1999**, *37*, 1023-1033.

(27) Tong, J. D.; Leclère, P.; Doneux, C.; Brédas, J. L.; Lazzaroni, R.; Jérôme, R. Morphology and Mechanical Properties of Poly(methylmethacrylate)-b-Poly(alkylacrylate)-b-Poly(methylmethacrylate). *Polymer* **2001**, *42*, 3503-3514.

(28) Tong, J.-D.; Jerôme, R. Dependence of the Ultimate Tensile Strength of Thermoplastic Elastomers of the Triblock Type on the Molecular Weight between Chain Entanglements of the Central Block. *Macromolecules* **2000**, *33*, 1479-1481.

(29) Hadjichristidis, N.; Pispas, S.; Floudas, G.: *Block copolymers: synthetic strategies, physical properties, and applications*; John Wiley & Sons, 2003.

(30) Matyjaszewski, K. Controlled radical polymerization. *Current Opinion in Solid State and Materials Science* **1996**, *1*, 769-776.

(31) Moineau, C.; Minet, M.; Teyssié, P.; Jérôme, R. Synthesis and Characterization of Poly(methyl methacrylate)-block-poly(n-butyl acrylate)-block-poly(methyl methacrylate) Copolymers by Two-Step Controlled Radical

Polymerization (ATRP) Catalyzed by NiBr2(PPh3)2, 1. *Macromolecules* **1999**, *32*, 8277-8282.

(32) Jean-Marc Boutillier, J.-P. D., Mickael Havel, Raber Inoubli, Stephanie Magnet, Christian Laurichesse, and Daniel Lebouvier. Self-Assembling Acrylic Block Copolymers for Enhanced Adhesives Properties. *ASI Adhesives & Sealants Industry,* May 1 2013, 2013.

(33) Nicolas, J.; Charleux, B.; Guerret, O.; Magnet, S. Nitroxide-Mediated Controlled Free-Radical Emulsion Polymerization Using a Difunctional Water-Soluble Alkoxyamine Initiator. Toward the Control of Particle Size, Particle Size Distribution, and the Synthesis of Triblock Copolymers. *Macromolecules* **2005**, *38*, 9963-9973.

(34) Hadjichristidis, N.; Iatrou, H.; Pispas, S.; Pitsikalis, M. Anionic polymerization: High vacuum techniques. *Journal of Polymer Science Part A: Polymer Chemistry* **2000**, *38*, 3211-3234.

(35) Uhrig, D.; Mays, J. W. Experimental techniques in high-vacuum anionic polymerization. *Journal of Polymer Science Part A: Polymer Chemistry* **2005**, *43*, 6179-6222.

(36) Baskaran, D. Strategic developments in living anionic polymerization of alkyl (meth)acrylates. *Progress in Polymer Science* **2003**, *28*, 521-581.

(37) Ishizone, T.; Yoshimura, K.; Hirao, A.; Nakahama, S. Controlled Anionic Polymerization of tert-Butyl Acrylate with Diphenylmethyl Anions in the Presence of Dialkylzinc. *Macromolecules* **1998**, *31*, 8706-8712.

(38) Lu, W.; Huang, C.; Hong, K.; Kang, N.-G.; Mays, J. W. Poly(1-adamantyl acrylate): Living Anionic Polymerization, Block Copolymerization, and Thermal Properties. *Macromolecules* **2016**, *49*, 9406-9414.

(39) Wang, J. S.; Jerome, R.; Bayard, P.; Teyssie, P. Anionic Polymerization of Acrylic Monomers. 21. Anionic Sequential Polymerization of 2-Ethylhexyl Acrylate and Methyl Methacrylate. *Macromolecules* **1994**, *27*, 4908-4913.

(40) Raj, D. J. A.; Wadgaonkar, P. P.; Sivaram, S. Controlled synthesis of dicarboxyl-terminated poly (methyl acrylate) macromonomers using a new blocked carboxyl functional metal-free carbanionic initiator. *Macromolecules* **1992**, *25*, 2774-2776.

(41) Leclère, P.; Moineau, G.; Minet, M.; Dubois, P.; Jérôme, R.; Brédas, J. L.; Lazzaroni, R. Direct Observation of Microdomain Morphology in “All-Acrylic” Thermoplastic Elastomers Synthesized via Living Radical Polymerization. *Langmuir* **1999**, *15*, 3915-3919.

(42) Hamada, K.; Morishita, Y.; Kurihara, T.; Ishiura, K.: Methacrylate-Based Polymers for Industrial Uses. In *Anionic Polymerization*; Springer, 2015; pp 1011-1031.

(43) Tong, J. D.; Moineau, G.; Leclère, P.; Brédas; Lazzaroni, R.; Jérôme, R. Synthesis, Morphology, and Mechanical Properties of Poly(methyl methacrylate)-b-poly(n-butyl acrylate)-b-poly(methyl methacrylate) Triblocks. Ligated Anionic Polymerization vs Atom Transfer Radical Polymerization. *Macromolecules* **2000**, *33*, 470-479.

(44) Laurer, J. H.; Mulling, J. F.; Khan, S. A.; Spontak, R. J.; Bukovnik, R. Thermoplastic elastomer gels. I. Effects of composition and processing on morphology and gel behavior. *Journal of Polymer Science Part B: Polymer Physics* **1998**, *36*, 2379-2391.

(45) Hiemenz, P. C.; Lodge, T. P.: *Polymer Chemistry, Second Edition*; Taylor & Francis, 2007.

(46) Kraus, G.; Rollmann, K. W. Dynamic viscoelastic behavior of ABA block polymers and the nature of the domain boundary. *Journal of Polymer Science: Polymer Physics Edition* **1976**, *14*, 1133-1148.

(47) Alfonzo, C. G.; Fleury, G.; Chaffin, K. A.; Bates, F. S. Synthesis and Characterization of Elastomeric Heptablock Terpolymers Structured by Crystallization. *Macromolecules* **2010**, *43*, 5295-5305.

(48) Hucul, D. A.; Hahn, S. F. Catalytic Hydrogenation of Polystyrene. *Advanced Materials* **2000**, *12*, 1855-1858.

(49) Fetters, L. J.; Firer, E. M.; Dafauti, M. Synthesis and Properties of Block Copolymers. 4. Poly(p-tert-butylstyrene-diene-p-tert-butylstyrene) and Poly(p-tert-butylstyrene-isoprene-styrene). *Macromolecules* **1977**, *10*, 1200-1207.

(50) Fetters, L. J.; Morton, M. Synthesis and Properties of Block Polymers. I. Poly-α-methylstyrene-Polyisoprene-Poly-α-methylstyrene. *Macromolecules* **1969**, *2*, 453-458.

(51) Kobayashi, S.; Kataoka, H.; Ishizone, T.; Kato, T.; Ono, T.; Kobukata, S.; Ogi, H. Synthesis and Properties of New Thermoplastic Elastomers Containing Poly[4-(1-adamantyl)styrene] Hard Segments. *Macromolecules* **2008**, *41*, 5502-5508.

(52) Wang, W.; Schlegel, R.; White, B. T.; Williams, K.; Voyloy, D.; Steren, C. A.; Goodwin, A.; Coughlin, E. B.; Gido, S.; Beiner, M.; Hong, K.; Kang, N.-G.; Mays, J. High Temperature Thermoplastic Elastomers Synthesized by Living Anionic Polymerization in Hydrocarbon Solvent at Room Temperature. *Macromolecules* **2016**, *49*, 2646-2655.

(53) Yu, J. M.; Dubois, P.; Teyssié, P.; Jérôme, R. Syndiotactic Poly(methyl methacrylate) (sPMMA)−Polybutadiene (PBD)−sPMMA Triblock Copolymers: Synthesis, Morphology, and Mechanical Properties. *Macromolecules* **1996**, *29*, 6090-6099.

(54) Hadjichristidis, N.; Pitsikalis, M.; Pispas, S.; Iatrou, H. Polymers with Complex Architecture by Living Anionic Polymerization. *Chemical Reviews* **2001**, *101*, 3747-3792.

(55) Pochan, D. J.; Gido, S. P.; Pispas, S.; Mays, J. W.; Ryan, A. J.; Fairclough, J. P. A.; Hamley, I. W.; Terrill, N. J. Morphologies of Microphase-Separated A2B Simple Graft Copolymers. *Macromolecules* **1996**, *29*, 5091-5098.

(56) Braunecker, W. A.; Matyjaszewski, K. Controlled/living radical polymerization: Features, developments, and perspectives. *Progress in Polymer Science* **2007**, *32*, 93-146.

(57) Aoshima, S.; Yoshida, T.; Kanazawa, A.; Kanaoka, S. New stage in living cationic polymerization: An array of effective Lewis acid catalysts and fast living polymerization in seconds. *Journal of Polymer Science Part A: Polymer Chemistry* **2007**, *45*, 1801-1813.

(58) Yu, J.; Wang, J.; Wang, C.; Liu, Y.; Xu, Y.; Tang, C.; Chu, F. UV-Absorbent Lignin-Based Multi-Arm Star Thermoplastic Elastomers. *Macromolecular Rapid Communications* **2015**, *36*, 398-404.

(59) Jiang, F.; Wang, Z.; Qiao, Y.; Wang, Z.; Tang, C. A Novel Architecture toward Third-Generation Thermoplastic Elastomers by a Grafting Strategy. *Macromolecules* **2013**, *46*, 4772-4780.

(60) Knoll, K.; Nießner, N. In *Tilte*1998; Wiley Online Library.

(61) Dair, B. J.; Honeker, C. C.; Alward, D. B.; Avgeropoulos, A.; Hadjichristidis, N.; Fetters, L. J.; Capel, M.; Thomas, E. L. Mechanical Properties and Deformation Behavior of the Double Gyroid Phase in Unoriented Thermoplastic Elastomers. *Macromolecules* **1999**, *32*, 8145-8152.

(62) Michler, G. H.; Adhikari, R.; Lebek, W.; Goerlitz, S.; Weidisch, R.; Knoll, K. Morphology and micromechanical deformation behavior of styrene/butadiene-block copolymers. I. Toughening mechanisms in asymmetric star block copolymers. *Journal of Applied Polymer Science* **2002**, *85*, 683-700.

(63) Shi, W.; Lynd, N. A.; Montarnal, D.; Luo, Y.; Fredrickson, G. H.; Kramer, E. J.; Ntaras, C.; Avgeropoulos, A.; Hexemer, A. Toward Strong Thermoplastic Elastomers with Asymmetric Miktoarm Block Copolymer Architectures. *Macromolecules* **2014**, *47*, 2037-2043.

(64) Imaeda, T.; Hashimoto, T.; Irie, S.; Urushisaki, M.; Sakaguchi, T. Synthesis of ABA‐triblock and star‐diblock copolymers with poly (2‐adamantyl vinyl ether) and poly (n‐butyl vinyl ether) segments: New thermoplastic elastomers composed solely of poly (vinyl ether) backbones. *Journal of Polymer Science Part A: Polymer Chemistry* **2013**, *51*, 1796-1807.

(65) Juhari, A.; Mosnáček, J.; Yoon, J. A.; Nese, A.; Koynov, K.; Kowalewski, T.; Matyjaszewski, K. Star-like poly (n-butyl acrylate)-b-poly (α-methylene-γ-butyrolactone) block copolymers for high temperature thermoplastic elastomers applications. *Polymer* **2010**, *51*, 4806-4813.

(66) Jacob, S.; Kennedy, J. P. Synthesis and characterization of novel octa-arm star-block thermoplastic elastomers consisting of poly (p-chlorostyrene-b-isobutylene) arms radiating from a calix[8]arene core. *Polymer Bulletin* **1998**, *41*, 167-174.

(67) Dufour, B.; Tang, C.; Koynov, K.; Zhang, Y.; Pakula, T.; Matyjaszewski, K. Polar Three-Arm Star Block Copolymer Thermoplastic Elastomers Based on Polyacrylonitrile. *Macromolecules* **2008**, *41*, 2451-2458.

(68) Dufour, B.; Koynov, K.; Pakula, T.; Matyjaszewski, K. PBA‐PMMA 3‐Arm Star Block Copolymer Thermoplastic Elastomers. *Macromolecular Chemistry and Physics* **2008**, *209*, 1686-1693.

(69) He, Z.; Liang, Y.; Yang, W.; Uchino, H.; Yu, J.; Sun, W.-H.; Han, C. C. Random hyperbranched linear polyethylene: One step production of thermoplastic elastomer. *Polymer* **2015**, *56*, 119-122.

(70) Hutchings, L. R.; Dodds, J. M.; Rees, D.; Kimani, S. M.; Wu, J. J.; Smith, E. HyperMacs to HyperBlocks: A Novel Class of Branched Thermoplastic Elastomer. *Macromolecules* **2009**, *42*, 8675-8687.

(71) Suksawad, P.; Yamamoto, Y.; Kawahara, S. Preparation of thermoplastic elastomer from natural rubber grafted with polystyrene. *European Polymer Journal* **2011**, *47*, 330-337.

(72) Zhu, Y.; Burgaz, E.; Gido, S. P.; Staudinger, U.; Weidisch, R.; Uhrig, D.; Mays, J. W. Morphology and Tensile Properties of Multigraft Copolymers with

Regularly Spaced Tri-, Tetra-, and Hexafunctional Junction Points. *Macromolecules* **2006**, *39*, 4428-4436.

(73) Zhang, J.; Li, T.; Mannion, A. M.; Schneiderman, D. K.; Hillmyer, M. A.; Bates, F. S. Tough and Sustainable Graft Block Copolymer Thermoplastics. *ACS Macro Letters* **2016**, *5*, 407-412.

(74) Fónagy, T.; Iván, B.; Szesztay, M. Polyisobutylene-graft-polystyrene by quasiliving atom transfer radical polymerization of styrene from poly(isobutylene-co-p-methylstyrene-co-p-bromomethylstyrene). *Macromolecular Rapid Communications* **1998**, *19*, 479-483.

(75) Uhrig, D.; Mays, J. Synthesis of well-defined multigraft copolymers. *Polymer Chemistry* **2011**, *2*, 69-76.

(76) Iatrou, H.; Mays, J. W.; Hadjichristidis, N. Regular comb polystyrenes and graft polyisoprene/polystyrene copolymers with double branches (“centipedes”). Quality of (1, 3-phenylene) bis (3-methyl-1-phenylpentylidene) dilithium initiator in the presence of polar additives. *Macromolecules* **1998**, *31*, 6697-6701.

(77) Mays, J. W.; Uhrig, D.; Gido, S.; Zhu, Y.; Weidisch, R.; Iatrou, H.; Hadjichristidis, N.; Hong, K.; Beyer, F.; Lach, R. In *Tilte*2004; Wiley Online Library.

(78) Uhrig, D.; Mays, J. W. Synthesis of combs, centipedes, and barbwires: poly (isoprene-graft-styrene) regular multigraft copolymers with

trifunctional, tetrafunctional, and hexafunctional branch points. *Macromolecules* **2002**, *35*, 7182-7190.

(79) Mijović, J.; Sun, M.; Pejanović, S.; Mays, J. W. Effect of molecular architecture on dynamics of multigraft copolymers: combs, centipedes, and barbwires. *Macromolecules* **2003**, *36*, 7640-7651.

(80) Duan, Y.; Rettler, E.; Schneider, K.; Schlegel, R.; Thunga, M.; Weidisch, R.; Siesler, H. W.; Stamm, M.; Mays, J. W.; Hadjichristidis, N. Deformation behavior of sphere-forming trifunctional multigraft copolymer. *Macromolecules* **2008**, *41*, 4565-4568.

(81) Duan, Y.; Thunga, M.; Schlegel, R.; Schneider, K.; Rettler, E.; Weidisch, R.; Siesler, H. W.; Stamm, M.; Mays, J. W.; Hadjichristidis, N. Morphology and deformation mechanisms and tensile properties of tetrafunctional multigraft copolymers. *Macromolecules* **2009**, *42*, 4155-4164.

(82) Schlegel, R.; Wilkin, D.; Duan, Y.; Weidisch, R.; Heinrich, G.; Uhrig, D.; Mays, J.; Iatrou, H.; Hadjichristidis, N. Stress softening of multigraft copolymers. *Polymer* **2009**, *50*, 6297-6304.

(83) Staudinger, U.; Weidisch, R.; Zhu, Y.; Gido, S.; Uhrig, D.; Mays, J.; Iatrou, H.; Hadjichristidis, N. In *Tilte*2006; Wiley Online Library.

(84) Uhrig, D.; Schlegel, R.; Weidisch, R.; Mays, J. Multigraft copolymer superelastomers: Synthesis morphology, and properties. *European Polymer Journal* **2011**, *47*, 560-568.

(85) Schulz, G. O.; Milkovich, R. Graft polymers with macromonomers. I. Synthesis from methacrylate-terminated polystyrene. *Journal of Applied Polymer Science* **1982**, *27*, 4773-4786.

(86) Wang, W.; Wang, W.; Lu, X.; Bobade, S.; Chen, J.; Kang, N.-G.; Zhang, Q.; Mays, J. Synthesis and Characterization of Comb and Centipede Multigraft Copolymers PnBA-g-PS with High Molecular Weight Using Miniemulsion Polymerization. *Macromolecules* **2014**, *47*, 7284-7295.

(87) Wang, W.; Wang, W.; Li, H.; Lu, X.; Chen, J.; Kang, N.-G.; Zhang, Q.; Mays, J. Synthesis and Characterization of Graft Copolymers Poly(isoprene-g-styrene) of High Molecular Weight by a Combination of Anionic Polymerization and Emulsion Polymerization. *Industrial & Engineering Chemistry Research* **2015**, *54*, 1292-1300.

(88) Li, H.; Wang, W.; Li, C.; Tan, J.; Yin, D.; Zhang, H.; Zhang, B.; Yin, C.; Zhang, Q. Synthesis and characterization of brush-like multigraft copolymers PnBA-g-PMMA by a combination of emulsion AGET ATRP and emulsion polymerization. *Journal of colloid and interface science* **2015**, *453*, 226-236.

(89) Radke, W.; Roos, S.; Stein, H. M.; Müller, A. H. E. Acrylic thermoplastic elastomers and comb-shaped poly(methyl methacrylate) via the macromonomer technique. *Macromolecular Symposia* **1996**, *101*, 19-27.

(90) Goodwin, A.; Wang, W.; Kang, N.-G.; Wang, Y.; Hong, K.; Mays, J. All-Acrylic Multigraft Copolymers: Effect of Side Chain Molecular Weight and

Volume Fraction on Mechanical Behavior. *Industrial & Engineering Chemistry Research* **2015**, *54*, 9566-9576.

(91) Roos, S. G.; Müller, A. H. E.; Matyjaszewski, K. Copolymerization of n-Butyl Acrylate with Methyl Methacrylate and PMMA Macromonomers: Comparison of Reactivity Ratios in Conventional and Atom Transfer Radical Copolymerization. *Macromolecules* **1999**, *32*, 8331-8335.

(92) Barra, G. M. O.; Jacques, L. B.; Oréfice, R. L.; Carneiro, J. R. G. Processing, characterization and properties of conducting polyaniline-sulfonated SEBS block copolymers. *European Polymer Journal* **2004**, *40*, 2017-2023.

(93) Söntjens, S. H. M.; Renken, R. A. E.; van Gemert, G. M. L.; Engels, T. A. P.; Bosman, A. W.; Janssen, H. M.; Govaert, L. E.; Baaijens, F. P. T. Thermoplastic Elastomers Based on Strong and Well-Defined Hydrogen-Bonding Interactions. *Macromolecules* **2008**, *41*, 5703-5708.

(94) Chen, Y.; Kushner, A. M.; Williams, G. A.; Guan, Z. Multiphase design of autonomic self-healing thermoplastic elastomers. *Nat Chem* **2012**, *4*, 467-472.

(95) Tobolsky, A. V.; Lyons, P.; Hata, N. Ionic clusters in high-strength carboxylic rubbers. *Macromolecules* **1968**, *1*, 515-519.

(96) Paroli, R. M.; Penn, J.: Measuring the glass transition temperature of EPDM roofing materials: comparison of DMA, TMA, and DSC techniques. In *Assignment of the Glass Transition*; ASTM International, 1994.

(97) Li, L.: Dynamic mechanical analysis (DMA) basics and beyond. ParkinElmer Inc. 2000.

(98) Moynihan, C. T.; Easteal, A. J.; Wilder, J.; Tucker, J. Dependence of the glass transition temperature on heating and cooling rate. *The journal of physical chemistry* **1974**, *78*, 2673-2677.

(99) Menard, K. P.: Thermomechanical Analysis Basics: Part 1 It's All Free Volume. PerkinElmer.

(100) Atake, T.; Angell, C. A. Pressure dependence of the glass transition temperature in molecular liquids and plastic crystals. *Journal of Physical Chemistry* **1979**, *83*, 3218-3223.

(101) Campbell, D.; Pethrick, R. A.; White, J. R.: *Polymer characterization: physical techniques*; CRC press, 2000.

(102) Honeker, C. C.; Thomas, E. L. Impact of Morphological Orientation in Determining Mechanical Properties in Triblock Copolymer Systems. *Chemistry of Materials* **1996**, *8*, 1702-1714.

(103) Magonov, S. N.; Reneker, D. H. Characterization of polymer surfaces with atomic force microscopy. *Annual Review of Materials Science* **1997**, *27*, 175-222.

(104) Zhong, Q.; Inniss, D.; Kjoller, K.; Elings, V. Fractured polymer/silica fiber surface studied by tapping mode atomic force microscopy. *Surface science* **1993**, *290*, L688-L692.

(105) Tamayo, J.; García, R. Deformation, Contact Time, and Phase Contrast in Tapping Mode Scanning Force Microscopy. *Langmuir* **1996**, *12*, 4430-4435.

(106) Knoll, A.; Magerle, R.; Krausch, G. Tapping Mode Atomic Force Microscopy on Polymers: Where Is the True Sample Surface? *Macromolecules* **2001**, *34*, 4159-4165.

(107) Bar, G.; Brandsch, R.; Whangbo, M.-H. Effect of Viscoelastic Properties of Polymers on the Phase Shift in Tapping Mode Atomic Force Microscopy. *Langmuir* **1998**, *14*, 7343-7347.

(108) Magonov, S. N.; Elings, V.; Whangbo, M. H. Phase imaging and stiffness in tapping-mode atomic force microscopy. *Surface Science* **1997**, *375*, L385-L391.

(109) Chu, B.; Hsiao, B. S. Small-angle X-ray scattering of polymers. *Chemical Reviews* **2001**, *101*, 1727-1762.

(110) Schnablegger, H.; Singh, Y. A practical guide to SAXS. *Anton Paar, Graz, Austria* **2006**.

(111) Libera, M. R.; Egerton, R. F. Advances in the Transmission Electron Microscopy of Polymers. *Polymer Reviews* **2010**, *50*, 321-339.

(112) Roberts, D. R. T.; Holder, S. J. Mechanochromic systems for the detection of stress, strain and deformation in polymeric materials. *Journal of Materials Chemistry* **2011**, *21*, 8256-8268.

(113) Morton, M.; McGrath, J. E.; Juliano, P. C. In *Tilte*1969; Wiley Online Library.

(114) Odom, E. M.; Adams, D. F. Specimen size effect during tensile testing of an unreinforced polymer. *Journal of Materials Science* **1992**, *27*, 1767-1771.

(115) Malkin, A. Y.; Arinstein, A.; Kulichikhin, V. G. Polymer extension flows and instabilities. *Progress in Polymer Science* **2014**, *39*, 959-978.

(116) Smith, T. L.; Dickie, R. A. In *Tilte*1969; Wiley Online Library.

(117) Smith, T. L. Ultimate tensile properties of elastomers. I. Characterization by a time and temperature independent failure envelope. *Journal of Polymer Science Part A: General Papers* **1963**, *1*, 3597-3615.

(118) Dealy, J.; Plazek, D. Time-temperature superposition—a users guide. *Rheol. Bull* **2009**, *78*, 16-31.

CHAPTER 2 POLY(1-ADAMANTYL ACRYLATE) - GOOD CANDIDATE FOR TPE WITH DISTINCT THERMAL PROPERTIES

A verision of this chapter has been published by Lu W et al. Macromolecules 2016, 49, 9406-9414.

The article was compiled and written by W. Lu. The reported synthesis and characterization was performed by W. Lu.

Abstract

In this chapter, the controlled synthesis of poly(1-adamatyl acrylate) (PAdA) was performed successfully for the first time via living anionic polymerization in tetrahydrofuran at -78 ^{o}C using custom glass-blowing and high vacuum techniques. PAdA synthesized via anionic polymerization using diphenylmethyl potassium (DPMK) as initiator, with a large excess (more than 40-fold to DPMK) of Et_2Zn as the ligand, yielded products that exhibited predicted molecular weights from 4.3 to 71.8 kg/mol and polydispersity indices of around 1.10. The produced PAdAs exhibit a low level of isotactic content (mm triads of 2.1%). The block copolymers of AdA and methyl methacrylate (MMA) were obtained by sequential anionic polymerization, and the distinct living properties of PAdAA over other acrylates was demonstrated based on the observation that the resulting PAdAA-b-PMMA block copolymers were formed with no residual PAdAA homopolymer. The PAdA homopolymers exhibit a very high glass transition temperature (133 ^{o}C) and outstanding thermal stability (T_d: 376 ^{o}C) as compared to other acrylic polymers such as poly(*tert*-butyl acrylate) and poly(methyl acrylate). The dilute solution properties and conformational characteristics of PAdA were evaluated

using different techniques. Based on the molecular weights and corresponding intrinsic viscosities acquired from size exclusion chromatography equipped with both viscosity and multiple angle laser light scattering detectors, the unperturbed dimensions of this polymer were evaluated by using different theories, including Mark-Howink relationship, Burchard-Stockmayer-Fixman (B-S-F) extrapolation and the touched-bead wormlike chain model. This polymer chain has a comparable persistence length, and diameter per bead to those of poly(methyl methacrylate) (PMMA) and polystyrene, and a characteristic ratio (C_∞) of 10.4, which is larger than that of PMMA. In addition, the second virial coefficient (A_2) of PAdA in different solvents were measured by static light scattering. Among the solvents investigated, tetrahydrofuran (THF) is a thermodynamically moderate solvent, with a Mark-Houwink coefficient of 0.67 at 40 ^{o}C and A_2 of 5×10^{-5} $cm^3 \cdot mol/g^2$. All these results indicate that PAdA is less flexible than common polyacrylates. These merits make PAdA a promising candidate for acrylic based thermoplastic elastomers with higher upper service temperature and enhanced mechanical strength.

2.1 Poly(1-adamantyl acrylate): Living Anionic Polymerization, Block Copolymerization, and thermal properties

2.1.1 Introduction

60 years have passed since Szwarc reported living anionic polymerization.[1] Even though many other so-called “living” polymerizations have been developed, including atom transfer radical polymerization (ATRP), reversible addition-fragmentation chain transfer (RAFT), “living” cationic polymerization and ring opening metathesis polymerization (ROMP),[2-4] anionic polymerization has remained widely used in industrial and academic fields because of its superior living properties, quantitative conversions, and predictable molecular weights with narrow polydispersities (PDI) even at extremely high molecular weights. Various monomers, such as styrene and its derivatives, conjugated dienes, vinylpyridines, alkene oxides, have been controllably polymerized anionically.[5]

The anionic polymerization of methacrylate-based monomers including methyl methacrylate has also been reported.[6] However, the anionic polymerization of acrylate-based monomers, especially acrylates with bulky alkyl substituents, is challenging because of side reactions such as nucleophilic attack of the carbanion either onto the monomer or the polymer chain (backbiting reaction), and the aggregation of the active chain ends with ester enolate structures.[7]

The anionic polymerization of alkyl methacrylates has been extensively reported, including the use of modified initiators,[8] lower temperature,[8] polar

solvents,[9] various additives,[10] and different counter ions.[11] One of the most effective approaches so far is their polymerization initiated with bulky organolithium compounds, such as 1,1-diphenylhexyl lithium (DPHLi) in tetrahydrofuran (THF) at -78 ^{o}C.[12] Lithium chloride is a commonly used additive to suppress backbiting reactions and reduce the PDI. For example, a 3-fold excess of LiCl to DPHLi is added typically to form the complex with carbanion chain ends.[13] Interestingly, the combination of solvent polarity along with the amount of LiCl added was reported to affect the stereochemistry of poly(methyl methacrylate) (PMMA).[14] It has been reported that the tacticity of poly(alkyl methacrylate) can also be tuned by changing the pendent group,[15] initiator, and additive used[16-19]. Another well-developed initiation system for alkyl methacrylate polymerization is diphenylmethyl potassium (DPMK) with diethyl zinc (Et_2Zn) as μ-type ligand, first reported by Nakahama et al.[20] This system forms a complex with carbanionic chain ends in THF at -78 ^{o}C which effectively suppresses the backbiting reactions, and polymers with predicted molecular weight and narrow PDI (below 1.10) are obtained.

As compared to alkyl methacrylates, the anionic polymerization of alkyl acrylates is still limited. In addition to the intramolecular backbiting reaction similar to that with alkyl methacrylates, proton abstraction of the acidic α-hydrogen in the backbone provides an additional critical obstacle to their controlled polymerization.[21] Teyssié et al. first reported the successful controlled copolymerization of MMA and *tert*-butyl acrylate (tBA) using the combination of α-

methyl styrenyl lithium (*α*-MStLi), DPMK, DPMNa or DPMLi as the initiator with the addition of a large excess of LiCl (more than 10-fold) and produced well-defined block copolymers of PMMA-*b*-PtBA with expected molecular weights. [22] Thereafter, they reported a series of more favorable ligands- lithium alkoxide, e.g. lithium 2-(2-methoxyethoxy) ethoxide (LiOEEM), that can polymerize 2-ethylhexyl acrylate (P2EtHA) with PDI as low as 1.03.[23] However, homopolymer of P2EtHA always remained after synthesis of P2EtHA-*b*-PMMA, which suggests the polyacrylate chain ends were not completely "living".

Nakahama and coworkers reported the anionic polymerization of N,N-dimethylacrylamide (DMAA) using the DPMK/Et_2Zn initiator system.[24] The polydispersity of the resulting polymer was broad (PDI ~1.28 even when 15-fold Et_2Zn to DPMK was applied), but the conversion was quantitative. Interestingly, they observed that PDMAA was highly syndiotactic when a certain amount of Et_2Zn was used. PtBA was also synthesized with DPMK/Et_2Zn system.[25] The polymerization was completed within minutes, with 100% yield, controlled molecular weight and narrow PDI (< 1.1). However, an estimated 61% of the living chain ends were deactivated even only after 5 min. The resulting PtBA showed no stereoselectivity as in the case of PDMAA. The polymerizations of primary and secondary alkyl acrylates including butyl acrylate and ethyl acrylate were also attempted.[26] However, their successful polymerization has been rarely reported until now and it still remains as a challenge to control the PDI. Compared to the

huge number of studies on alkyl methacrylates, new approaches to control the anionic polymerization of alkyl acrylates are required.

In this section, the anionic polymerization of 1-adamantyl acrylate (PAdA) using the DPMK/Et_2Zn initiation system is studied. The pendent group, adamantane (tricycle[3.3.1.1]decane), is a symmetric tricyclic hydrocarbon with three fused chair-form cyclohexyl rings in a diamond lattice. Even compared to other bulky pendant groups such as benzene rings, adamantane shows a drastic impact on the physical and chemical properties, especially the glass transition temperature (T_g). The bulky adamantyl moiety can also contribute to the decrease of chain mobility and increase of rotational barrier, which could further increase the T_g of the final polymer.[27-30] In addition, adamantyl substituents have been reported to increase the decomposition temperature of polymers, e.g. poly(1-adamantyl methacrylate) exhibits a degradation temperature (T_d) ~300 ^{o}C.[31] We thus envision that PAdA is a promising candidate for acrylic based thermoplastic elastomers with high upper service temperatures and enhanced mechanical strength which may be synthesized by block copolymerization with polyacrylates having low T_gs such as poly(n-butyl acrylate).[32,33] Another attractive property of adamantane is its strong host-guest inclusion complexation with β-cyclodextrin and Cucurbit[7]uril because of its size matching to their cavities.[34,35] Such complexes have shown distinct self-healing behavior.[36,37]

Even though AdA has been previously polymerized through radical polymerization,[38,39] and anionic polymerizations of styrene[40] and methacrylate[31] bearing 1-adamantyl pendent groups were also studied, the anionic synthesis of PAdA and its block copolymers has not been reported, mainly because of the inherent difficulty in the anionic polymerization of acrylates as discussed above. We expected that the bulky size of adamantane and its tertiary carbon connected with the ester group might make the anionic polymerization less problematic than that of PtBA. However, we found that the anionic polymerization of AdA was still not an easy task, requiring more carefully chosen reaction conditions as compared to that of PtBA, including a specific initiation system and a large excess of suitable additive.

In this study, the anionic polymerization of 1-adamantyl acrylate (AdA) was performed with *sec*-butyllithium/diphenylethylene/lithium chloride (*sec*-BuLi/DPE/LiCl), diphenylmethyl potassium/diethyl zinc (DPMK/Et_2Zn), and sodium naphthalenide/diphenylethylene/diethyl zinc (Na-Naph/DPE/Et_2Zn) initiator systems in THF at -78 ^{o}C. These initiator systems have been generally applied for the anionic polymerization of (meth)acrylates.[6] The living nature and reactivity of poly(1-adamantyl acrylate) and the block copolymerization of AdA with methyl methacrylate (MMA) were also studied. The resulting PAdA was characterized using nuclear magnetic resonance spectroscopy (NMR), size exclusion

chromatography (SEC), thermogravimetric analysis (TGA), and differential scanning calorimetry (DSC).

2.1.2 Experimental Part

Materials. 1-adamantanol (Acros Organics, 99%), acryloyl chloride (Aldrich, 97%), triethylamine (Acros Organics, 99%), and ammonium chloride (Acros Organics, 99.5%) were used as received. *Sec*-butyllithium (*sec*-BuLi), 1,1-diphenylethylene (DPE, Acros Organics, 98%), THF (Fisher, GR grade) and methanol (Fisher, GR grade) were purified as previously described.[41] Sodium naphthalenide (Naph-Na) was prepared using naphthalene and sodium metal in THF. Diphenylmethyl potassium (DPMK) was prepared according to previously reported work.[42] LiCl (Alfa Aesar, 99.995%) was dried at 130 ^{o}C for 2 days, ampulized and diluted in THF under high vacuum conditions, giving a concentration of 0.6 mmol/ml. Diethyl zinc was ampulized and diluted in THF under high vacuum condition, giving the concentration 1 mmol/ml. Methyl methacrylate (MMA, Aldrich, 99%) was passed through aluminum oxide (Acros Organics, basic) column to remove inhibitor, stirred for 24 h over anhydrous CaH_2 and distilled over CaH_2 and trioctylaluminum sequentially under reduced pressure. The resulting MMA was ampulized and diluted immediately with THF under high vacuum condition, giving a concentration of 0.83 mmol/ml. All ampules of the reactants, equipped with break seals were stored at -30 ^{o}C. *Tert*-butyl acrylate (tBA, Sigma-Aldrich, 98%) and methyl acrylate (MA, Acros Organics, 99%) were used directly

after passed through aluminum oxide (Acros Organics, basic) column to remove inhibitor. 2,2-Azobis-(isobutyronitrile) (AIBN, Sigma-Aldrich, 90%) was recrystallized before use and the S-1-dodecyl-S'-(α,α'-dimethyl-α'-acetic acid)trithiocarbonate chain transfer agent (CTA) was synthesized following the procedure previously published by Lai et al.[43] Copper(I) bromide (CuBr, Sigma-Aldrich, 99.9999%), Ethylene bis(2-bromoisobutyrate) (EBIB, Sigma-Aldrich, 97%), N,N,N',N",N"-pentamethyldiethylenetriamine (PMDETA, Sigma-Aldrich, 99%), Benzene (Sigma-Aldrich, ≥99.9%), Anisole (Acros Organics, 99%) were used as received.

Characterization. The molecular weights (MWs) of the polymers were measured using size exclusion chromatography (SEC) with the EcoSEC GPC system, which allows for the use of three semimicro GPC columns (2 Tosoh TSKgel SuperMultiporeHZ-M; 4.6x150 mm; 4 µm; and a TSKgel SuperMultiporeHZ-M guard). RI detector with flow rate at 0.35 ml/min was utilized for MW estimation based on a PMMA standard curve ranging from 600 to 7,500,000 Daltons. The ^{1}H and ^{13}C NMR spectra were measured with Varian VNMR 500 MHz, and using $CDCl_3$ as the solvent. Chemical shifts were referred to $CDCl_3$ solvent peak at 7.26 ppm for ^{1}H NMR spectra and 77.16 ppm for ^{13}C NMR spectra. Thermal properties were characterized using thermogravimetric analysis (TGA, TA-50) and differential scanning calorimetry (DSC, TA2000) under nitrogen with a heating rate of 10 ^{o}C/min.

Synthesis of 1-Adamantyl Acrylate (AdA). The monomer AdA was synthesized following the previously reported work.[38] (**Scheme 2-1**) Briefly, the procedure was as follows: 1-adamantanol (10.0 g, 65.7 mmol), and triethylamine (33.2 g, 328.1 mmol) were dissolved in freshly dried THF (60 ml) and cooled to 0 ^{o}C with an ice bath. The THF solution of acryloyl chloride (11.9 g, 131.5 mmol, 4.38 M) was added dropwise. The reaction solution was raised to room temperature and left stirring overnight. After the reaction was complete, the precipitated salt was filtered out. The solution mixture was extracted with saturated ammonium water solution until the aqueous layer became colorless. The collected organic layer was evaporated, mixed with a large excess of silica gel, and purified using a flash column with n-hexane as the eluent. Colorless crystals were obtained after the evaporation of n-hexane. The resulting product was obtained with a yield of 59.2% and the chemical structure is shown in **Scheme 2-1**. ^{1}H NMR spectra ($CDCl_3$, 500 MHz), δ (ppm): 6.27 and 5.27 (d, 2H, -C=CH2), 6.04 (t, 1H, O=C-CH-C), 1.60-2.22 (15H, -CH2-CH-CH2- of 1-adamantyl pendent group).

For anionic polymerization, AdA was further freeze dried with benzene three times and directly flame sealed in an ampule equipped with a break-seal under high vacuum conditions. The purified monomer was diluted with anhydrous THF. The solution (0.81 mmol/ml) was stored at -30 ^{o}C until polymerization.

Homopolymerization of AdA. All anionic polymerizations were carried out under high-vacuum conditions (10^{-6} mmHg) in a glass apparatus equipped with

break-seals in the usual manner.[41,44] The polymerization was performed in THF at -78 ^{o}C. Initiator (DPHLi, DPMK or NaphNa/DPE), additive (LiCl or Et_2Zn), and monomer AdA were introduced sequentially via break-seals. Polymerization was terminated with degassed methanol at -78 ^{o}C. To remove additives used during polymerization, the product was poured into acidified methanol with vigorous stirring. The precipitated polymer was filtered, rinsed with methanol, and vacuum dried overnight. The resulting polymer was characterized by SEC, ^{1}H and ^{13}C NMR spectroscopies. ^{1}H NMR spectra ($CDCl_3$, 500 MHz) (**Figure 2-1, Figure 2-2**), δ (ppm): 2.2- 2.3 (br, 1H, O=C-CH-C), 1.7– 1.9 (br, 2H, -C-CH2). ^{13}C NMR spectra ($CDCl_3$, 500 MHz), δ (ppm): 173- 174.1 (C=O), 42.3, 41.4, 36.4, 34.5, 31.0.

Block copolymerization of AdA with MMA. The sequential anionic polymerization of AdA and MMA were carried out to synthesize block copolymers of poly(1-adamantyl acrylate)-*b*-poly(methyl methacrylate) (PAdA-*b*-PMMA). The solution was performed in THF at -78 ^{o}C. DPMK/Et_2Zn, which was used for the homopolymerization of AdA, was introduced via break-seals. Depending on the sequence of the block composition, the two sequential orders of the first addition of AdA and second of MMA as well as the opposite sequential monomer addition was carried out. Aliquots of the first block were withdrawn to an attached receiver for characterization of the first block. Polymerizations were terminated with degassed methanol at -78 ^{o}C. To remove additives used during polymerization, the product solution was poured into acidified methanol with vigorous stirring. The

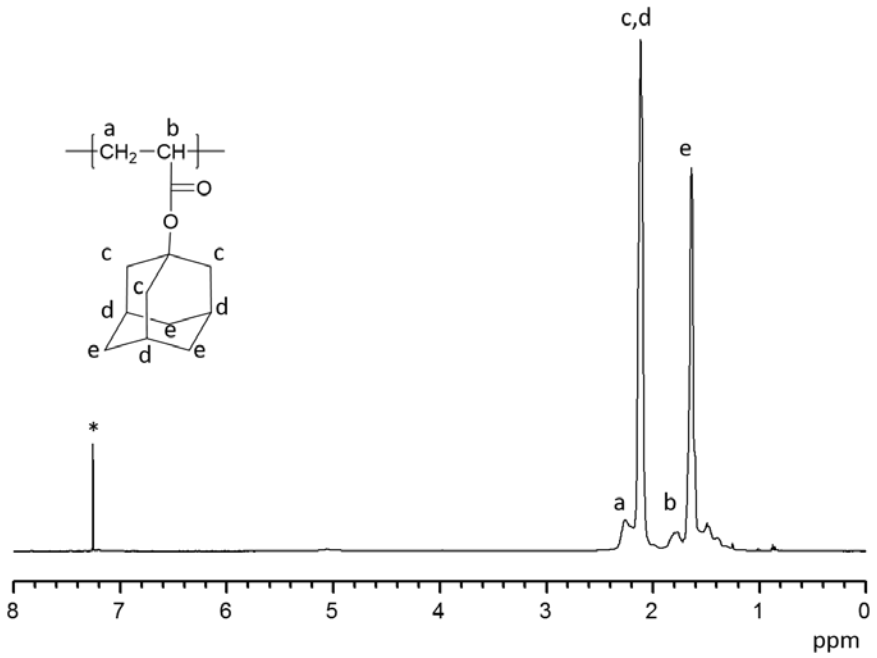

Figure 2-1. ^{1}H NMR spectra of PAdA.

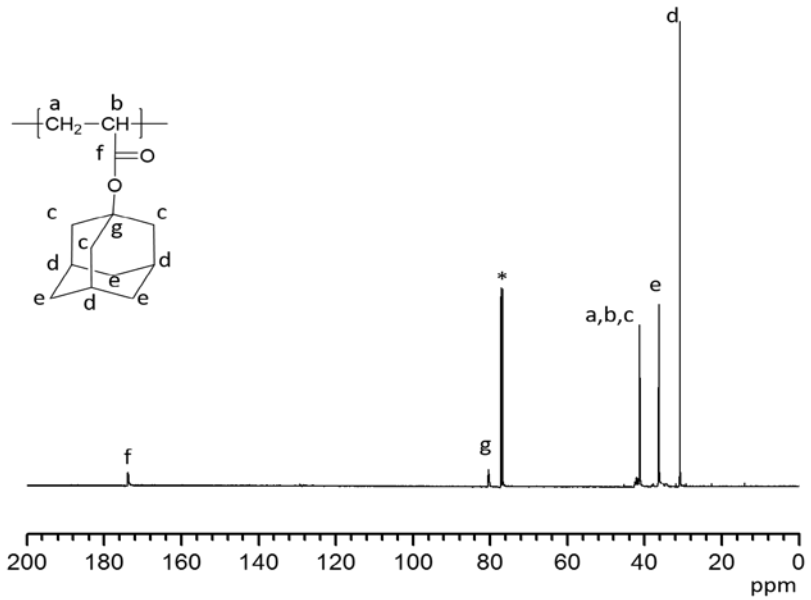

Figure 2-2. ^{13}C NMR spectra of PAdA.

precipitated polymer was filtered, rinsed with methanol, and vacuum dried. The resulting polymer was characterized by SEC.

Homopolymerization of tBA. PtBA was polymerized through reversible addition–fragmentation chain transfer (RAFT) polymerization under high-vacuum conditions (10^{-6} mmHg) in a glass apparatus. After mixing CTA (0.1 M in benzene, 1.00ml), AIBN (0.1 M in benzene, 0.22 ml), tBA (10.00g) and Benzene (5.00 ml) in a vial, the solution was transferred to an ampule, which was degassed by three freeze-thaw-evacuate cycles. The ampule was flame sealed under vacuum and immersed in an oil bath at 75 ^{o}C for 10 h. The polymerization was quenched with liquid nitrogen. The product solution was precipitated twice in large excess of methanol/H2O (60/40) with vigorous stirring and vacuum dried overnight. The resulting polymer was characterized by using size exclusion chromatography (SEC). Mn: 54.2 Kg/mol, PDI: 1.89, as shown in **Figure 2-3**.

Homopolymerization of MA. PMA was polymerized through atom-transfer radical-polymerization (ATRP) under high-vacuum conditions (10^{-6} mmHg) in a glass apparatus. EBIB (0.1 mmol), CuBr (0.1 mmol), MA (30 g), Anisole (100 ml) and PMDETA (0.1 mmol) were sequentially added to an ampule, which was degassed by three freeze-thaw-evacuate cycles. The ampule was flame sealed under vacuum and immersed in an oil bath at 85 ^{o}C for 7 days. The polymerization was quenched with liquid nitrogen. The product solution was passed through aluminum oxide (Acros Organics, neutral) column to remove salt, precipitated

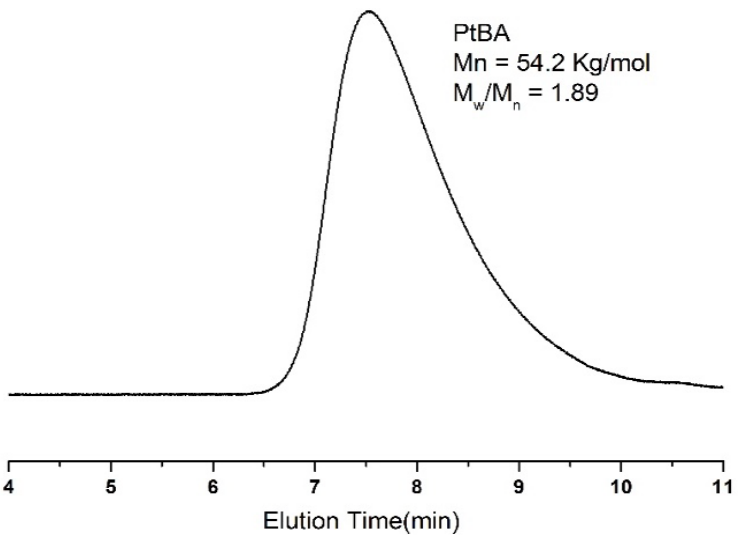

Figure 2-3. SEC profiles of PtBA by RAFT polymerization.

twice in large excess of methanol and vacuum dried overnight. The resulting polymer was characterized by using size exclusion chromatography (SEC). M_n: 110.4 Kg/mol, PDI: 1.15, as shown in **Figure 2-4**.

2.1.3 Result and Discussion

Effect of Initiators on Anionic Polymerization. The initiator systems of sec-BuLi/DPE/LiCl, DPMK/Et_2Zn and NaNaph/DPE/Et_2Zn have been generally applied for the anionic polymerization of (meth)acrylate.[6] To optimize living anionic polymerization of AdA monomer, which was prepared as shown in Scheme 1, various initiator systems of *sec*-BuLi/DPE, NaphNa/DPE, and DPMK with LiCl and Et_2Zn were employed, as shown in **Scheme 2-1.** The detailed results of the polymerization are summarized in **Table 2-1**.

For the anionic polymerization using *sec*-BuLi initiator, the combination of *sec*-BuLi/DPE was used to decrease the nucleophilicity, as previously reported with polymerization of (meth)acrylates.[9] The polymeric solution changed from colorless to red once DPE was introduced to *sec*-BuLi solution in -78 ^{o}C, indicating the formation of diphenylethyl anions. Sequentially, LiCl was used to form the complexation with living chain ends, which was reported to be helpful in suppressing the back-biting reaction and decreasing the propagation rate.[45]

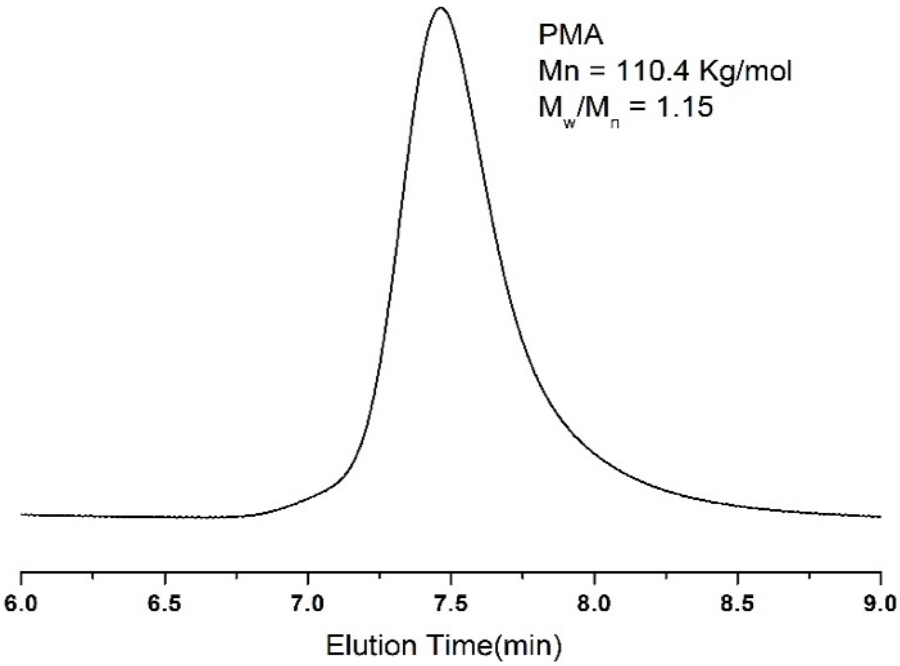

Figure 2-4. SEC profiles of PMA by ATRP.

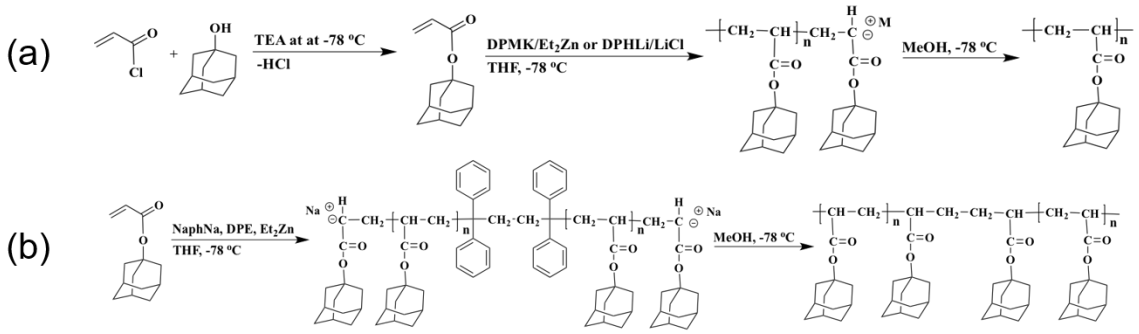

Scheme 2-1. (a) Synthesis of 1-adamantyl acrylate (AdA)[38] and anionic polymerization of AdA initiated by DPMK or DPHLi in the presence of Et_2Zn or LiCl. Denote: TEA: triethylamine, DPMK: diphenylmethyl potassium, Et_2Zn: diethyl zinc, DPHLi: diphenylhexyl lithium, and LiCl: lithium chloride. M is Li or K metal.(b) Anionic polymerization of AdAA using NaphNa/DPE initiator in the presence of Et_2Zn in THF at -78 ^oC.

Table 2-1. Anionic Polymerization of AdA Using Various Initiators[a]

runs	initiator/Additive (mmol/mmol)	AdA (mmol)	time (min)	M_n (kg/mol) calcd[c]	M_n (kg/mol) obsd	M_w/M_n[b]
	sec-BuLi/DPE/LiCl[d]					
01	0.10/0.20/1.00	4.85	30	10.0	13.0	1.83
	NaphNa/DPE/ Et_2Zn[e]					
02[f]	0.04/2/1.00	2.42	30	25.0	94.3, 42.2	1.03, 1.10
03	0.04/0.20/1.6	2.42	5.0	25.0	55.7	1.86
	DPMK/ Et_2Zn[e]					
04	0.05/0.75	1.21	30	5.0	104.3, 4.4	1.03, 1.21
05	0.05/1.00	1.21	30	5.0	4.3	1.37
06	0.05/2.00	1.21	30	5.0	4.5	1.09
07	0.05/2.00	1.21	60	5.0	4.3	1.10
08	0.05/2.00	1.21	5	5.0	4.8	1.19

Table 2-1 Continued

runs	initiator/Additive (mmol/mmol)	AdA (mmol)	time (min)	M_n (kg/mol) calcd[c]	M_n (kg/mol) obsd	M_w/M_n[b]
09[g]	0.05/2.00	2.42	<1	10.0	8.5	1.14
10	0.05/2.00	16.97	5	70.0	71.8	1.10

[a]All the polymerization showed quantitative yields. [b]Number-average molecular weight Mn (obsd) and PDI were measured by SEC calibration using a PMMA standard in THF as the eluent at 40 °C [c] $M_n(\text{calcd}) = \frac{[\text{AdA}]}{[\text{initiator}]} \times \text{MW}(\text{AdA}) \times \text{yield of polymerization } (\%)$. [d]LiCl was applied as the additive for the anionic polymerization of AdA initiated by *sec*-BuLi/DPE. [e]Et_2Zn was applied as the additive for the anionic polymerization of AdA initiated by NaphNa/DPE and DPMK. [f]Bimodal peak was obtained in SEC curve. [g]The sample demonstrated Mn:8.5 kg/mol, PDI: 1.14 from SEC with refractive index (RI) detector based on PMMA standard and Mn: 9.1 kg/mol, PDI: 1.06 from SEC with a viscometer and multi-angle light scattering (MALLS) detectors.

However, the polymerization of AdA using the initiation system of *sec*-BuLi/DPE/LiCl was poorly controlled and lead to a broad molecule weight distribution (PDI= 1.83) as described in **Table 2-1 run 01** and **Figure 2-5a** (black line). Thus, another initiation system of NaphNa/DPE was used for the anionic polymerization to adjust the nucleophilicity to comparable with carbanion of (meth)acrylate, as reported in the polymerization of (meth)acrylates.[6] In the polymerization, the additive Et_2Zn was introduced with a molar ratio of $[NaphNa]_0/[Et_2Zn]_0$ = 25 and 40 (Run 02 and 03 in **Table 2-1**) to form the complex with living chain ends as well as the coordination bonding with the carbonyl group of AdA monomers to suppress the side reactions. However, the polymerization using NaphNa/DPE/Et_2Zn ($[NaphNa]_0/[Et_2Zn]_0$ = 25, Run 02 in **Table 2-1**) produced bimodal molecular weight distributions as shown in **Figure 2-5a** (red line), that could be the heterogeneous growth of polymer chains from the difunctional initiation site formed by the radical coupling reaction.[46] With Na^+ as the counter ion, the complexation formed between the enolate ion and the ligand is not strong enough to suppress the side reactions like backbiting reactions, inter-molecular polymer terminations, etc.[6] The combination of these side reactions, as well as possible limitation in initiation efficiency, make the molecular weight produced higher than expected. Therefore, we carried out one more polymerization of AdA using NaphNa and Et_2Zn with the feeding ratio of 40-fold excess to overcome side reactions and to control anionic polymerization.

Interestingly, the different concentration of NaphNa/DPE/Et_2Zn with $[NaphNa]_0/[Et_2Zn]_0$ = 40 (Run 03 in **Table 2-1**) overwhelmed the bimodal curve but exhibited 1.86 of very high PDI. (**Figure2-6**) Although the sodium cation is more favorable for the AdA polymerization generally, this initiation system was still not well controlled.

Alternatively, the anionic polymerization of AdA was performed by the initiation system of DPMK/Et_2Zn. The solution of DPMK in THF changed from red to orange immediately after Et_2Zn was introduced at -78 ^oC, due to the complexation between the additive and diphenylmethyl anion. Once AdA was added, the solution became colorless or pale yellow, which is typical for living poly(meth)acrylates. With a certain amount of Et_2Zn, PAdA was successfully obtained with target molecular weight and almost 100% yield, giving PDI lower than 1.1. (**Table 2-1 Run 06** and **Figure 2-5a**, blue line). Similar results were also reported previously.[47,48] An equilibrium of the ligand with enolate ion is presumably involved that endows K with a better ability to control the polymerization than Na and Li.[49] For alkali metals, the increase of size leads to higher polarizability of the carbanion with K^+ than that with Na^+ and Li^+. The radii of K^+, Na^+, and Li^+ were verified at 133, 95, and 60 pm, respectively.[50] Thus the complexation of K^+ with the ligand is easier, which restricts either the intermolecular termination or intramolecular backbiting between carbanion and carbonyl group.

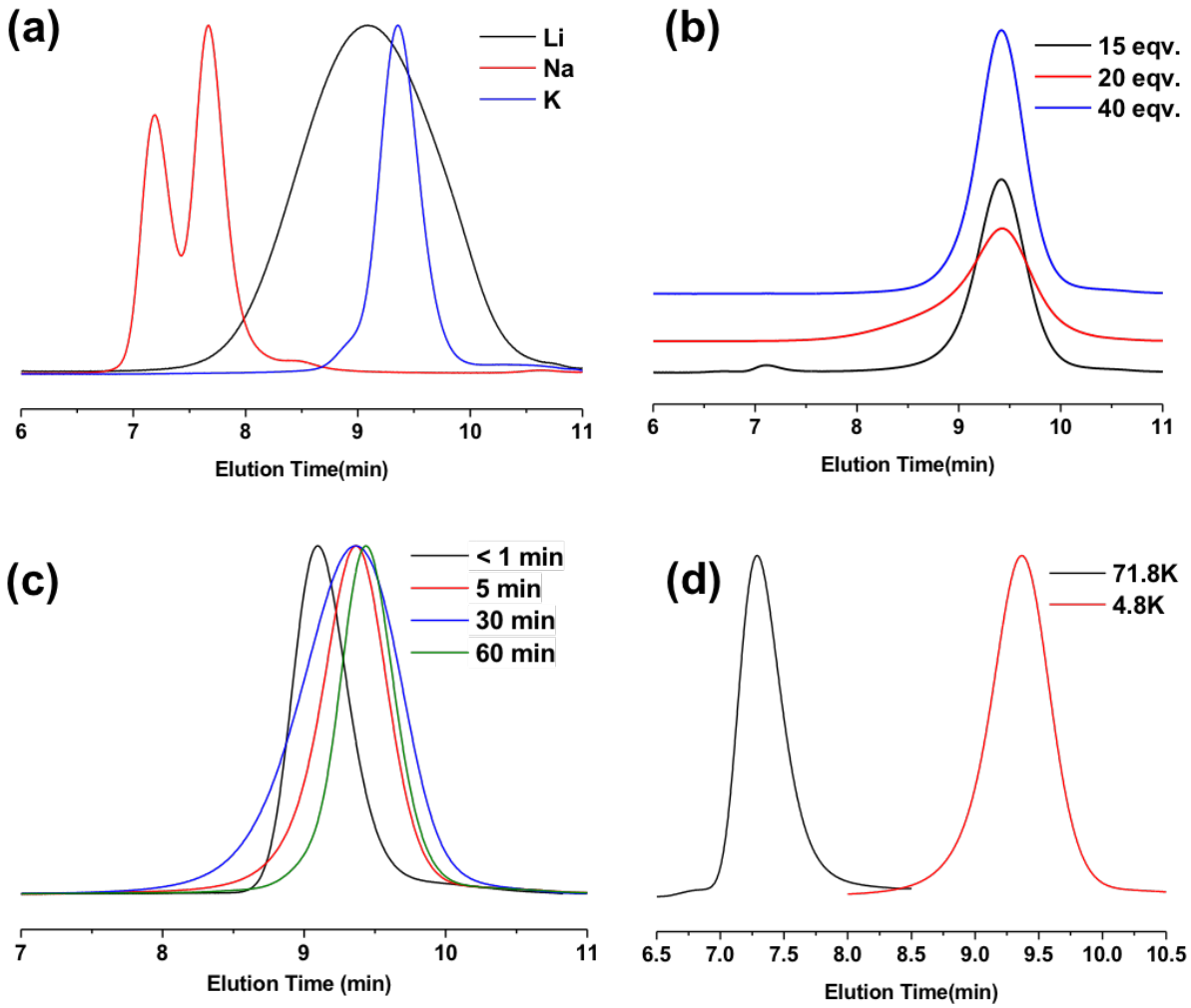

Figure 2-5. SEC profiles of PAdA synthesized by anionic polymerization with a) initiation system with different cations, results shown as Run 01, 02 and 06 in Table 2-1; b) different amount of Et_2Zn added, results shown as Run 04, 05 and 06 in Table 2-1; c) different reaction time, results shown as Run 06 to Run 09 in Table 2-1; d) wide molecular range, results shown as Run 08 and 10 in Table 2-1.

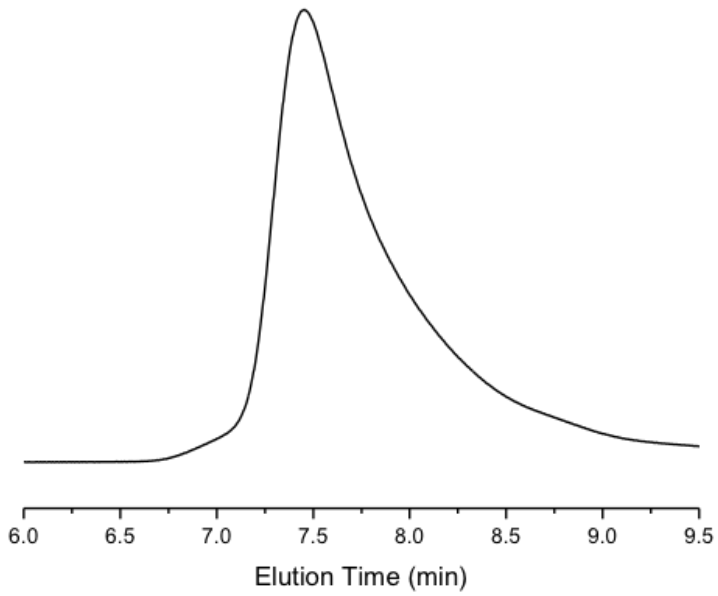

Figure 2-6. SEC profiles of PAdA synthesized by NaphNa/DPE/Et2Zn via anionic polymerization with 40-fold excess of Et2Zn (Run 03 in Table 2-1).

Effect of Additive/Initiator Ratio on Anionic Polymerization. The coordination of ligands with enolate ion pairs has been classified into μ-type ligands, σ-type ligands, and μ / σ -type dual ligands.[51] As mentioned above, anionic polymerization of methyl methacrylate,[20] *N,N*-Dialkylacrylamides,[24] and *tert*-butyl acrylate[25] have been controlled well by the introduction of Et_2Zn. The strong electrostatic interactions lead to μ-type of complexation between potassium or sodium enolate and Et_2Zn. This complexation forms the steric hindrance that restricts the backbiting termination. On the other hand, the strong electrostatic interactions decrease the reactivity of living chain ends and suppress its attack on carbonyl groups. As reported previously, for the anionic polymerization of MMA, only 3~10-fold excess of Et_2Zn/initiator is necessary to suppress the side reaction.[20] When Et_2Zn/initiator is higher than 11-folds, the polymerization of tBA could be well controlled.[25]

As shown in **Figure 2-5b**, however, the previously used ratio of Et_2Zn/DPMK is not sufficient for the controlled polymerization of AdA. When Et_2Zn/DPMK was 15 fold, unexpectedly high molecular weight polymer was produced which might be caused by multi-coupling reactions. With a 20-fold excess of Et_2Zn, this side reaction was somewhat suppressed, which made the molecular weight lower. However, the side reaction still occurred to some extent and gave a broad shoulder in SEC profiles. The polymerization was controlled completely when a 40-fold excess of Et_2Zn/DPMK was used. As studied

previously, the 1-adamantyl group has a higher ability to pull the electrons away from the ester group than *tert*-butyl group.[52] This enolate is more vulnerable to carbanion attack. More ligand is thus necessary to stabilize enolate and to suppress the side reaction.

Polymerization Kinetics and Molecular Weight Range. Compared to methacrylates, the anionic polymerization of acrylate monomers is much faster, e.g. the conversion of the anionic polymerization of tBA reached 100% within 1 minute.[25] Even though it is reported that the presence of additive can distinctly reduce the propagation rate,[20] and a large excess of Et_2Zn was used during the polymerization of AdA, the polymerizations undergoing 30 min and 60 min showed the same MWs as for the polymerization for 5 min. Even though the anionic polymerization was performed for less than 1 min, the well-defined PAdA was synthesized completely with quantitative yield, controlled Mn of 8.5K g/mol, and narrow PDI of 1.14 as shown in **Table 2-1** run09 and **Figure 2-5c** blue line. The polymerization of AdA to high molecular weight also proceeded in 5min, giving the Mn 71.8 kg/mol with a narrow polydispersity of 1.10 in **Figure 2-5d** and it is the highest Mw of PAdA polymer synthesized in this study.

Tacticity of PAdA. In general, the tacticity of a poly(alkyl methacrylate) is dictated by the size of the alkyl group.[15] It can also be effectively tuned by changing initiator and/or ligand. Thus poly(alkyl methacrylate) with highly syndiotactic[16,17] or isotactic[18,19] structures could be obtained. Ligated anionic polymerization has been

widely reported to influence tacticity of (metha)acrylate polymers. The formation of highly isotactic[18,19] and highly syndiotactic[16,17] structures have been achieved with the selection of different additives.

The tacticity of PAdA with Mn 71.8 kg/mol (Run 10 in **Table 2-1**) was determined by integration of the triad peaks of the carbonyl group in ^{13}C NMR spectra as shown in **Figure 2-7**. The resonances at 174.1~173.7 ppm and 173.7~173.4 ppm were assigned to rr and mr triads, with the proportion of 76.8% and 21.1% respectively. The content of mm triad at 173.4~173.2 ppm was only 2.1%. As reported by S. Nakahama et. al, Et_2Zn also accounts for the increase of syndiotactic proportion of poly(*N,N*-dialkylacrylamides) synthesized via anionic polymerization. Even though they have different structures from (meth)acrylate, a large excess of Et_2Zn is used to coordinate with the propagating chain end to suppress the side reactions in the polymerization of both acrylamides and acrylates.[24] In addition, as the (meth)acrylate monomers, even though the influence of Et_2Zn on tacticity was not observed in the polymerization of tBA,[25] it has been reported that the tacticity of a poly(alkyl methacrylate) is affected by the size of the alkyl group.[15] Based on the works above, it is anticipated that the selectivity of tacticity found in the anionic polymerization of AdA could be attributed to both the ligand effect and the bulkiness of the pendent group.

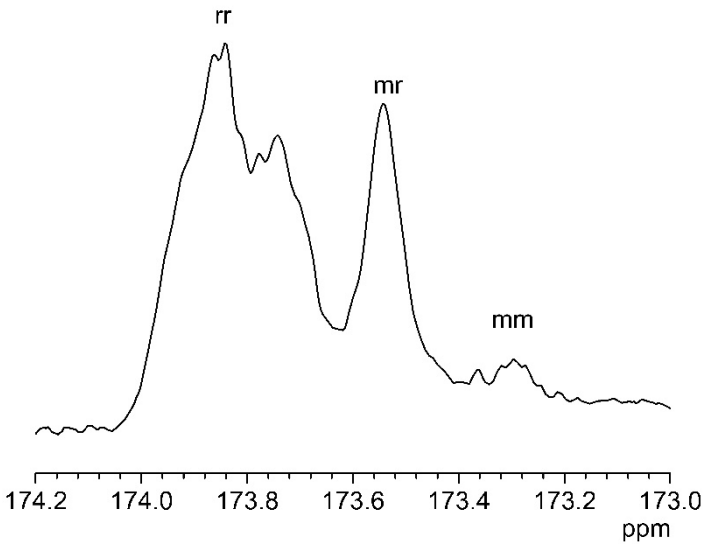

Figure 2-7. ^{13}C NMR spectra of the carbonyl carbons of the PAdA with Mn 71.8 kg/mol (Run 10 in Table 2-1) measured in $CDCl_3$.

Block Copolymerization of AdA with MMA. One of the merits of living anionic polymerization is the easy preparation of well-defined block copolymers through the sequential addition of different monomers. Through the block copolymerization of AdA with MMA, we evaluated the living properties of PAdA, and the nucleophilicity of the living PAdA chain ends.

Block copolymerization was carried out in THF at -78 ^{o}C using DPMK as the initiator and 40 equiv of Et_2Zn. For the synthesis of PMMA-*b*-PAdA, the first block was polymerized for 1 h, followed by the addition of AdA. The polymerization was quenched with degassed methanol after the propagation of PAdA for 10 min in THF at -78 ^{o}C. For the synthesis of PAdA-*b*-PMMA, the first block of PAdA was carried out for 10 min, followed by the polymerization of MMA for 1 h. All the polymeric solutions were precipitated in a large excess of acidified methanol after termination of living polymer chains with methanol. This gave a direct indication of PAdA production, based on the fairly good solubility of PMMA in methanol. The details of the polymerization results are summarized in **Table 2-2.**

Clear shifts were observed in the SEC profiles in both PMMA to PMMA-*b*-PAdA (**Figure 2-8a**) and PAdA to PAdA-*b*-PMMA (**Figure 2-8b**). Block copolymers were successfully synthesized by living anionic polymerization via both sequences, with 100% conversion of each monomer. It is thus demonstrated that the PAdA living chain end has similar nucleophilicity to that of PMMA.

Table 2-2. Diblock Copolymerization of AdA with MMA in THF at -78 $^{o}C^{a}$

Run	Initiator (mmol)	1st monomer (mmol)	2nd monomer (mmol)	Time (min)	Block copolymer (homopolymer) M_n (kg/mol) calcd[c]	obsd	Mw/Mn[b]
11	0.02	MMA, 2.00	AdA, 2.42	60/10	25(10)	25.1(8.5)	1.09(1.05)
12	0.05	AdA, 2.50	MMA, 2.42	10/60	15(5)	14.6(4.3)	1.06(1.10)

[a]The polymerization was initiated by DPMK with Et_2Zn as the additive at concentration of [Et_2Zn]/[DPMK] = 40. All the polymerization demonstrated quantitative yields. [b]Mn (obsd) and M_w/M_n were measured by SEC calibration using a PMMA standard in THF as the eluent at 40 ^{o}C. [c] $M_n(\text{calcd}) = \frac{[\text{AdA}]}{[\text{initiator}]} \times \text{MW(AdA)} \times \text{yield of polymerization (\%)} + \frac{[\text{MMA}]}{[\text{initiator}]} \times \text{MW(MMA)} \times \text{yield of polymerization (\%)}$

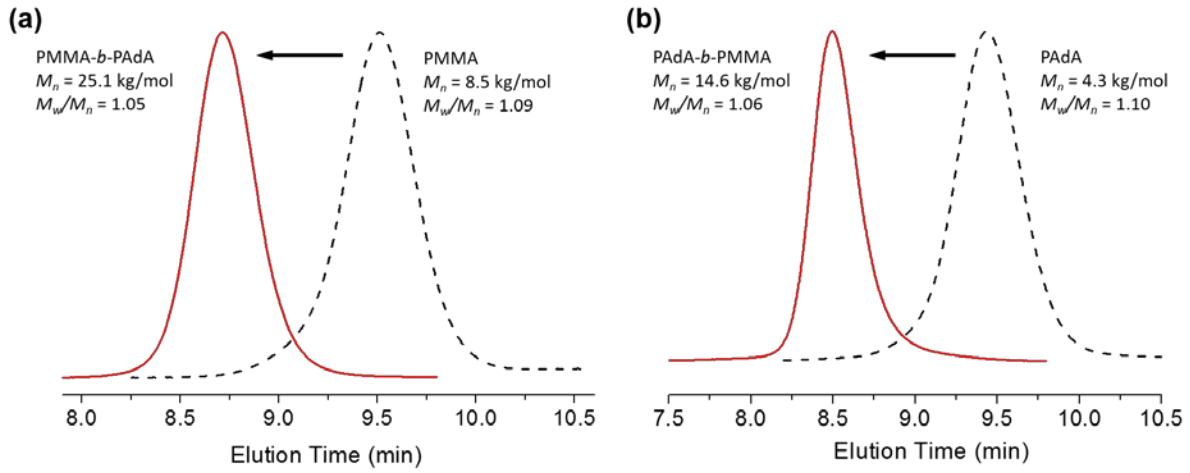

Figure 2-8. SEC profiles from a) PMMA homopolymer to PMMA-*b*-PAdA block copolymer, and b) PAdA homopolymer to PAdA-*b*-PMMA block copolymer.

For the synthesis of PAdA-*b*-PMMA, the diblock copolymer gave a clean unimodal molecular weight distribution and quite narrow polydispersity, as shown in **Figure 2-8b**. Accordingly, it was proven that living AdA initiates MMA completely with 100% conversion of PAdA. From this observation, it was surmised that living PAdA has a distinct 100% living property as compared to other acrylates like 2EtHA and tBA. For the anionic polymerization of tBA by Et_2Zn/DPMK, it was demonstrated that 61% of the living chains were deactivated in only 5min.[25] In addition, a trace of P2EtHA also existed in the SEC curve of diblock copolymer of P2EtHA-*b*-PMMA.[24] In the case of 1-adamantyl acrylate, the bulky side group contributes to the steric hindrance for backbiting termination, and the large excess of Et_2Zn also helps to stabilize the living chain ends.

Thermal Properties of PAdA. It has been reported that the bulky adamantane moiety can contribute to the decrease of chain mobility and increase of rotational barrier to backbone bond rotation upon incorporation, which further increase the T_g of the final polymer.[27] In addition, the enhancement of decomposition temperature of polymers by adamantane incorporation was also reported.[31] To evaluate these effects on PAdA, DSC and TGA were used for the characterization of thermal properties. T_g of PAdA with Mw 71.8 kg/mol reached 133 ^oC (**Figure 2-9a**), and is much higher than that of PMA (T_g: 8 ^oC) and PtBA (T_g: 11 ^oC). Compared to polymethacrylates, polyacrylates have greatly increased flexibility of the polymer backbone due to the absence of the α-methyl group so

that polyacrylates have much lower T_gs than the corresponding polymethacrylates. The T_g of 133 ^oC of PAdA is distinctively high and very unique, to the best of our knowledge, because it is rare to find polyacrylates with high T_g—the highest found from the literature is 94 ^oC for poly(isobornyl acrylate), which also has a very bulky side group.[53] The unique T_g makes PAdA a promising candidate for use in acrylic based thermoplastic elastomers with high upper service temperature and enhanced mechanical strength by block copolymerization with acrylates with low T_gs such as poly(*n*-butyl acrylate).[32,33]

The thermal behavior of PAdA synthesized by free radical polymerization and ATRP was studied previously.[33,54] Compared to T_gs of 153 ^oC and 145-151 ^oC as they reported, the PAdA sample in this study is around 20 ^oC lower (133 ^oC). In addition, we measured T_g of another PAdA synthesized by reversible addition fragmentation chain transfer (RAFT) polymerization and obtained similar T_g as 134 ^oC. In general, T_g correlated with molecular weight (MW) so that we measured Tg of PAdA with high MW of 71.8 kg/mol. However, the Tg of PAdA was not increased by increasing MW from 4.3 to 71.8 kg/mol. The effect of tacticity can also be disregarded, since the low isotactic content are normally expected to increase of T_g.[55] Based on the T_g ranges of PMMA from 105 ^oC to 128 ^oC,[56,57] it could be anticipated that the T_g deviation is caused by the difference in synthesis methods, instruments or the characterization parameters.

Figure 2-9b shows the TGA thermograms of a series of polyacrylates. Poly(methyl acrylate) (PMA) and PtBA were synthesized by radical polymerization, and the PAdA shown was polymerized anionically, as shown in **Run 10 Table 2-1**. As reported previously, the *tert*-butyl ester moiety of PtBA decomposed at 228 ^{o}C to yield isobutene and poly(acrylic acid) (PAA). This can be confirmed by the weight ratio left after the first transition, with around 56% left, corresponding to the molecular weight ratio of PAA to PtBA. The weight loss afterward from 255 ^{o}C to 445 ^{o}C was attributed to the degradation of the PAA remaining. In contrast, PMA gave the degradation temperature (T_d) at 343 ^{o}C (with 5% weight loss). The thermal stability of PMA is reasonable, since the degradation occurred with no decomposition of the side chain. Surprisingly, even containing the ester group connecting with a tertiary carbon like PtBA, PAdA showed a sufficiently high T_d of 376 ^{o}C. The decomposition of the distorted bridgehead alkene, adamantane, is thermodynamically unfavorable,[58] thus leading to the outstanding thermal stability of PAdA.

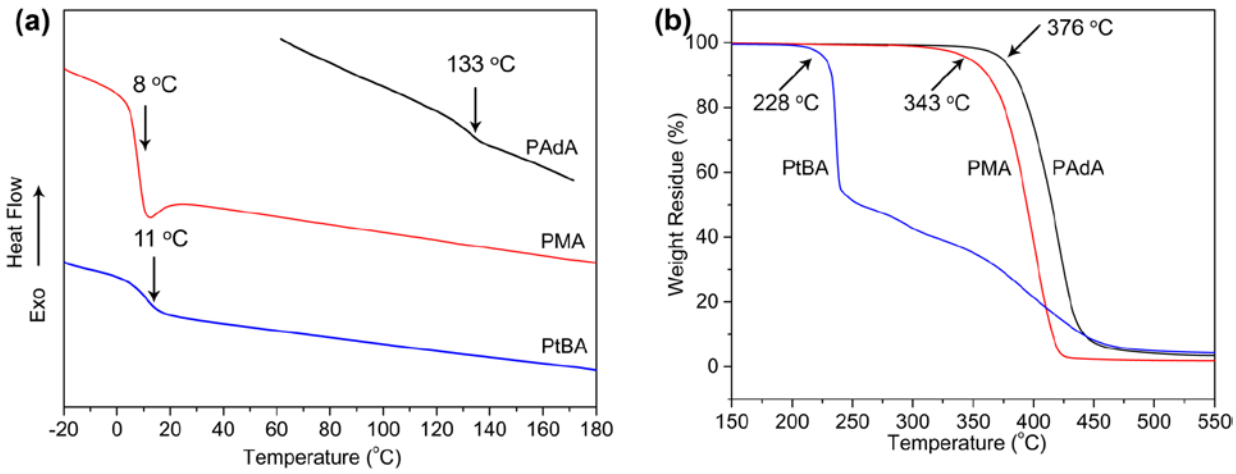

Figure 2-9. The thermal properties of polymers including PAdA with Mn 71.8 kg/mol, PtBA 54.2 kg/mol, and PMA 110.4 kg/mol. a) DSC thermogram of polymers under nitrogen at a heating rate of 10 ^{o}C min^{-1}; b) TGA thermograms of polymers under nitrogen at a heating rate of 10 ^{o}C min^{-1}.

2.1.4 Conclusion

The living anionic polymerization of 1-adamantyl acrylate (AdA) was successfully achieved for the first time using DPMK as an initiator, with a large excess of diethyl zinc (Et_2Zn) in THF at -78 ^oC. Compared to other acrylates like tBA and 2EtHA, a lager excess (40-fold relative to DPMK) of Et_2Zn is required to control the polymerization. The polymerization was completed within 5 min, giving various molecular weight from 4.3 kg/mol to 71.8 kg/mol with PDIs lower than 1.1 and quantitative yields. The PAdA made exhibited a low level of isotactic content, attributing to the bulk pendent group and coordination complex between enolate and zinc cation. It was demonstrated that the living chain end of PAdA has comparable reactivity to that of PMMA via sequential block copolymerization. Moreover, the chain ends of PAdA showed distinct living properties superior to that of other acrylates which were used to build PAdA-*b*-PMMA with 100% incorporation of PAdA homopolymer. The homopolymer of PAdA exhibits outstanding thermal behavior with a much higher glass transition temperature (T_g: 133 ^oC) and degradation temperature (T_d: 376 ^oC) than other acrylic polymers such as poly(*tert*-butyl acrylate) and poly(methyl acrylate).

2.2 Solution Properties, Unperturbed Dimensions and Chain Flexibility of Poly(1-Adamantyl Acrylate)

2.2.1 Introduction

The very high glass transition temperature and thermal stability make PAdA a promising candidate for acrylic-based thermoplastic elastomers with elevated upper service temperature and enhanced mechanical strength. It has been reported that the decrease of chain mobility and an increase of rotational barrier to backbone rotation upon incorporation of the bulky 1-adamantyl moiety contributes to this exceptional thermal behavior.[27] However, the quantitative evaluation of the stiffness of this polymer chain has not been previously reported.

Many series of polymers, including polymethacrylates and polystyrene derivatives, have been investigated previously, and these studies showed the influence of the rigidity and the bulkiness of the side groups on conformational characteristics.[59-61] However to date, the systematic study on the conformation of polyacrylates is much more limited, due to the lack of studies on polymers with varied structure, controlled molecular weights, and low polydispersities.

Herein, we report the dilute solution properties and conformational characteristics of PAdA in different solvents based on different techniques, including nuclear magnetic resonance spectroscopy (NMR), size exclusion chromatography (SEC) equipped with viscometric and multi-angle light scattering (MALLS) detectors, and stand-alone multiangle laser light scattering.

2.2.2 Experimental Part

Sample preparation. Different samples of poly(1-adamantyl acrylate) (PAdA) were synthesized via anionic polymerization based on our previously reported procedure,[62] in order to meet the requirements of low polydispersity indices (PDIs) and consistent tacticity. Among them, the polymer produced by diphenylmethylpotassium/diethylzinc (DPMK/Et_2Zn) initiator system exhibited the narrow PDI of 1.10 (PAdA-N in **Table 2-3**). In contrast, the PAdA specimens obtained using the sec-butyllithium/diphenylethylene/lithium chloride (*sec*-BuLi/DPE/LiCl) initiator system showed rather broad PDI of 2.57. (PAdA-B in **Table 2-3**).

Measurements. The tacticity of the polymers was calculated based on ^{13}C NMR spectra measured by a Varian VNMR 500 MHz with $CDCl_3$ as the solvent. Chemical shifts were referenced to the $CDCl_3$ solvent peak at 77.16 ppm.

The specific refractive index increment (*dn/dc*) of PAdA in tetrahydrofuran (THF) at 40 ^oC was determined as 0.1227 mL/g, with a Wyatt Technology Optlab rEX (690 nm). The molecular weights (MWs) and intrinsic viscosities ([η]) were measured in THF at 40 ^oC using a Polymer Laboratories PL-120 SEC system equipped with four detectors consisting of a Polymer Laboratories refractometer, a Precision Detector PD 2040 (2-angle static light scattering detector), a Precision Detector PD2000DLS (2-angle light scattering detector), and a Viscotek 220

Table 2-3. Molecular Characteristics of Poly(1-adamantyl acrylate)[a]

runs	name	initiator system	M_n[b] (kg/mol)	M_w/M_n	triad ratio (mol%)[c]		
					mm	mr	rr
01	PAdA-N	DPMK/Et_2Zn	174.8	1.01	2.1	21.1	76.8
02	PAdA-B	*sec*-BuLi/DPE/LiCl	8.3	2.57	6.3	13.5	80.2

[a]All the polymers were synthesized by anionic polymerization as reported previously.[62] [b]Number-average molecular weight M_n and PDI were measured in THF at 40 ^oC using the Polymer Laboratories PL-120 SEC system, with *dn/dc* as 0.1227 mL/g. [c]Triad ratios were calculated based on the ^{13}C NMR spectra using a Varian VNMR 500 MHz and $CDCl_3$ as the solvent.

differential viscometer. The column set employed consisted of Polymer Laboratories PLgel; 7.5 × 300 mm; 10 μm; 500, 1 × 104, 1 × 106, and 1 × 107 Å.

Static light scattering (SLS) measurements on PAdA-N solutions in different solvents and at different concentrations were performed on a commercial Brookhaven laser scattering spectrometer equipped with a λ = 637 nm laser. The measurement angles ranged from 30° to 100° with an interval of 5°. The radius of gyration (R_g) and second virial coefficient (A_2) were directly calculated using the Rayleigh-Gans-Debye equation and the Brookhaven software.[63]

2.2.3 Result and Discussion

Molecular Characterization of PAdA. The molecular characteristics of polymer samples are summarized in **Table 2-3**. The assignment of the triad peaks of the carbonyl carbons of PAdA is shown in **Figure 2-10**. The resonances at 174.2−173.8, 173.8−173.6 and 173.6−173.3 ppm were assigned to rr, mr and mm triads respectively. As discussed in previous work,[62] the bulkiness of the pendent group and the ligand effect, especially when a large excess of Et_2Zn was used, contribute to the low isotactic (mm) ratio.

Based on the rotational isomeric state (RIS) theory, the unperturbed dimensions of the polymers can be influenced by their stereoregularity.[64] Although the influence is not universal for all kind of polymers either experimentally or theoretically,[65] its role on polymethacrylates are well studied, which can give us

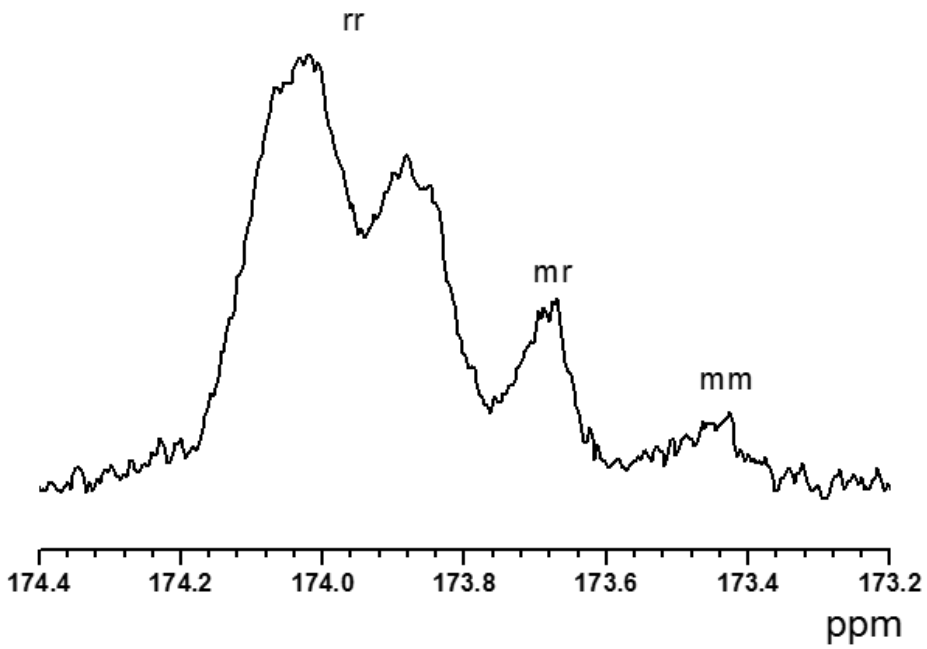

Figure 2-10. ^{13}C NMR spectra of the carbonyl carbons of the PAdA with M_n 8.3 kg/mol (**PAdA-B in Table 1**) measured in $CDCl_3$.

hints on polyacrylates with similar structures.[66] The lower fraction of isotactic diads leads to reduced intrinsic viscosities and smaller unperturbed dimensions. The flexibility of the polymer chains may also be influenced by different tacticities.

Investigation of the Unperturbed Dimensions. Instead of the traditional off-line measurements of molecular weights and intrinsic viscosities using narrowly dispersed polymer samples obtained by controlled synthesis or from solvent-nonsolvent fractionations, the development of modern SEC instrumentation with size sensitive detectors provides a convenient approach for establishing the molecular weight dependence of intrinsic viscosity by using SEC with both light scattering and viscosity detectors. Especially, when a multiple angle laser light scattering detector (MALLS) is used, the radius of gyration, as well as the molecular weight of each near-monodisperse eluting fraction can be determined.[67]

Both PAdA-N and PAdA-B samples were mixed together in a weight ratio around 50/50 to ensure a wide measurement window of molecular weights and intrinsic viscosities. The SEC chromatograph of the resulting PAdA in THF at 40 ^{o}C is shown in **Figure 2-11**. From left to right, the peaks represent light-scattering intensity, differential refractive index (DRI), and viscosity.

The results for molecular weight (M_w) and the intrinsic viscosity ([η]) of each near-monodisperse eluting fraction are plotted, as shown in **Figure 2-12**. Results for radius of gyration showed excessive scatter (due to very low concentrations used) and are not included. The viscosity data may be fitted to the Mark-Houwink

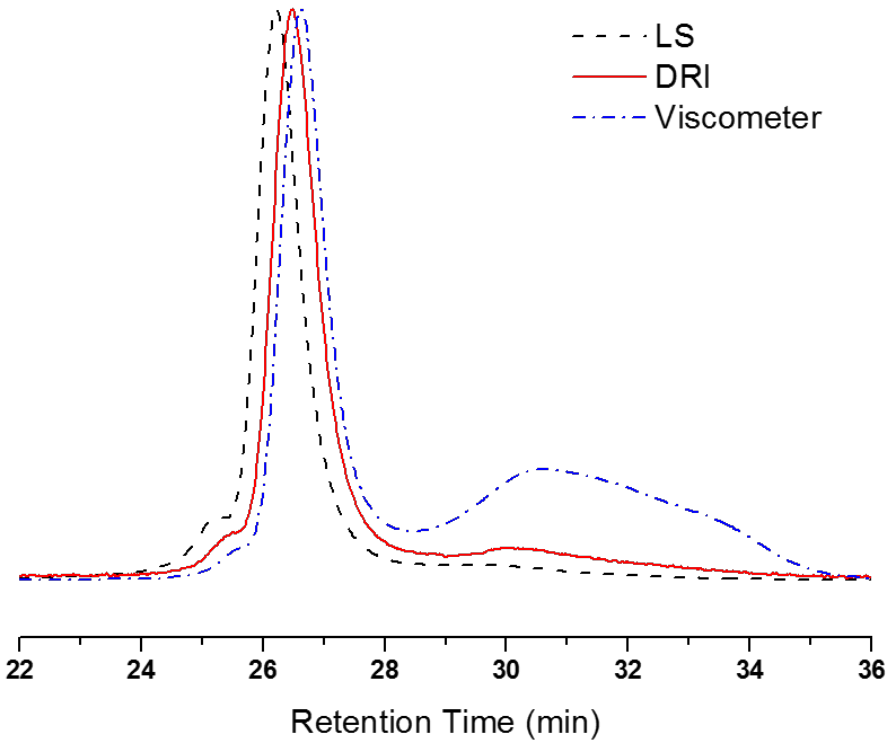

Figure 2-11. SEC chromatograph tracings for the polymer mixture of PAdA-N and PAdA-B (weight ratio around 50/50).

equation and expressed as:

$$[\eta] = 7.0\times10^{-5}{M_w}^{0.67} \qquad \text{(dL/g)} \qquad \textbf{(1)}$$

It is well known that the value of the exponent can be used to evaluate qualitatively the solubility, chain flexibility, and temperature influences on conformational characteristics. The value of 0.5 indicates the theta condition. The coefficient of 0.67 indicates that the polymer has a flexible conformation in THF solution, and that THF is thus a thermodynamically moderate solvent for PAdA.

The [η] of a wormlike chain is calculated for the touched-bead wormlike chain model based on the following equation:[68,69]

$$[\eta] = f(\lambda L, \lambda d_B)(\lambda^2 M_L) \qquad \textbf{(2)}$$

where L, λ^{-1}, and d_B are the contour length, the Kuhn segment length, and the diameter of a bead, respectively. L is related to M_w by $L = M_w/M_L$, for which M_L is the molar mass per unit contour length of the polymer chain. For PAdA in THF, the M_L is 820 nm^{-1} based on the molecular weight of the monomer unit of 206 g/mol. The persistence length of PAdA is 1.2 nm, which is comparable to that of poly(methyl methacrylate) (PMMA, persistence length ~2 nm)[70,71] and polystyrene (PS, persistence length ~1.2 nm).[72] The diameter of a bead (d_B) is 1.0 nm, which is also similar to that of PMMA (~0.8 nm) [22,23] and PS (~1.0 nm).[72] Even though the lack of α-methyl group makes the backbone of polyacrylates more flexible than those for polymethacrylates, the bulky adamantyl group greatly restrained the rotation of the polymer chains and leads to a size comparable to PMMA and PS.

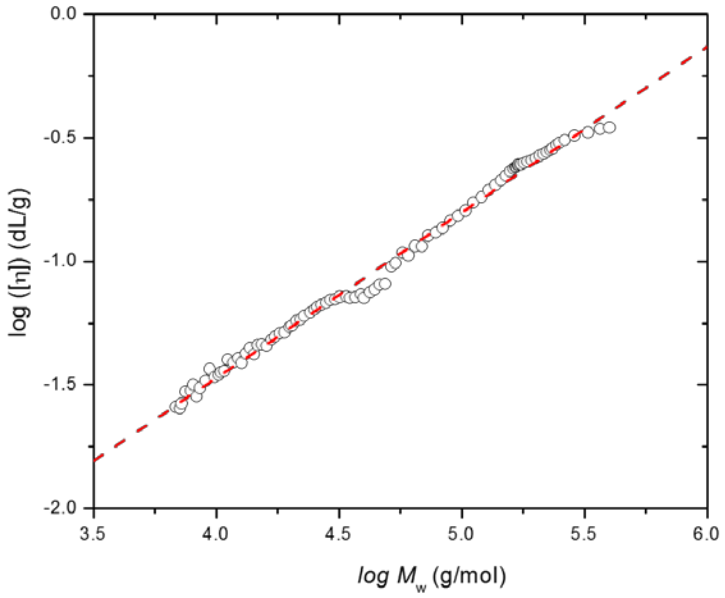

Figure 2-12. Relationships between log [η] and log M_w of PAdA in THF at 40 ^oC.

Further investigation of the unperturbed dimensions of PAdA was performed based on the Burchard-Stockmayer-Fixman (B-S-F) extrapolation procedure for intrinsic viscosity.[73,74] The B-S-F relation can be expressed as the equation below:

$$\frac{[\eta]}{M_w^{\frac{1}{2}}} = K_\theta + 0.51 B \Phi M_w^{\frac{1}{2}} \quad \textbf{(3)}$$

where B is a function of Flory's interaction parameter, polymer specific volume, molar volume of solvent and Avogadro's number. Φ is the universal Flory constant (2.5×10^{21}mol^{-1}). K_θ can be expressed by the Flory-Fox equation as below:[64]

$$K_\theta = \Phi(\langle R^2\rangle_0/M_w)^{3/2} \quad \textbf{(4)}$$

where $\langle R^2\rangle_0$ is the unperturbed mean-square end-to-end distance. Even when theta conditions cannot be achieved experimentally, the B-S-F relationship can still be used to estimate the unperturbed dimensions of the polymer chain.

The other more commonly used term for the estimation of the unperturbed dimension, the characteristic ratio C_∞ can be further calculated, which is defined by Flory as[64]

$$C_\infty = \lim_{n\to\infty}\left[\frac{\langle R^2\rangle_0}{nl^2}\right] = \left(\frac{K_\theta}{\Phi}\right)^{2/3}\frac{M_b}{l^2} \quad \textbf{(5)}$$

where *n* is the number of bonds in the backbone, *l* is the bond length ($l = 0.153\ nm$), M_b is the molecular mass per bond.

The B-S-F plot is shown in **Figure 2-13**. It yields the K_θ as the intercept of $2.9\times10^{-4}\ dL/g$. The characteristic ratio C_∞ is thus 10.4. The K_θ and C_∞ of several

other reported poly(meth)acrylates are also listed in **Table 2-4** for comparison. The unperturbed dimensions in solution (C_∞) and glass transition temperature (T_g) in bulk roughly follow similar trends. With an increase of chain stiffness, they both tend to increase.[75,76] Among polyacrylates studied, the bulky and very rigid 1-adamantyl group makes PAdA the least flexible. Thus both its C_∞ and T_g are much larger than those of poly(methyl acrylate) (PMA) and poly(tetrahydrofurfuryl acrylate) (PTHFA). However, although PMA is more compact, it exhibits a higher T_g than that of PTHFA. The bulky tetrahydrofurfurylmethylene group makes the unperturbed dimension of the latter larger. It should be noted that the reported value of PMA's C_∞ is still inconsistent, ranging from 5.4 to 7.2 depending on different measuring systems and models applied.[77] The existence of the α-methyl group greatly enhances the steric hindrance of the polymer chains in bulk, which causes the T_gs of polymethacrylates to always be larger than polyacrylates with the same pendant groups, this difference is also observed in solution, from the comparison of the C_∞ values between PAdA/PAdMA, PMA/PMMA and PTHF/PTHFMA. Meanwhile, the properties of PAdA, either in bulk or in solution, are outstanding and even superior to polymethacrylates like PMMA and PTHFMA, due to 1-adamantyl group's unique compact structure (diamond lattice and bridged nature).

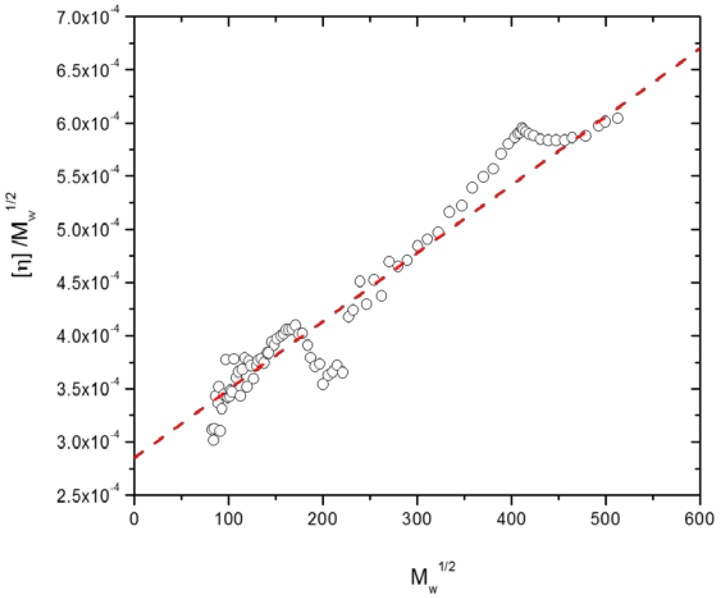

Figure 2-13. Burchard-Stockmayer-Fixman relation for PAdA in THF at 40 ºC.

Table 2-4. Values of K_θ and C_∞ of Poly(meth)acrylates

Polymer	K_θ ($\times 10^4$) (dL/g)	C_∞	T_g (°C)	Ref.
PAdA	2.9	10.4	133	This work, [62]
PMA[a]	5.3	5.4- 7.2	8	75,[78]
PTHFA[b]	3.3	8.6	-11	[79]
PMMA	4.8	7.3	105	[80]
PTHFMA[c]	3.5	9.6	57	[81,82]
PAdMA[d]	5.3	16.9	202	[31,60]

[a]PMA: poly(methayl acrylate); [b]PTHFA: poly(tetrahydrofurfuryl acrylate); [c]PTHFMA: poly(tetrahydrofurfuryl methacrylate); [d]PAdMA: poly(1-adamantyl methacrylate).

Light Scattering. The PAdA sample with narrow PDI (PAdA-N in **Table 2-3**) was used to prepare solutions in various solvents and at different concentrations for light scattering measurements. Different solvent characteristics were evaluated from Zimm plots using static light scattering at 30 ^{o}C, based on the equation below.[83]

$$\frac{Kc}{R_\theta} = \frac{1}{M_w}\left(1 + \frac{1}{3}q^2R_g^2 + \cdots\right) + 2A_2c \qquad \textbf{(6)}$$

where *K* is the constant depending on the studied system, R_θ is the Rayleigh ratio depending on the intensity of the light scattered, *q* is scattering wavevector, R_g is the root-mean-square z-average radium of radius of gyration, *c* is the polymer concentration, and A_2 is the second virial coefficient. The value of A_2 can be used to evaluate the thermodynamic interactions between the solvent and the polymer, i.e. $A_2 > 0$ means it is a good solvent for the polymer; $A_2 < 0$ means it is a poor solvent for polymer; while $A_2 = 0$ means it is a theta solvent.

A typical Zimm plot is shown in **Figure 2-14**, using PAdA in toluene as an example. Based on **Equation 6**, two extrapolations to zero scattering angle ($\theta = 0\ or\ q = 0$) and to zero concentration ($A_2c = 0$) result in the production of $1/M_w$. The slope of $\left(\frac{Kc}{R_\theta}\right)_{c\to 0}$ vs q^2 corresponds to R_g, and the slope of $(\frac{Kc}{R_\theta})_{q\to 0}$ vs c corresponds to A_2. The values of A_2 and R_g for the polymer in different solvents are summarized in **Table 2-5**. The A_2 in THF is rather small, of the order 10^{-5}, which is closer to the theta condition than other solvents studied. Considering that the increase of temperature can enhance the solubility of the polymer, this value

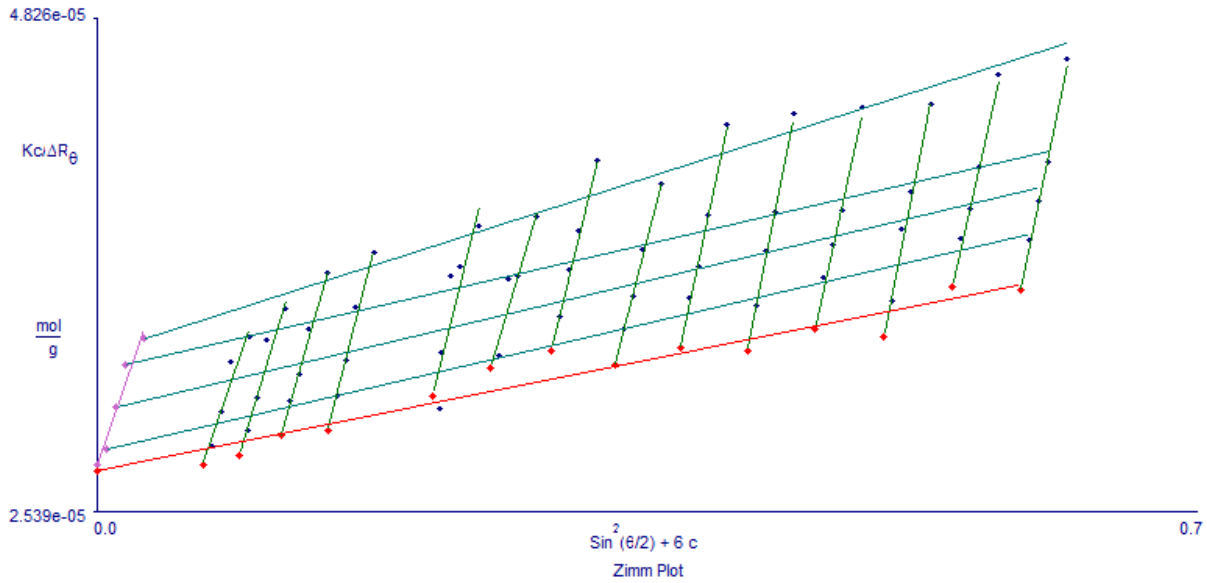

Figure 2-14. Zimm plot for PAdA in toluene at 30 ºC.

Table 2-5. The Values of A_2 and R_g for PAdA in Different Solvents at 30 ^oC.

Solvent	A_2 (X10^4) (cm^3 mol g^{-2})	R_g (nm)
THF	0.5 ± 0.18	60.2 ± 2.7
Toluene	6.3 ± 1.40	43.2 ± 2.0
Cyclohexanone	3.2 ± 0.69	52.0 ± 1.6
Cyclopentanone	2.2 ± 0.32	30.3 ± 1.2
3-Pentanone	-2.1 ± 0.22	16.8 ± 4.9
3-Hexanone	-6.3 ± 3.20	122.0 ± 51
Hexane	-138.0 ± 12	N/A

*Other solvents tested includes 1,4-dioxane (Partially soluble. For 3 mg/mL, cloudy point at around 45 ^oC), methyl ethyl ketone (insoluble) and acetone (insoluble).

of A_2 at 30 ^oC, as well as the Mark-Houwink coefficient of 0.67 in THF at 40 ^oC, indicate that THF is a thermodynamically moderate solvent for PAdA. Several theta solvents of other poly(meth)acrylates and the molecules with similar structures were also evaluated, like hexane (for poly(tert-butyl acrylate at 24.2 ^oC)),[84] and acetone (for poly(phenyl methacrylate at 25 ^oC)).[80] With the increase of solution power, the polymer chain becomes more expanded, thus the R_g will increase. An exception is the observed behavior in toluene and THF which might be caused by specific solvent effects[85] and /or small experimental error. On the other hand, when the solubility is poor enough like that in 3-hexanone and hexane, aggregation and ultimately precipitation occurs that greatly increase the value of R_g. We can expect that in theta condition, the R_g of PAdA tested ranges from 16.8 nm and 30.3 nm from our results.

2.2.4 Conclusion

In this section, the solution properties of poly(1-adamantyl acrylate) (PAdA) in various solvents derived from NMR, SEC with viscometer and MALLS detectors, and multiangle static light scattering were studied. Among all the solvents evaluated, THF is a moderate solvent for PAdA, with a Mark-Houwink coefficient of 0.67 at 40 ^oC and A_2 as 5×10^{-5} $cm^3 \cdot mol/g^2$. The polymer chain has a comparable persistence length, and diameter per bead to those of PMMA and PS. Its characteristic ratio (C_∞) of 10.4 is larger than that of PMMA. All these results

indicate that PAdA is less flexible than common polyacrylates. Even though it lacks the α-methyl group that induces the steric hindrance for polymethacrylates and makes them less flexible than most polyacrylates, the bulky structure of three fused chair-form cyclohexyl rings in a diamond lattice and the bridged nature of the 1-adamantyl pendant group makes PAdA extraordinary low in flexibility as an acrylic polymer. In addition, the second virial coefficient (A_2) of PAdA in different solvents has been measured, which can be used as a reference for further investigations on the theta condition of this polymer. The unperturbed radius of gyration of the polymer sample tested was also expected to be ranging from 16.8 nm to 30.3 nm from the SLS study of these solvents.

References

(1) Szwarc, M. Living'Polymers. *Nature* **1956**, *178*, 1168-1169.

(2) Aoshima, S.; Kanaoka, S. A Renaissance in Living Cationic Polymerization. *Chemical Reviews* **2009**, *109*, 5245-5287.

(3) Bielawski, C. W.; Grubbs, R. H. Living ring-opening metathesis polymerization. *Progress in Polymer Science* **2007**, *32*, 1-29.

(4) Braunecker, W. A.; Matyjaszewski, K. Controlled/living radical polymerization: Features, developments, and perspectives. *Progress in Polymer Science* **2007**, *32*, 93-146.

(5) Hirao, A.; Loykulnant, S.; Ishizone, T. Recent advance in living anionic polymerization of functionalized styrene derivatives. *Progress in polymer science* **2002**, *27*, 1399-1471.

(6) Baskaran, D. Strategic developments in living anionic polymerization of alkyl (meth)acrylates. *Progress in Polymer Science* **2003**, *28*, 521-581.

(7) Baskaran, D.; Müller, A. H. E. Anionic vinyl polymerization—50 years after Michael Szwarc. *Progress in Polymer Science* **2007**, *32*, 173-219.

(8) Anderson, B. C.; Andrews, G. D.; Arthur, P.; Jacobson, H. W.; Melby, L. R.; Playtis, A. J.; Sharkey, W. H. Anionic polymerization of methacrylates. Novel functional polymers and copolymers. *Macromolecules* **1981**, *14*, 1599-1601.

(9) Varshney, S. K.; Hautekeer, J. P.; Fayt, R.; Jerome, R.; Teyssie, P. Anionic polymerization of (meth)acrylic monomers. 4. Effect of lithium salts as

ligands on the "living" polymerization of methyl methacrylate using monofunctional initiators. *Macromolecules* **1990**, *23*, 2618-2622.

(10) Wang, J. S.; Jérôme, R. Mechanistic aspects of ‘ligated’anionic living polymerization (LAP): The case of (meth) acrylic ester monomers. *Journal of Physical Organic Chemistry* **1995**, *8*, 208-221.

(11) Ballard, D. G. H.; Bowles, R. J.; Haddleton, D. M.; Richards, S. N.; Sellens, R.; Twose, D. L. Controlled polymerization of methyl methacrylate using lithium aluminum alkyls. *Macromolecules* **1992**, *25*, 5907-5913.

(12) Allen, R.; Long, T.; McGrath, J. Preparation of high purity, anionic polymerization grade alkyl methacrylate monomers. *Polymer Bulletin* **1986**, *15*, 127-134.

(13) Fayt, R.; Forte, R.; Jacobs, C.; Jerome, R.; Ouhadi, T.; Teyssie, P.; Varshney, S. K. New initiator system for the living anionic polymerization of tert-alkyl acrylates. *Macromolecules* **1987**, *20*, 1442-1444.

(14) Wang, J. S.; Jerome, R.; Warin, R.; Teyssie, P. Anionic polymerization of (meth)acrylic monomers. 12. Effect of lithium chloride on the stereochemistry of the anionic polymerization of methyl methacrylate in THF and in a 9/1 toluene/THF mixture. *Macromolecules* **1993**, *26*, 5984-5990.

(15) Mays, J. W.; Hadjichristidis, N.; Lindner, J. Synthesis and unperturbed dimensions of poly (diphenylmethyl methacrylate). *Journal of Polymer Science Part B: Polymer Physics* **1990**, *28*, 1881-1889.

(16) Kitayama, T.; Shinozaki, T.; Masuda, E.; Yamamoto, M.; Hatada, K. Highly syndiotactic poly (methyl methacrylate) with narrow molecular weight distribution formed by tert-butyllithium-trialkylaluminium in toluene. *Polymer Bulletin* **1988**, *20*, 505-510.

(17) Kitayama, T.; Shinozaki, T.; Sakamoto, T.; Yamamoto, M.; Hatada, K. Living and highly syndiotactic polymerization of methyl methacrylate and other methacrylates by tert - butyllithiumtrialkylaluminium in toluene. *Die Makromolekulare Chemie* **1989**, *15*, 167-185.

(18) Hatada, K.; Ute, K.; Tanaka, K.; Kitayama, T.; Okamoto, Y. Preparation of highly isotactic poly (methyl methacrylate) of low polydispersity. *Polymer journal* **1985**, *17*, 977-980.

(19) Zundel, T.; Teyssié, P.; Jérôme, R. New ligands for the living isotactic anionic polymerization of methyl methacrylate in toluene at 0° C. 1. Ligation of butyllithium by lithium silanolates. *Macromolecules* **1998**, *31*, 2433-2439.

(20) Ozaki, H.; Hirao, A.; Nakahama, S. Anionic polymerization of alkyl methacrylates in the presence of diethylzinc. *Macromolecular Chemistry and Physics* **1995**, *196*, 2099-2111.

(21) Davis, T. P.; Haddleton, D. M.; Richards, S. N. Controlled Polymerization of Acrylates and Methacrylates1. *Journal of Macromolecular Science, Part C* **1994**, *34*, 243-324.

(22) Varshney, S. K.; Jacobs, C.; Hautekeer, J. P.; Bayard, P.; Jerome, R.; Fayt, R.; Teyssie, P. Anionic polymerization of acrylic monomers. 6. Synthesis, characterization, and modification of poly(methyl methacrylate)-poly(tert-butyl acrylate) di- and triblock copolymers. *Macromolecules* **1991**, *24*, 4997-5000.

(23) Wang, J. S.; Jerome, R.; Bayard, P.; Teyssie, P. Anionic Polymerization of Acrylic Monomers. 21. Anionic Sequential Polymerization of 2-Ethylhexyl Acrylate and Methyl Methacrylate. *Macromolecules* **1994**, *27*, 4908-4913.

(24) Nakahama, S.; Kobayashi, M.; Ishizone, T.; Hirao, A.; Kobayashi, M. Polymerization of N,N-Dialkylacrylamides with Anionic Initiators Modified by Diethylzinc. *Journal of Macromolecular Science, Part A* **1997**, *34*, 1845-1855.

(25) Ishizone, T.; Yoshimura, K.; Hirao, A.; Nakahama, S. Controlled Anionic Polymerization of tert-Butyl Acrylate with Diphenylmethyl Anions in the Presence of Dialkylzinc. *Macromolecules* **1998**, *31*, 8706-8712.

(26) Nugay, N.; Nugay, T.; Jérôme, R.; Teyssié, P. Anionic polymerization of primary acrylates as promoted by lithium 2-(2-methoxyethoxy) ethoxide. *Journal of Polymer Science Part A: Polymer Chemistry* **1997**, *35*, 361-369.

(27) Acar, H. Y.; Jensen, J. J.; Thigpen, K.; McGowen, J. A.; Mathias, L. J. Evaluation of the Spacer Effect on Adamantane-Containing Vinyl Polymer Tg's. *Macromolecules* **2000**, *33*, 3855-3859.

(28) Cypcar, C. C.; Camelio, P.; Lazzeri, V.; Mathias, L. J.; Waegell, B. Prediction of the glass transition temperature of multicyclic and bulky substituted acrylate and methacrylate polymers using the energy, volume, mass (EVM) QSPR model. *Macromolecules* **1996**, *29*, 8954-8959.

(29) Mays, J. W.; Siakali-Kioulafa, E.; Hadjichristidis, N. Glass transition temperatures of polymethacrylates with alicyclic side groups. *Macromolecules* **1990**, *23*, 3530-3531.

(30) Ozaki, A.; Sumita, K.; Goto, K.; Matsumoto, A. Synthesis of Poly (decahydro-2-naphthyl methacrylate) s with Different Geometric Structures and Effects of Side-Group Dynamics on Polymer Properties Investigated by Thermal and Dynamic Mechanical Analyses and DFT Calculations. *Macromolecules* **2013**, *46*, 2941-2950.

(31) Ishizone, T.; Tajima, H.; Torimae, H.; Nakahama, S. Anionic Polymerizations of 1-Adamantyl Methacrylate and 3-Methacryloyloxy-1,1′-biadamantane. *Macromolecular Chemistry and Physics* **2002**, *203*, 2375-2384.

(32) Goodwin, A.; Wang, W.; Kang, N.-G.; Wang, Y.; Hong, K.; Mays, J. All-Acrylic Multigraft Copolymers: Effect of Side Chain Molecular Weight and Volume Fraction on Mechanical Behavior. *Industrial & Engineering Chemistry Research* **2015**, *54*, 9566-9576.

(33) Nakano, Y.; Sato, E.; Matsumoto, A. Synthesis and thermal, optical, and mechanical properties of sequence‐controlled poly (1‐adamantyl

acrylate) ‐ block ‐ poly (n ‐ butyl acrylate) containing polar side group. *Journal of Polymer Science Part A: Polymer Chemistry* **2014**, *52*, 2899-2910.

(34) Eftink, M. R.; Andy, M. L.; Bystrom, K.; Perlmutter, H. D.; Kristol, D. S. Cyclodextrin inclusion complexes: studies of the variation in the size of alicyclic guests. *Journal of the American Chemical Society* **1989**, *111*, 6765-6772.

(35) Li, J.; Zhou, L.; Luo, Q.; Wang, Y.; Zhang, C.; Lu, W.; Xu, J.; Liu, J. Cucurbit[7]uril-Based Vesicles Formed by Self-assembly of Supramolecular Amphiphiles. *Chinese Journal of Chemistry* **2012**, *30*, 2085-2090.

(36) Kakuta, T.; Takashima, Y.; Harada, A. Highly Elastic Supramolecular Hydrogels Using Host–Guest Inclusion Complexes with Cyclodextrins. *Macromolecules* **2013**, *46*, 4575-4579.

(37) Li, L.; Guo, X.; Wang, J.; Liu, P.; Prud'homme, R. K.; May, B. L.; Lincoln, S. F. Polymer Networks Assembled by Host−Guest Inclusion between Adamantyl and β-Cyclodextrin Substituents on Poly(acrylic acid) in Aqueous Solution. *Macromolecules* **2008**, *41*, 8677-8681.

(38) Kavitha, A. A.; Singha, N. K. High temperature resistant tailor-made poly(meth)acrylates bearing adamantyl group via atom transfer radical polymerization. *Journal of Polymer Science Part A: Polymer Chemistry* **2008**, *46*, 7101-7113.

(39) Wang, K.; Cui, R.; Gu, J.; Yu, Q.; Ma, G.; Nie, J. Photopolymerization of 1‐adamantyl acrylate pohotoinitiated by free radical photoinitiators. *Journal of Applied Polymer Science* **2012**, *123*, 26-31.

(40) Kobayashi, S.; Matsuzawa, T.; Matsuoka, S.-i.; Tajima, H.; Ishizone, T. Living anionic polymerizations of 4-(1-adamantyl) styrene and 3-(4-vinylphenyl)-1, 1'-biadamantane. *Macromolecules* **2006**, *39*, 5979-5986.

(41) Uhrig, D.; Mays, J. W. Experimental techniques in high-vacuum anionic polymerization. *Journal of Polymer Science Part A: Polymer Chemistry* **2005**, *43*, 6179-6222.

(42) Candau, F.; Afchar-Taromi, F.; Rempp, P. Synthesis and characterization of polystyrene-poly(ethylene oxide) graft copolymers. *Polymer* **1977**, *18*, 1253-1257.

(43) Lai, J. T.; Filla, D.; Shea, R. Functional polymers from novel carboxyl-terminated trithiocarbonates as highly efficient RAFT agents. *Macromolecules* **2002**, *35*, 6754-6756.

(44) Hadjichristidis, N.; Iatrou, H.; Pispas, S.; Pitsikalis, M. Anionic polymerization: High vacuum techniques. *Journal of Polymer Science Part A: Polymer Chemistry* **2000**, *38*, 3211-3234.

(45) Janata, M.; Lochmann, L.; Müller, A. H. E. Mechanisms and kinetics of the anionic polymerization of acrylates, 3. Effect of lithium chloride and lithium

tert-butoxide on the oligomerization of tert-butyl acrylate. *Die Makromolekulare Chemie* **1993**, *194*, 625-636.

(46) Cho, Y.-S.; Kim, S.-W.; Ihn, C.-S.; Lee, J.-S. Anionic polymerization of 4-(9-carbazolyl)methylstyrene. *Polymer* **2001**, *42*, 7611-7616.

(47) Kang, N.-G.; Changez, M.; Kim, M.-J.; Lee, J.-S. Effect of Biphenyl Spacers on the Anionic Polymerization of 2-(4′ -Vinylbiphenyl-4-yl) pyridine. *Macromolecules* **2014**, *47*, 6706-6714.

(48) Lochmann, L.; Rodová, M.; Trekoval, J. Anionic polymerization of methacrylate esters initiated with esters of α-metallocarboxylic acids. *Journal of Polymer Science: Polymer Chemistry Edition* **1974**, *12*, 2091-2094.

(49) Welch, F. J. Polymerization of Styrene by n-Butyllithium. II. Effect of Lewis Acids and Bases1. *Journal of the American Chemical Society* **1960**, *82*, 6000-6005.

(50) Shannon, R. Revised effective ionic radii and systematic studies of interatomic distances in halides and chalcogenides. *Acta Crystallographica Section A* **1976**, *32*, 751-767.

(51) Wang, J.-S.; Jérôme, R.; Teyssieacute; Philippe. Mechanistic aspects of ‘ligated’ anionic living polymerization (LAP): The case of (meth)acrylic ester monomers. *Journal of Physical Organic Chemistry* **1995**, *8*, 208-221.

(52) Bentley, T. W.; Carter, G. E. The SN2-SN1 spectrum. 4. The SN2 (intermediate) mechanism for solvolyses of tert-butyl chloride: a revised Y scale of

solvent ionizing power based on solvolyses of 1-adamantyl chloride. *Journal of the American Chemical Society* **1982**, *104*, 5741-5747.

(53) Wouters, D.; Van Camp, W.; Dervaux, B.; Du Prez, F. E.; Schubert, U. S. Morphological transition during the thermal deprotection of poly(isobornyl acrylate)-b-poly(1-ethoxyethyl acrylate). *Soft Matter* **2007**, *3*, 1537-1541.

(54) Matsumoto, A.; Tanaka, S.; Otsu, T. Synthesis and characterization of poly (1-adamantyl methacrylate): effects of the adamantyl group on radical polymerization kinetics and thermal properties of the polymer. *Macromolecules* **1991**, *24*, 4017-4024.

(55) Thompson, E. V. Dependence of the glass transition temperature of poly (methyl methacrylate) on tacticity and molecular weight. *Journal of Polymer Science Part A‐2: Polymer Physics* **1966**, *4*, 199-208.

(56) Condo, P. D.; Paul, D. R.; Johnston, K. P. Glass transitions of polymers with compressed fluid diluents: type II and III behavior. *Macromolecules* **1994**, *27*, 365-371.

(57) Zawada, J. A.; Ylitalo, C. M.; Fuller, G. G.; Colby, R. H.; Long, T. E. Component relaxation dynamics in a miscible polymer blend: poly(ethylene oxide)/poly(methyl methacrylate). *Macromolecules* **1992**, *25*, 2896-2902.

(58) Gagosian, R. B.; Dalton, J. C.; Turro, N. J. Molecular photochemistry. XXXIII. Photochemistry of 1-adamantylacetone. *Journal of the American Chemical Society* **1970**, *92*, 4752-4754.

(59) Hadjichristidis, N.; Mays, J.; Ferry, W.; Fetters, L. J. Properties and chain flexibility of poly(dl-isobornyl methacrylate). *Journal of Polymer Science: Polymer Physics Edition* **1984**, *22*, 1745-1751.

(60) Matsumoto, A.; Tanaka, S.; Otsu, T. Local conformation of poly(1-adamantyl methacrylate) evaluated from intrinsic viscosity. *Colloid and Polymer Science* **1992**, *270*, 17-21.

(61) Mays, J. W.; Ferry, W. M.; Hadjichristidis, N.; Funk, W. G.; Fetters, L. J. Solution properties and chain flexibility of poly(p-tert-butylstyrene). *Polymer* **1986**, *27*, 129-132.

(62) Lu, W.; Huang, C.; Hong, K.; Kang, N.-G.; Mays, J. W. Poly(1-adamantyl acrylate): Living Anionic Polymerization, Block Copolymerization, and Thermal Properties. *Macromolecules* **2016**, *49*, 9406-9414.

(63) Hiemenz, P. C.; Rajagopalan, R.: *Principles of colloid and surface chemistry*; CRC press, 1997.

(64) Flory, P.; Volkenstein, M.: Statistical mechanics of chain molecules. Wiley Online Library, 1969.

(65) Jenkins, R.; Porter, R. S.: Unperturbed dimensions of stereoregular polymers. In *Properties of Polymers*; Springer, 1980; pp 1-20.

(66) Jenkins, R.; Porter, R. S. Measurement of the unperturbed dimensions of stereoregular poly(methyl methacrylate). *Polymer* **1982**, *23*, 105-111.

(67) Jackson, C.; Chen, Y. J.; Mays, J. W. Dilute solution properties of randomly branched poly (methyl methacrylate). *Journal of applied polymer science* **1996**, *59*, 179-188.

(68) Yamakawa, H.; Yoshizaki, T.: *Helical wormlike chains in polymer solutions*; Springer, 1997; Vol. 1.

(69) Yun, S. I.; Terao, K.; Hong, K.; Melnichenko, Y. B.; Wignall, G. D.; Britt, P. F.; Mays, J. W. Solution properties of 1, 3-cyclohexadiene polymers by laser light scattering and small-angle neutron scattering. *Macromolecules* **2006**, *39*, 897-899.

(70) Fujii, Y.; Tamai, Y.; Konishi, T.; Yamakawa, H. Intrinsic viscosity of oligo- and poly(methyl methacrylate)s. *Macromolecules* **1991**, *24*, 1608-1614.

(71) Yoshizaki, T.; Nitta, I.; Yamakawa, H. Transport coefficients of helical wormlike chains. 4. Intrinsic viscosity of the touched-bead model. *Macromolecules* **1988**, *21*, 165-171.

(72) Yamada, T.; Yoshizaki, T.; Yamakawa, H. Transport coefficients of helical wormlike chains. 5. Translational diffusion coefficient of the touched-bead model and its application to oligo- and polystyrenes. *Macromolecules* **1992**, *25*, 377-383.

(73) Burchard, V. W. ÜBer den einfluß der lösungsmittel auf die struktur linearer makromoleküle. I. *Macromolecular Chemistry and Physics* **1961**, *50*, 20-36.

(74) Stockmayer, W. H.; Fixman, M. On the estimation of unperturbed dimensions from intrinsic viscositiesxcin. *Journal of Polymer Science Part C: Polymer Symposia* **1963**, *1*, 137-141.

(75) Hooshmand-Mozaffar, F.; Hoseinalizadeh-Khorasani, M.; Huglin, M. B. Unperturbed dimensions of poly (phenyl acrylate). *Polymer* **1980**, *21*, 413-416.

(76) Xu, Z.; Hadjichristidis, N.; Fetters, L.; Mays, J.: Structure/chain-flexibility relationships of polymers. In *Physical Properties of Polymers*; Springer, 1995; pp 1-50.

(77) Matsuda, H.; Yamano, K.; Inagaki, H. Styrene-methyl acrylate copolymers and acrylate homopolymers in solution. *Journal of Polymer Science Part A-2: Polymer Physics* **1969**, *7*, 609-633.

(78) Takahashi, A. T. Kamei, and I. Kagawa. *Nippon Kagaku Zasshi* **1962**, *83*, 14.

(79) Zioga, A.; Ekizoglou, N.; Siakali-Kioulafa, E.; Hadjichristidis, N. Characteristic ratio of poly(tetrahydrofurfuryl acrylate) and poly(2-ethylbutyl acrylate). *Journal of Polymer Science Part B: Polymer Physics* **1997**, *35*, 1589-1592.

(80) Mays, J. W.; Hadjichristidis, N. Characteristic Ratios of Polymethacrylates. *Journal of Macromolecular Science, Part C* **1988**, *28*, 371-401.

(81) Zafar, M. M.; Mahmood, R. Viscosities of dilute solutions of poly (tetrahydrofurfuryl methacrylate). *Macromolecular Chemistry and Physics* **1974**, *175*, 903-912.

(82) Goh, S. H. Miscible blends of poly(tetrahydrofurfuryl methacrylate) with two hydroxyl-containing polymers. *Polymer Bulletin* **1987**, *17*, 221-224.

(83) Zimm, B. H. The scattering of light and the radial distribution function of high polymer solutions. *The Journal of chemical physics* **1948**, *16*, 1093-1099.

(84) Jerome, R.; Desreux, V. Hydrodynamic properties and unperturbed dimensions of polytert.butylacrylate in different solvents. *European Polymer Journal* **1970**, *6*, 411-421.

(85) Graessley, W. W. Polymer chain dimensions and the dependence of viscoelastic properties on concentration, molecular weight and solvent power. *Polymer* **1980**, *21*, 258-262.

CHAPTER 3 ALL ACRYLIC-BASED THERMOPLASTIC ELASTOMERS WITH HIGH SERVICE TEMPERATURE AND DISTINCT MECHANICAL STRENGTH

Abstract

All acrylic based thermoplastic elastomers (TPEs) offer potential alternates to the widely-used styrenic TPEs. However, the high entanglement molecular weight (M_e) of polyacrylates leads to “disappointing” mechanical performance as compared to styrenic TPEs. In this study, the triblock copolymers composed of alkyl acrylates with different pendant groups and glass transition temperatures (T_gs), i.e. 1-adamatyl acrylate (AdA) and tetrahydrofurfuryl acrylate (THFA), were synthesized via reversible addition-fragmentation chain transfer (RAFT) polymerization. Thermal characterization of the resulting polymers was performed using differential scanning calorimetry (DSC) and the T_gs of both segments were observed. The distinct microphase separation behavior was further demonstrated using atomic-force microscopy (AFM) and small angle X-ray scattering (SAXS). Dynamic mechanical analysis (DMA) showed the softening temperature of PAdA domain was 123 ^{o}C, which is higher than that of both styrenic TPEs and commercial acrylic based TPEs with poly(methyl methacrylate) (PMMA) hard block. The resulting triblock copolymers exhibited stress-strain behavior superior to the conventional all acrylic based TPEs composed of PMMA and poly(*n*-butyl acrylate) (PBA).

3.1 Introduction

In this chapter, a new type of all-acrylic TPE composed of poly(1-adamantyl acrylate) (PAdA) and poly(tetrahydrofurfuryl acrylate) (PTHFA) is reported. PAdA was used as the glassy segment with T_g of around 133 ^oC, which is extraordinarily high for polyacrylates. Its distinct thermal property has been discussed in our previous publication and in Chapter 2. The bulky adamantyl group contributes to the decrease of chain mobility and an increase of rotational barrier to backbone bond rotation upon its incorporation.[1] PTHFA was used as the elastomeric domain, with T_g of around -13 ^oC. We expected that the great difference in glass transition temperatures and the dipole moments of the pendent groups (Adamantane: 0.237 D,[2] and THF: 1.404 D[3]) can lead to great thermodynamic mismatch and good microphase separation behavior. This will, in return, help to improve the mechanical property of the block copolymer synthesized.[4]

The triblock copolymer of PAdA-b-PTHFA-b-PAdA was synthesized via RAFT polymerization using dibenzyl trithiocarbonate (DBTTC) as the difunctional chain transfer agent (CTA). This CTA has been generally applied for the polymerization of triblock copolymers of (meth)acrylates.[5] Triblock copolymers with different molecular weights and different ratios between hard and soft segments were produced. The resulting polymers were characterized using nuclear magnetic resonance spectroscopy (NMR) and size exclusion chromatography (SEC) to confirm the chemical structure and composition. The microphase separation

behavior was studied via various methods including differential scanning calorimetry (DSC), atomic-force microscopy (AFM) and small angle X-ray scattering (SAXS). The mechanical properties and viscoelastic properties were characterized by dynamic mechanical analysis (DMA) and uniaxial tensile tests.

3.2 Experimental Part

Materials. The monomer of AdA was synthesized as reported in previous work.[6] Tetrahydrofurfuryl acrylate (TCI America, >98.0%) were used directly after passed through aluminum oxide (Acros Organics, basic) column to remove inhibitor. 2,2-Azobis-(isobutyronitrile) (AIBN, Sigma-Aldrich, 90%) was recrystallized before use and the dibenzyl trithiocarbonate (DBTTC) was synthesized following the procedure previously published.[7] Benzene (Sigma-Aldrich, ≥99.9) was used as received. Both AIBN and DBTTC was dissolved in benzene to make the stock solutions (0.1 mmol/ml) before use.

Preparation of PAdA Macromolecular Chain Transfer Agent (PAdA-CTA-PAdA). PAdA-CTA-PAdA was polymerized through reversible addition–fragmentation chain transfer (RAFT) polymerization under high-vacuum conditions (10^{-6} mmHg) in a glass apparatus. AdA, AIBN, DBTTC, and benzene were mixed together in a vial. The solution was transferred to an ampule, which was degassed by three freeze-thaw-evacuate cycles. The ampule was flame sealed under vacuum and immersed in an oil bath at 70 ^{o}C for the desired time. The polymerization was quenched with liquid nitrogen. The product solution was

precipitated in large excess of methanol with vigorous stirring and vacuum dried overnight. A similar procedure was used to prepare PTHFA homopolymer for the comparison of the thermal properties with triblock copolymers.

Preparation of PAdA-b-PTHFA-b-PAdA (ATA) Triblock Copolymers. ATA triblock copolymers were made by RAFT polymerization using PAdA-CTA-PAdA as the macro chain transfer agent and AIBN as the initiator in benzene. All the polymerizations were carried out under high-vacuum conditions (10^{-6} mmHg) in a glass apparatus. THFA monomer, AIBN, AdA-CTA-PAdA, and benzene were mixed together in a vial. The solution was transferred to an ampule, which was degassed by three freeze-thaw-evacuate cycles. The ampule was flame sealed under vacuum and immersed in an oil bath at 75 ^{o}C. Different reaction time was used to reach different target molecular weights. The polymerization was quenched with liquid nitrogen. The product solution was precipitated in a large excess of methanol with vigorous stirring and vacuum dried overnight.

Chemical and Thermal Property Characterization. The molecular weights (MWs) of the polymers were tested using a Polymer Laboratories PL-120 SEC system equipped with four detectors consisting of a Polymer Laboratories refractometer, a Precision Detector PD 2040 (2-angle static light scattering detector), a Precision Detector PD2000DLS (2-angle light scattering detector), and a Viscotek 220 differential viscometer. The column set employed consisted of Polymer Laboratories PLgel; 7.5 × 300 mm; 10 μm; 500, 1 × 104, 1 × 106, and 1

× 107 Å. Thermal properties were characterized by differential scanning calorimetry (DSC, TA instrument Q-2000) under nitrogen with a heating rate of 10 ^{o}C/min.

Microphase Separation Behavior Characterization. Morphological measurements were performed using atomic force microscopy (AFM) and small-angle X-ray scattering (SAXS).

To prepare samples for AFM measurement, a solution of 50 mg of polymer in 2ml of toluene was stirred overnight at room temperature. Silicon wafers were cleaned by soaking in deionized water, acetone, and isopropanol for one hour in each solvent. Then, the polymer solution was spin-cast on the silicon wafer (1500 rpm for 30 s and 300 rpm for another 30 s). The resulting thin films were dried and annealed at 160 ^{o}C for 2 days prior to the measurement. AFM images were collected on Asylum Research MFP3D with a multimode controller at room temperature in tapping mode with an Al reflex coated Si tip (radius 9±2 nm) at a line scanning frequency of 1 Hz.

Samples for SAXS were prepared as follows: A solution of 100 mg of polymer in 1 ml of toluene was stirred overnight at room temperature and cast into a 1 ml PTFE Griffin beaker and evaporated slowly over 7 days, resulting in film thicknesses of 0.5-1 mm. All dried samples were annealed at 160 ^{o}C under vacuum (10^{-6} mmHg) before measurements. SAXS/WAXS experiments were conducted at 12-ID-B at Advanced Photon Source at Argonne National Laboratory. X-rays of

wavelength λ= 0.89Å were used, and each measurement was performed at two different sample-to-detector distances to cover a q-range of 0.0026 < q < 4.4 $Å^{-1}$, where $q = \left(\frac{4\pi}{\lambda}\right)\sin(\theta/2)$ is the magnitude of the scattering vector, and θ is the scattering angle.

Measurements of Mechanical Properties. The characterization of mechanical properties included dynamic mechanical analysis (DMA) and tensile tests. The samples tested were prepared as follows: A solution of 2.0 g of polymer in 20 ml of toluene was stirred overnight at room temperature and cast into a 25 ml PTFE evaporating dish and evaporated slowly over 7 days, resulting in film thicknesses of around 0.5 mm. Then the samples were dried for 2 days in a vacuum oven at around 50 ^{o}C. The resulting films were cut into uniform dog-bone shaped specimens (ISO 37-4).

Dynamic mechanical analysis was performed on a TA Instruments Q-800 dynamic mechanical analyzer equipped with a single cantilever clamp. The temperature ramp/frequency sweep experiments were run at 1 Hz over a temperature range of −50 to +200 °C. Uniaxial tensile tests were carried out using Instron 4465 with a cross-head velocity of 50 mm/min. For each polymer sample, three identical specimens were tests.

3.3 Results and Discussion

3.3.1 Molecular Characterization of Homopolymers and Triblock Copolymers of PAdA and PTHFA.

The triblock copolymer of ATA was synthesized via RAFT polymerization as shown in **Scheme 3-1**. DBTTC was used as the difunctional CTA to ensure the same molecular weight of the end blocks. Three batches of PAdA-CTA-PAdA samples was synthesized. Based on the PAdA-CTA-PAdA, different feeding ratios and reaction time were applied for the further synthesis of ATA triblock copolymers, details of which as shown in **Table 3-1**. The typical SEC profiles are as shown in **Figure 3-1.**

3.3.2 Thermal Properties of ATA Triblock Copolymers

Thermal properties of the ATA triblock copolymers were investigated using DSC to determine the glass transition temperatures (T_gs). **Figure 3-2** shows a typical DSC thermogram for ATA-26.2-33.5 as the example. Two glass transitions were observed with T_gs at -9 ^oC and 118 ^oC. As compared to the T_gs of PTHFA (-11 ^oC)[8] and PAdA (133 ^oC)[1], the small shifts indicated that the blocks of PAdA and PTHF are slightly miscible with each other. Instead of the only T_g of 49 ^oC for fully miscible copolymers based on the Fox Equation ($\frac{1}{Tg} = \frac{\omega_1}{T_{g,1}} + \frac{\omega_2}{T_{g,2}}$, where ω is the weight fractions of each component)[9], the observation of two T_gs with similar

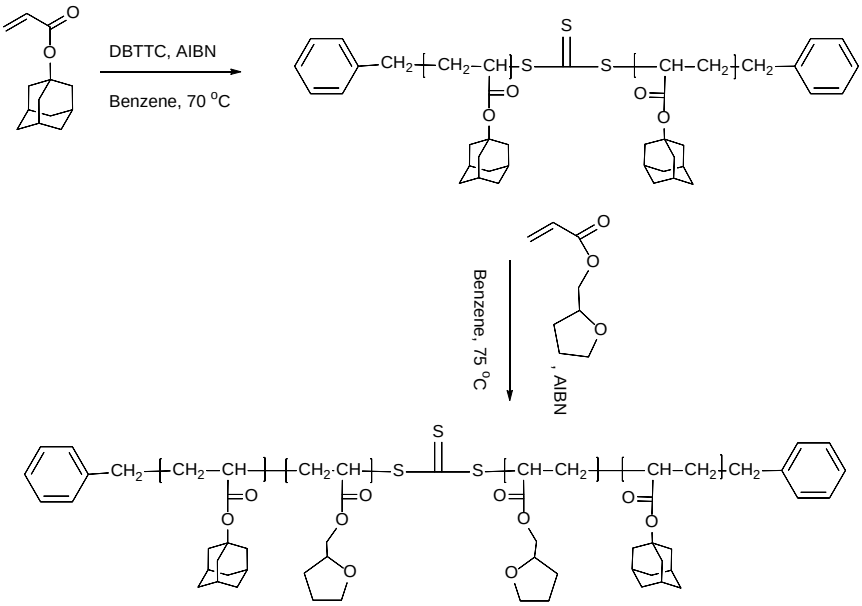

Scheme 3-1. Synthesis of PAdA-b-PTHFA-b-PAdA triblock copolymers.

Table 3-1. Molecular Characteristics of ATA Triblock Copolymers

Sample ID[a]	M_n(PAdA)/PDI[b] (kg/mol)	M_n(Triblock)/PDI[b] (kg/mol)	M_n(THFA)[c] (kg/mol)	wt% of PAdA[d]
ATA-28.6-14.3	28.6/1.21	200.7/3.03	172.1	14.3
ATA-28.6-60.6	28.6/1.21	47.2/1.97	18.6	60.6
ATA-28.6-27.1	28.6/1.21	105.4/2.20	76.8	27.1
ATA-26.2-33.5	26.2/1.08	78.1/1.98	51.9	33.5
ATA-26.2-53.0	26.2/1.08	49.5/1.66	23.3	53.0
ATA-16.2-18.7	16.2/1.16	86.8/2.07	70.6	18.7
ATA-16.2-25.4	16.2/1.16	63.7/1.90	47.5	25.4
PAdA	26.2/1.08	N/A	N/A	N/A
PTHFA	N/A	N/A	14.7/1.14	N/A

[a]Sample identification ATA-M_n(PAdA)-wt% of PAdA. [b]Number-average molecular weight M_n and PDI were measured in THF at 40 °C using the Polymer Laboratories PL-120 SEC system, with *dn/dc* as 0.1227 mL/g for PAdA and 0.065 for PTHFA. [c]M_n(THFA)= M_n(Triblock) - M_n(PAdA). [d]wt% of PAdA = M_n(PAdA)/M_n(Triblock)× 100%

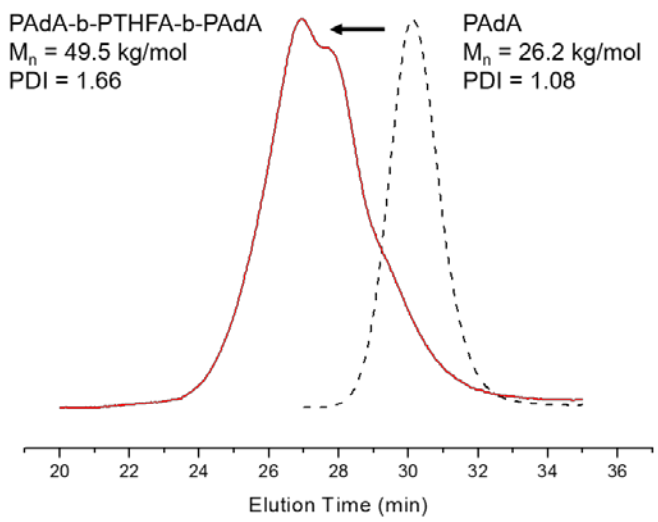

Figure 3-1. SEC profile of ATA-26.2-53.0 from **Table 3-1.**

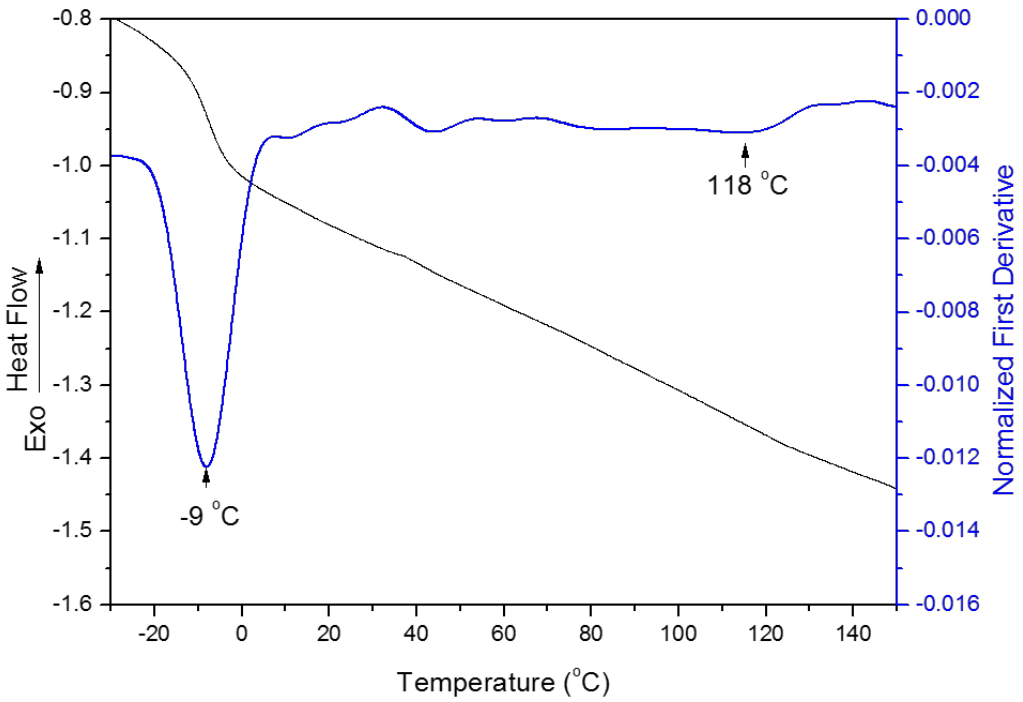

Figure 3-2. DSC thermograph of ATA-26.2-33.5 from **Table 3-1** and its normalized first derivative.

values of each homopolymer gave the indirect indication of the microphase separation behavior in the ATA triblock copolymers.

3.3.3 Microphase Separation Behaviors of ATA Triblock Copolymers

The microphase separation behaviors of the resulting ATA triblock copolymers were directly investigated using AFM and SAXS. As shown in **Figure 3-3**, clear microphase separation can be observed by the comparison of the height image and phase image of ATA-16.2-25.4. The bright regions of the phase image represent the stiff domain, i.e. PAdA, due to the increase of phase angle of the probe oscillation.[10] More precise identification of the morphology can be observed by the SAXS profiles shown in **Figure 3-4**. With the weight percent of PAdA changes from 60.6% to 25.4% and 14.3%, the bulk morphology of the resulting polymers changes from lamella structure to hexagonal and spherical structures. It should be noticed that the further growth of the polymer chain lead to the broadening of the polydispersity indices. Thus, the long range order of the resulting polymers was damaged, resulting in the broadening of the peaks in SAXS profiles and the absence of several peaks. Domain spacings ($D = 2\pi/q^*$), were calculated from the principla scattering peak position (q*), and gave the value of 40.5 nm for ATA-28.6-60.6 and 69.8 nm for ATA-16.2-25.4 and ATA-28.6-14.3.

The distinct microphase separation behavior of the triblock copolymers demonstrated by both AFM and SAXS indicate the great thermodynamic incompability between PAdA and PTHFA domains. Even though these polymers

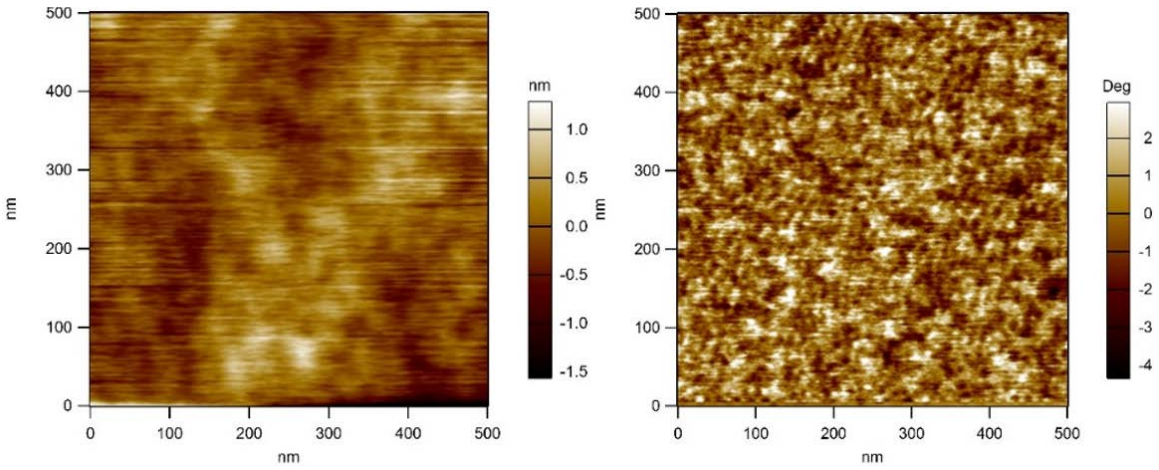

Figure 3-3. AFM images of ATA-16.2-25.4 in **Table 3-1**: (left) height image; (right) phase image.

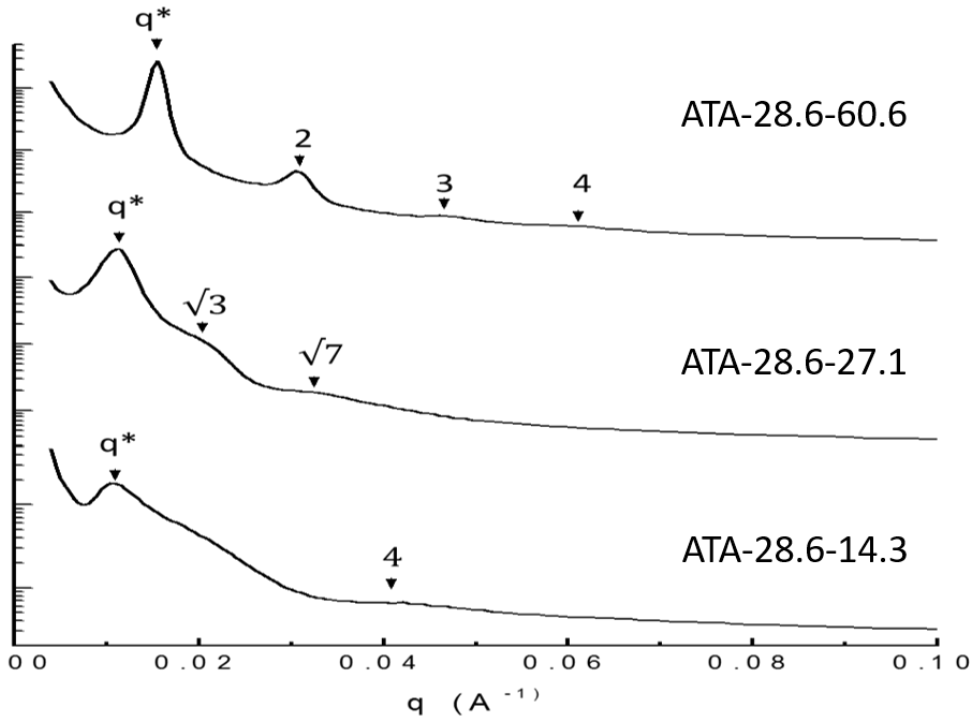

Figure 3-4. SAXS profiles of ATA-28.6-14.3, ATA-16.2-25.4, ATA-28.6-60.6 in **Table 3-1.**

have the same backbone, the great difference in the dipole moment might lead to the increase in Flory-Huggins interaction parameter (χ), which helps to improve the phase separation behavior[11]. The formation of the soft matrix by PTHFA and physical crosslinking junctions by the aggregation of PAdA can be reinforced, which can contribute to the enhancement of the mechanical property of the resulting TPEs.

3.3.4 Mechanical Properties of ATA Triblock Copolymers

The storage modulus, loss modulus, and tan δ over a temperature range from -50 ^{o}C to 200 ^{o}C were investigated through dynamic mechanical analysis (**Figure 3-5**). At low temperature, the relaxation process was observed at -4 ^{o}C corresponding to the glass-rubber transition of the PTHFA phase indicated by a stepwise decrease in storage modulus and a peak in loss modulus. This transition temperature is close to the T_g of PTHF in the ATA triblock copolymers as observed from DSC thermograph (-9 ^{o}C, the first transition as shown in **Figure 3-2**). The further heating caused the storage modulus to drop sharply until reaching the rubbery plateau starting from around 43 ^{o}C, where the storage modulus did not experience obvious change with the increase of temperature. The pronounced drop of the storage modulus was observed again when the temperature reached around 123 ^{o}C, which indicated the softening temperature of the material. Similar to the first transition, this temperature was also close to the T_g of PAdA in the ATA triblock copolymers as observed from DSC thermograph (118 ^{o}C, the second

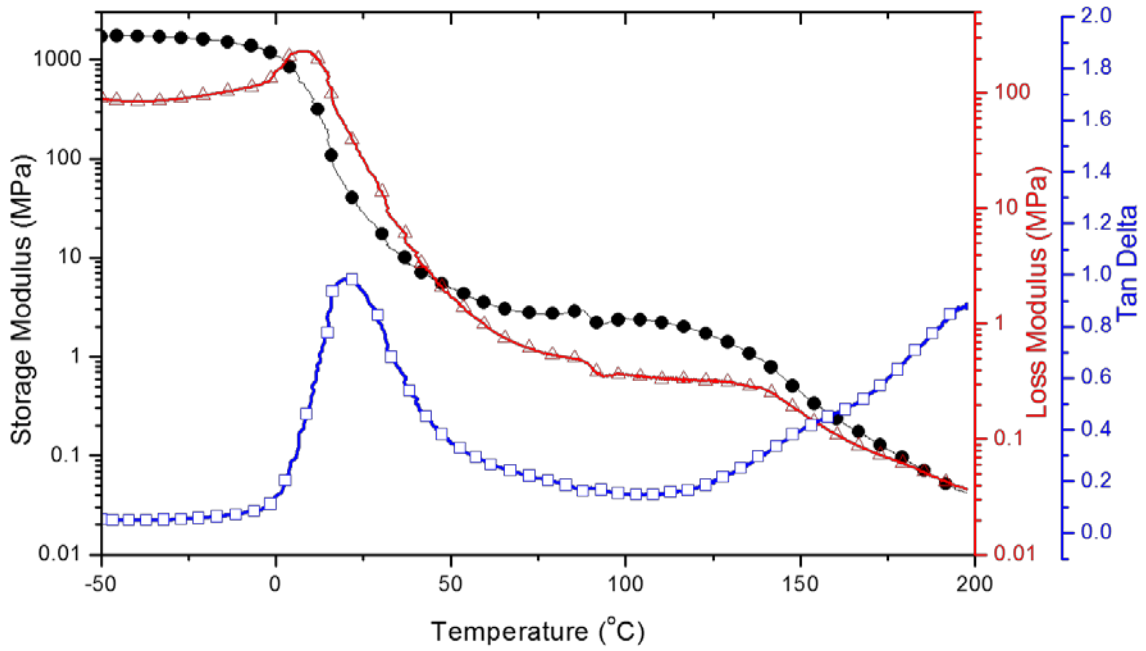

Figure 3-5. Storage modulus (black), loss modulus (red), and tan δ (blue) for ATA-26.2-33.5.

trandition as shown in **Figure 3-2**). Compared to other commercial TPEs, either acrylic TPEs with PMMA as the hard segment (UST around 100 ^{o}C)[12] or styrenic TPEs with PS as the hard segment (UST around 100 ^{o}C),[13] the ATA triblock copolymer has an exceptionally improved UST of 123 ^{o}C due to the use of PAdA as the hard segment with a high glass transition temperature of 133 ^{o}C.

The stress-strain behavior of the ATA triblock copolymers was evaluated by the uniaxial tensile tests, as summarized in **Table 3-2** and the stress-strain curves in **Figure 3-6**. As compared to commercial all acrylic based thermoplastic elastomers based on poly(methyl methacrylate)-b-poly(butyl acrylate)-b-poly(methyl methacrylate) (PMMA-b-PBA-b-PMMA) triblock colymers, such as Arkema's Nanostrength® with stress lower than 1 MPa and elongation only around 500%,[14] both the mechanical strength and the elongation of the material were exceptional. The mechanical strength of all the ATA triblock copolymers tested was higher than 1 MPa, which was also much beyond the commercial products. Although we expected the soft domain has a much larger value of M_e as compared to other polyacrylates such as poly(ethyl acrylate) (PEA), poly(*n*-propyl acrylate) (PPA) and poly(*n*-butyl acrylate) (PBA) due to the bulky pendent group that increases the packing length,[15] the ATA triblock copolymer exhibited higher strain than other all acrylic based TPEs. For instance, ATA-16.2-18.7 exhibited the elongation of 803%, which was higher than other all acrylic TPEs.[16] This exceptional elongation property may be attributed to the distinct microphase

Table 3-2. Mechanical Property Parameters of ATA Triblock Copolymers

Sample ID	E (MPa)	σ_B (MPa)	ε_B (%)
ATA-16.2-18.7	2.2	1.1	803
ATA-16.2-25.4	3.0	1.4	639
ATA-26.2-33.5	1.8	2.2	532
ATA-26.2-53.0	52.4	2.6	240

*E: Young's modulus, σ_B: stress at breaking point, ε_B: elongation at break

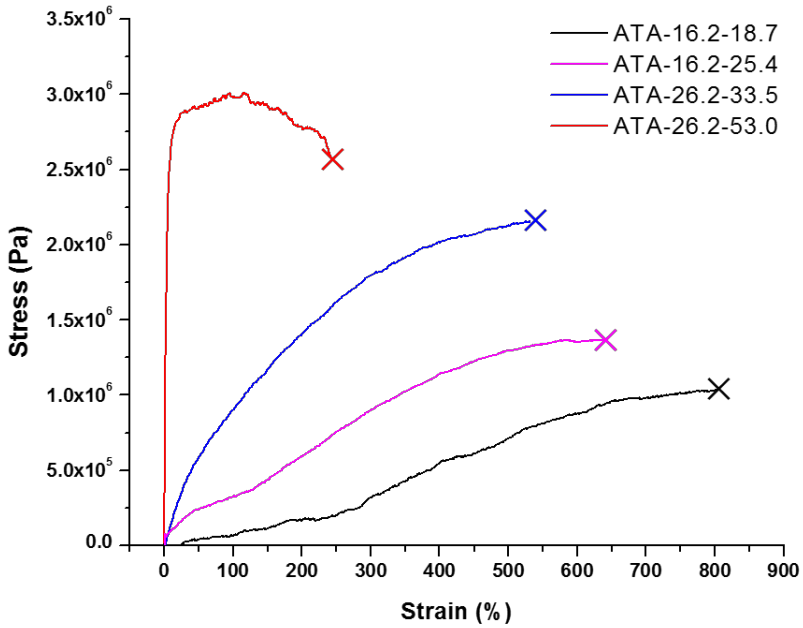

Figure 3-6 Stress-strain curves of ATA triblock copolymers.

separation behavior of the ATA triblock copolymers, for which the material can be stretched longer due to the formation of a well dispersed soft matrix. The distinct mechanical strength of the ATA triblock copolymers may be contributed to the high rigidity of PAdA as the hard domain that is expected to have a large modulus.

Meanwhile, the influences of molecular weights and composition on the mechanical properties were also investigated. The increase of the molecular weight and the weight ratio of PAdA can lead to the improvement in the mechanical strength. However, the elongation of the material can be sacrificed.

3.4 Conclusion

A series of poly(1-adamantyl acrylate)-b-poly(tetrahydrofurfuryl acrylate)-b-poly(1-adamantyl acrylate) (ATA) triblock copolymers has been prepared by reversible addition−fragmentation chain transfer (RAFT) polymerization. All the characterization methods including differential scanning calorimetry (DSC), dynamic mechanical analysis (DMA), atomic force microscopy (AFM) and small angle X-ray scattering (SAXS) indicated the strong microphase separation behaviors of the resulting polymers. The high glass transition temperature of PAdA lead to the upper service temperature of 123 ^{o}C, which was higher than other conventional acrylic or styrenic TPEs with PMMA or PS as the hard segments. Moreover, the high rigidity of PAdA and the distinct phase separation behaviors gave rise to the exceptional mechanical strength and elongation properties of the ATA triblock copolymers over other acrylic based TPEs.

References

(1) Lu, W.; Huang, C.; Hong, K.; Kang, N.-G.; Mays, J. W. Poly(1-adamantyl acrylate): Living Anionic Polymerization, Block Copolymerization, and Thermal Properties. *Macromolecules* **2016**, *49*, 9406-9414.

(2) Deady, L. W.; Kendall, M.; Topsom, R. D.; Jones, R. A. Y. The dipole moments of substituted adamantanes and the correlation of the dipole moments of aliphatic compounds with substituent constants. *Journal of the Chemical Society, Perkin Transactions 2* **1973**, 416-420.

(3) Aminabhavi, T. M.; Gopalakrishna, B. Density, Viscosity, Refractive Index, and Speed of Sound in Aqueous Mixtures of N,N-Dimethylformamide, Dimethyl Sulfoxide, N,N-Dimethylacetamide, Acetonitrile, Ethylene Glycol, Diethylene Glycol, 1,4-Dioxane, Tetrahydrofuran, 2-Methoxyethanol, and 2-Ethoxyethanol at 298.15 K. *Journal of Chemical & Engineering Data* **1995**, *40*, 856-861.

(4) Jha, K. C.; Tsige, M. Molecular Modeling of Thermal and Mechanical Properties of Elastomers: A Review. *Rubber Chemistry and Technology* **2013**, *86*, 401-422.

(5) Chen, S.; Binder, W. H. Controlled copolymerization of n-butyl acrylate with semifluorinated acrylates by RAFT polymerization. *Polymer Chemistry* **2015**, *6*, 448-458.

(6) Lu, W.; Huang, C.; Hong, K.; Kang, N.-G.; Mays, J. W. Poly(1-adamantyl acrylate): Living Anionic Polymerization, Block Copolymerization, and Thermal Properties. *Macromolecules* **2016**.

(7) Bai, R. K.; You, Y. Z.; Pan, C. Y. 60Co γ - Irradiation - Initiated "Living" Free - Radical Polymerization in the Presence of Dibenzyl Trithiocarbonate. *Macromolecular rapid communications* **2001**, *22*, 315-319.

(8) Zioga, A.; Ekizoglou, N.; Siakali-Kioulafa, E.; Hadjichristidis, N. Characteristic ratio of poly(tetrahydrofurfuryl acrylate) and poly(2-ethylbutyl acrylate). *Journal of Polymer Science Part B: Polymer Physics* **1997**, *35*, 1589-1592.

(9) Fox, T. G. Influence of diluent and of copolymer composition on the glass temperature of a polymer system. *Bull Am Phys Soc* **1956**, *1*, 123-135.

(10) Magonov, S. N.; Elings, V.; Whangbo, M. H. Phase imaging and stiffness in tapping-mode atomic force microscopy. *Surface Science* **1997**, *375*, L385-L391.

(11) Kumar, R.; Sumpter, B. G.; Muthukumar, M. Enhanced Phase Segregation Induced by Dipolar Interactions in Polymer Blends. *Macromolecules* **2014**, *47*, 6491-6502.

(12) Oshita, S.; Chapman, B.; Hirata, K. Acrylic Block Copolymer for Adhesive Application. *PSTC Tape Summit 2012* **2012**.

(13) Wang, W.; Schlegel, R.; White, B. T.; Williams, K.; Voyloy, D.; Steren, C. A.; Goodwin, A.; Coughlin, E. B.; Gido, S.; Beiner, M.; Hong, K.; Kang, N.-G.; Mays, J. High Temperature Thermoplastic Elastomers Synthesized by Living Anionic Polymerization in Hydrocarbon Solvent at Room Temperature. *Macromolecules* **2016**, *49*, 2646-2655.

(14) Jean-Marc Boutillier, J.-P. D., Mickael Havel, Raber Inoubli, Stephanie Magnet, Christian Laurichesse, and Daniel Lebouvier. Self-Assembling Acrylic Block Copolymers for Enhanced Adhesives Properties. *ASI Adhesives & Sealants Industry,* May 1 2013, 2013.

(15) Fetters, L. J.; Lohse, D. J.; Graessley, W. W. Chain Dimensions and Entanglement Spacings in Dense Macromolecular Systems. *Journal of Polymer Science Part B: Polymer Physics* **1999**, *37*, 1023-1033.

(16) Tong, J. D.; Leclère, P.; Doneux, C.; Brédas, J. L.; Lazzaroni, R.; Jérôme, R. Morphology and Mechanical Properties of Poly(methylmethacrylate)-b-Poly(alkylacrylate)-b-Poly(methylmethacrylate). *Polymer* **2001**, *42*, 3503-3514.

CHAPTER 4 ALL ACRYLIC MULTIGRAFT COPOLYMER SUPERELASTOMER

Abstract

In the work reported in this chapter, all acrylic multigraft copolymers of poly(butyl acrylate)-g-poly(methyl methacrylate) (PBA-g-PMMA) were prepared using graft-through methodology. The resulting materials exhibit extensively higher strain at break than conventional acrylic and styrenic triblock copolymers and are comparable to that of styrenic multigraft copolymer superelatomers (higher than 1500%). The PMMA macromonomers were synthesized by anionic polymerization using sec-butyl lithium/N-isopropyl-4-vinylbenzylamine (sec-BuLi/PVBA) initiation system, with quantitative yield, quick reaction time and simple operation. Thermal characteristics of the materials were analyzed using differential scanning calorimetry (DSC). The microphase separation behavior and morphologies of these materials were characterized by atomic force microscopy (AFM) and small angle X-ray scattering (SAXS). The mechanical performance of the graft materials was characterized by dynamic mechanical analysis (DMA) and uniaxial tensile tests. This innovative approach greatly expands the potential application range of all-acrylic thermoplastic elastomers (TPEs).

4.1 Introduction

All acrylic based TPE can be used as high performance pressure sensitive adhesives, taking advantages of their optical transparency, versatility of adhesion, weatherability, and low viscosity.[1] However, the higher average molecular weight between chain entanglements (M_e) leads to much poorer mechanical properties of all acrylic TPEs as compared to styrenic TPEs.[2] The design of complex architectures gives a potential approach to overcome this issue. As compared to linear block copolymers, polymers with complex architectures exhibit superior physical and mechanical properties. Furthermore, block copolymers with miktoarm star architectures and graft/multigraft architectures allow additional capacity to tune morphology and long range order.[3] We have previously reported the multigraft copolymers composed of polyisoprene (PI) as the backbone and polystyrene (PS) as the side chains, which were termed “superelastomers”, due to their typical 1500% elongation at break, far exceeding that of polystyrene-b-polyisoprene-b-polystyrene (SIS) triblock copolymers with strain at break less than 1000%.[4-7]

Multigraft copolymers are normally synthesized through three strategies: graft onto, graft from and graft through (macromonomers).[8] Among them, “graft through” methodology has a superior ability to produce a graft copolymer with side chains with fixed chain length.[9] All acrylic multigraft copolymers, e.g. poly(n-butyl acrylate)-g-poly(methyl methacrylate) (PBA-g-PMMA), have been exploited with good elongations (>400% strain at break) and tunable stress.[10] The PMMA

macromonomer was synthesized by anionic polymerization using 1-(tert-butyldimethylsiloxy)-3-butyllithium as a protected initiator that was later converted to the PMMA macromonomer (MM-PMMA). Similarly, the macromonomer was also synthesized through a coupling reaction with 4-vinylbenzyl chloride.[11] However, both routes involve the linking reaction or post-modification reaction that have limitations including complex operation, low conversion and long reaction time.

In this work, we report a novel way to synthesize PBA-g-PMMA graft copolymer using graft through methodology. The PMMA macromonomer was produced by anionic polymerization using glass blowing and high-vacuum techniques and utilizing sec-butyl lithium/N-isopropyl-4-vinylbenzylamine (*sec*-BuLi/PVBA) as the initiation system. As previously reported, the activity gap between carbanion and nitranion can give rise to the polymerization of methacrylates, with the styrenic vinyl group intact.[12] Thus the synthesis of macromonomer can be achieved with 100% conversion and short reaction time, taking advantage of the “living” nature of anionic polymerization.[13,14] For the first time, this promising method was used to make all acrylic TPEs. Through the initiation system of *sec*-BuLi/PVBA, PMMA macromonomers were synthesized by anionic polymerization directly in one batch with no post-modification. The final PBA-g-PMMA graft copolymer was synthesized by reversible addition−fragmentation chain-transfer (RAFT) polymerization. The resulting graft

copolymer was characterized using nuclear magnetic resonance spectroscopy (NMR), size exclusion chromatography (SEC) for molecular information. Differential scanning calorimetry (DSC) was used to characterize the thermal properties of the materials. The microphase separation behaviors were investigated using atomic force microscopy (AFM) and small angle X-ray scattering (SAXS). In addition, the mechanical properties of the graft copolymers were studied using dynamic mechanical analysis (DMA) and uniaxial tensile tests.

4.2 Experimental Part

Materials. Isopropylamine (Acros Organics, 99%), 4-vinylbenzyl chloride (Acros Organics, 90%), *Sec*-butyl lithium (*sec*-BuLi), 1,1-diphenyl ethylene (DPE, Acros Organics, 98%), tetrahydrofuran (THF) (Fisher, GR grade) and methanol (Fisher, GR grade) were prepared and purified as previously described.[14] LiCl (Alfa Aesar, 99.995%) was dried at 130 ^{o}C for 2 days and ampulized under high vacuum conditions. Methyl methacrylate (MMA, Aldrich, 99%) was passed through aluminum oxide (Acros Organics, basic) column to remove the inhibitor, stirred for 24 h over anhydrous CaH_2 and distilled over CaH_2 and trioctylaluminum sequentially under reduced pressure. The resulting MMA was ampulized and diluted immediately with THF under high vacuum condition, giving a concentration of 0.83 mmol/mL. All ampules of the reactants equipped with break seals were stored at -30 ^{o}C.

N-butyl acrylate (BA, Acros Organics, 99%) was used directly after passed through aluminum oxide (Acros Organics, basic) column to remove the inhibitor. 2,2-Azobis-(isobutyronitrile) (AIBN, Sigma-Aldrich, 90%) was recrystallized before use and the S-1-dodecyl-S'-(α,α'-dimethyl-α'-acetic acid)trithiocarbonate chain transfer agent (CTA) was synthesized following the procedure previously published by Lai et al.[15] Benzene (Aldrich, ≥99.9%), sodium hydroxide (Acros Organics, 98%), magnesium sulfate (Aldrich, 99.5%), sodium chloride (Acros Organics, 99.5%) were used as received.

Synthesis of N-isopropyl-4-vinylbenzylamine (PVBA). PVBA was synthesized following the previously reported work.[16] Briefly, the procedure was as follows: The reaction was carried out under an atmosphere of nitrogen. A 250 mL round bottom flask with 4-vinylbenzyl chloride (10 g, 65.5 mmol) was cooled to 0 ^{o}C with an ice bath. Isopropylamine (15.5 g, 262.2 mol) was added to the flask. The reaction solution was raised to room temperature and left stirring for 24 h. After the reaction was completed, the solution was diluted with dichloromethane, and extracted with saturated sodium hydroxide aqueous solution, saturated aqueous sodium chloride solution and DI water sequentially. The combined organic layer was dried over anhydrous magnesium sulfate, evaporated, and purified using a flash column with n-hexane as the eluant. Light orange oil-like liquid was obtained after the evaporation of n-hexane. The resulting product was obtained with the yield of 73%. ^{1}H NMR spectra ($CDCl_3$, 500 MHz), δ (ppm): 7.31

and 7.37 (d, 4H, -Ar), 6.74 (dd, 1H, C=CH-Ar), 5.72 and 5.24 (dd, 2H, CH_2=C-Ar), 3.76 (s, 2H, N-CH_2-Ar), 2.83 (sept, 1H, N-CH-C_2), 1.09 (d, 6H, CH_3-C-N).

For anionic polymerization, PVBA was further stirred over CaH_2 overnight, and distilled into an ampule equipped with a break-seal under high vacuum conditions. The purified colorless liquid was diluted with anhydrous THF. The solutions (0.5 mmol/mL and 0.05 mmol/mL) were stored at -30 ^{o}C until polymerization.

Homopolymerization of PMMA Macromonomer. All anionic polymerizations were carried out under high-vacuum conditions (10^{-6} mmHg) in a glass apparatus equipped with break-seals in the usual manner.[13,14] The polymerization was performed in THF at -78 ^{o}C. The initiation system was prepared by the anion exchange reaction between *sec*-BuLi and PVBA at -78 ^{o}C for 30 min. LiCl and MMA were introduced sequentially via break-seals. Polymerization was performed for 1 h and terminated with degassed methanol at -78 ^{o}C. The product was poured into a large excess of hexane with vigorous stirring. The precipitated polymer was filtered and vacuum dried overnight. The resulting polymer was characterized by SEC. The intact vinyl group was confirmed by ^{1}H NMR spectroscopy.

Synthesis of PBA-g-PMMA Graft Copolymer. All the PBA-g-PMMA graft copolymers were polymerized through reversible addition–fragmentation chain transfer (RAFT) polymerization under high-vacuum conditions (10^{-6} mmHg) in a

glass apparatus. PMMA macromonomer, CTA, AIBN were mixed and dissolved in a vial. The solution was transferred to a round bottom flask, which was degassed by three freeze-thaw-evacuate cycles. The flask was flame sealed under vacuum and immersed in an oil bath at 80 ^{o}C for certain time, depending on different target molecular weights. The polymerization was quenched with liquid nitrogen. The product solution was precipitated in a large excess of methanol with vigorous stirring and vacuum dried overnight. The resulting polymer was characterized by SEC. The ratio of PMMA to PBA was investigated by ^{1}H NMR.

Chemical and Thermal Property Characterization. The molecular weights (MWs) of the polymers were characterized by size exclusion chromatography (SEC) in THF at 40 ^{o}C with a flow rate of 1.0 mL/min using a Polymer Laboratories PL-120 SEC system equipped with four detectors consisting of a Polymer Laboratories refractometer, a Precision Detector PD 2040 (2-angle static light scattering detector), a Precision Detector PD2000DLS (2-angle light scattering detector), and a Viscotek 220 differential viscometer. The column set employed consisted of Polymer Laboratories PLgel; 7.5 × 300 mm; 10 μm; 500, 1 × 104, 1 × 106, and 1 × 107 Å. The ^{1}H NMR spectra were measured with Varian VNMR 500 MHz, and using $CDCl_3$ as the solvent. Chemical shifts were referred to $CDCl_3$ solvent peak at 7.26 ppm. Thermal properties were characterized by differential scanning calorimetry (DSC, TA2000) under nitrogen with a heating rate of 10 ^{o}C/min.

Phase Separation Behavior Characterization. Morphological measurements were performed using atomic force microscopy (AFM) and small-angle X-ray scattering (SAXS).

To prepare samples for AFM measurement, a solution of 50 mg of polymer in 1 mL of toluene was stirred overnight at room temperature. Silicon wafers were cleaned by soaking in deionized water, acetone, and isopropanol for one hour in each solvent. Then, the polymer solution was spin-cast on the silicon wafer (1500 rpm for 30 s and 300 rpm for another 30 s). The resulting thin films were dried and annealed at 160 ^{o}C for 7 days prior to the measurement. AFM images were collected using Asylum Research MFP3D with a multimode controller at room temperature in tapping mode with an Al reflex coated Si tip (radius 9±2 nm) at a line scanning frequency of 1 Hz.

Samples for SAXS were prepared as follows: a solution of 50 mg of polymer in 1 mL of toluene was stirred overnight at room temperature and cast into a 1 mL PTFE Griffin beaker and evaporated slowly over 7 days, resulting in a film with the thicknesses of around 0.5 mm. All dried samples were annealed at 160 ^{o}C for 7 days under vacuum (10^{-6} mmHg) before measurements. SAXS/WAXS experiments were conducted at 12-ID-B at the Advanced Photon Source at Argonne National Laboratory. X-rays of wavelength λ= 0.89Å were used, and each measurement was performed at two different sample-to-detector distances to

cover a q-range of 0.0026 < q < 4.4 Å^{-1}, where $q = \left(\frac{4\pi}{\lambda}\right)\sin(\theta/2)$ is the magnitude of the scattering vector, and θ is the scattering angle.

Measurements of the Mechanical Property. The characterization of mechanical properties of polymers included dynamic mechanical analysis (DMA) and uniaxial tensile tests. The samples tested were prepared as follows: A solution of 2.0 g of polymer in 20 ml of toluene was stirred overnight at room temperature and cast into a 25 ml PTFE evaporating dish and evaporated slowly over 7 days, resulting in a film with the thicknesses of around 0.5 mm. Then the samples were dried for 2 days in a vacuum oven at around 50 ^{o}C. The resulting films were cut into uniform dog-bone shaped specimens (ISO 37-4).

Dynamic mechanical analysis was performed on a TA Instruments Q-800 dynamic mechanical analyzer equipped with a single cantilever clamp. The temperature ramp/frequency sweep experiments were run at 1 Hz over a temperature range of −60 to +140 °C. Uniaxial tensile tests were carried out using Instron 4465 with a cross-head velocity of 50 mm/min. For each polymer sample, three identical specimens were tests.

4.3 Results and Discussion

4.3.1 Synthesis PVBA-PMMA Macromonomer

As compared to other reported approaches to synthesize the macromonomers, the advantages of the method in this study including 100%

conversion, short reaction time and simple operations make it possible to produce a large quantity of the macromonomer with narrow polydispersity through the one-batch reaction using *sec*-BuLi/PVBA initiation system. The synthesis of PVBA and the PMMA macromonomer can be illustrated by **Scheme 4-1 (a)**.

PVBA was synthesized by the alkylation of isopropylamine by 4-vinylbenzyl chloride. The anionic polymerization was performed by the sequential addition of PVBA, sec-BuLi, LiCl and MMA monomer, and terminated with degassed methanol. The mixing of PVBA and sec-BuLi leads to the formation of greenish yellow color (**Figure 4-1 (a)**), which changed to light orange color after the reaction for 30 min (**Figure 4-1 (b)**). Otherwise, when PVBA was added to the sec-BuLi solution, a deep orange color was observed due to the attack of extra sec-BuLi to the vinyl group of PBVA. The initiator solution is stable at elevated temperature and was left at room temperature for around 10 min for the removal of possible remaining *sec*-BuLi by its reaction with THF at room temperature.[17] A large excess of LiCl was added to the initiation solution before the addition of MMA at -78 ^{o}C to coordinate with the nitrogen anion and suppress the backbiting reactions during the polymerization.[18] The color change from light orange to a blue color indicated the formation of a complex between the LiCl salt and the nitrogen anion (**Figure 4-1 (c)**). The solution became colorless once MMA was added, which was the typical phenomenon for living polymethacrylates (**Figure 4-1 (d)**). The intact vinyl group of the resulting macromonomer was confirmed by the ^{1}H NMR spectra, with

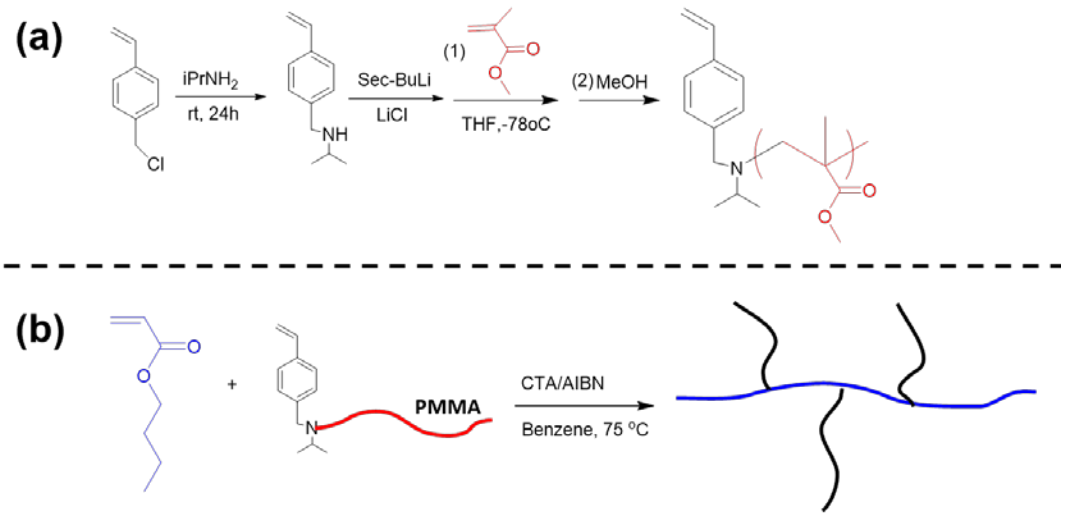

Scheme 4-1. Synthesis of PBA-g-PMMA graft copolymer.

Figure 4-1. Reaction solutions on the synthesis of PMMA macromonomer: (a) activation of PVBA by *sec*-BuLi upon mixing; (b) the completion of the activation of PVBA by *sec*-BuLi; (c) formation of a complex between LiCl and nitrogen anion; (d) Solutions of living PMMA.

the chemical shifts at 6.7 ppm, 5.8 ppm, and 5.2 ppm. (**Figure 4-2**). Detailed polymerization conditions and molecular weight information are shown in **Table 4-1**. The number average molecular weights of the resulting macromonomers were always higher than the calculated values, which might be caused by the trace amount of impurities existing in PVBA ampules, since it was only distilled once over CaH_2 during the ampulization. Still, all the polymers synthesized had a quantitative yield and exhibited very narrow PDI, which indicated the typical characteristics of anionic polymerization.

4.3.2 Synthesis of PBA-g-PMMA Graft Copolymers

The final PBA-g-PMMA graft copolymers were synthesized by RAFT polymerization of BA with the PMMA macromonomer. (**Scheme 4-1(b)**) The composition of each graft copolymer was calculated based on the ratio of integrated areas between the peaks at around 3.6 ppm (-OCH_3 of PMMA) and 4.0 ppm (-O-CH_2- of PBA) in ^{1}H NMR spectra. (**Figure 4-3**) The typical SEC curves of PMMA macromonomer and resulting PBA-g-PMMA are shown in **Figure 4-4**. Graft copolymers with different molecular weights and different compositions were summarized in **Table 4-2**.

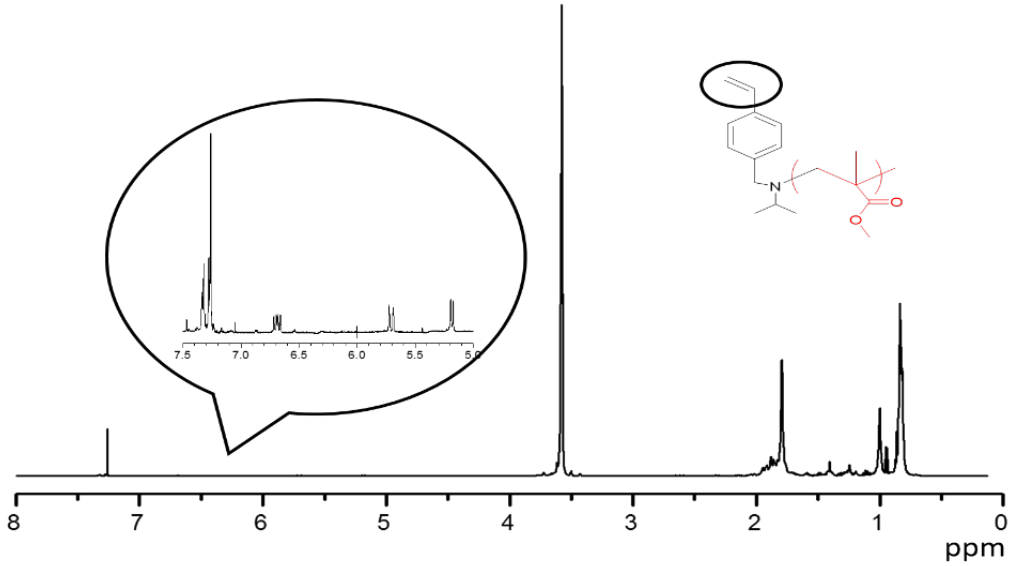

Figure 4-2. ^{1}H NMR spectrum of PMMA macromonomer (PMMA-18 in **Table 4-1**).

Table 4-1. Synthesis of PMMA macromonomer by living anionic polymerization [a]

Sample ID	*Sec*-BuLi (mmol)	PVBA (mmol)	LiCl (mmol)	MMA (mmol)	Time (min)	M_n (kg/mol) calcd[c]	M_n (kg/mol) obsd	M_w/M_n[b]
PMMA-8	0.92	1.50	10.20	30.0	60	3.3	8.4	1.04
PMMA-18	0.80	1.00	10.00	50.0	60	6.3	18.1	1.02
PMMA-29	0.12	0.2	0.1	25.0	60	20.8	29.3	1.01

[a]All the polymerization showed quantitative yields. [b]Number-average molecular weight M_n and PDI were measured in THF at 40 ^oC using the Polymer Laboratories PL-120 SEC system, with *dn/dc* as 0.085 mL/g for PMMA. [c]M_n (calcd)=[MMA]/[*sec*-BuLi] ×MW(MMA)×yield of polymerization (%).

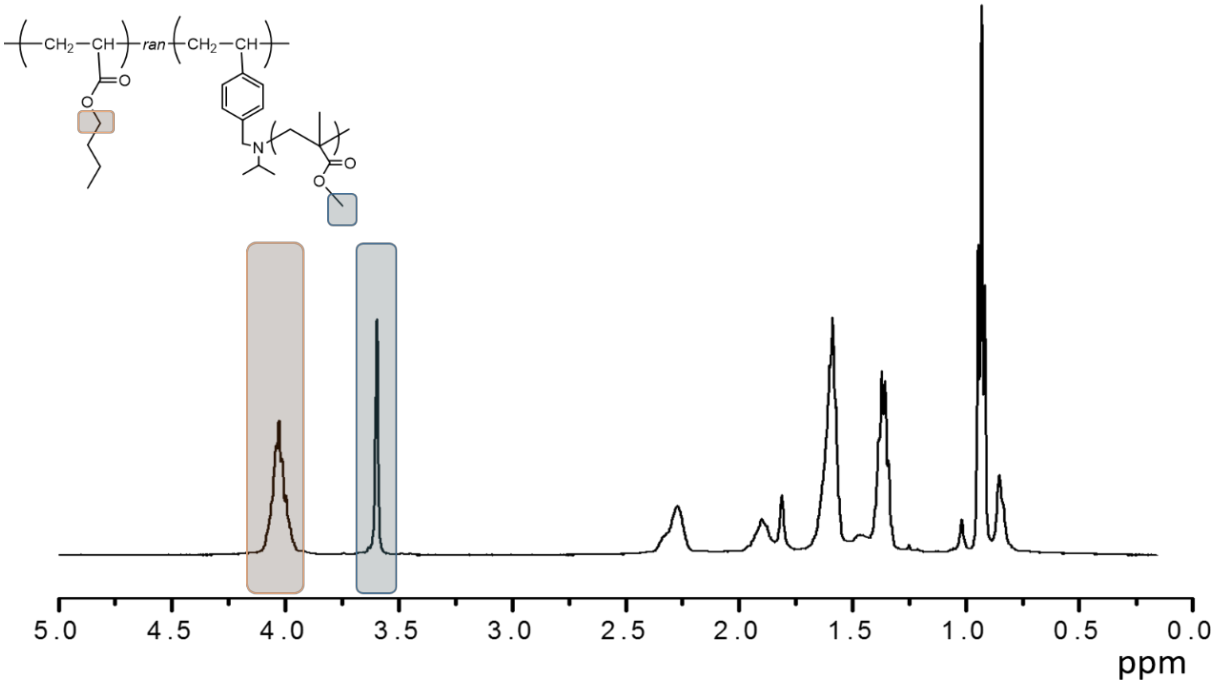

Figure 4-3. ^{1}H NMR spectrum of PBA-g-PMMA(MG-18.1-2.8-18.4 in **Table 4-2**)

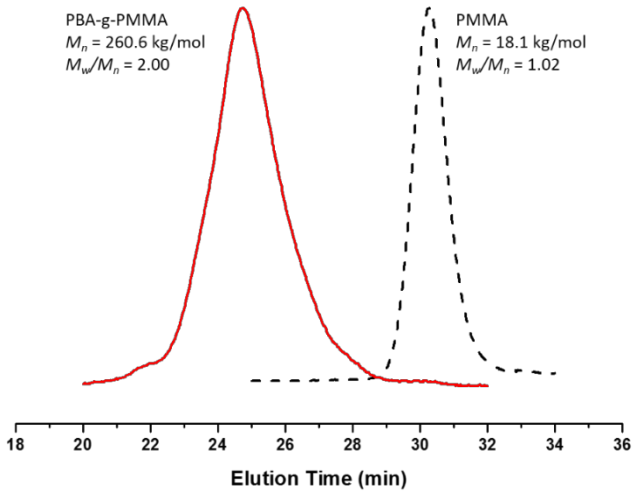

Figure 4-4. SEC profiles of PBA-g-PMMA (MG-18.1-2.8-18.4 in **Table 4-2**) and PMMA macromonomer (PMMA-18 in **Table 4-1**)

Table 4-2. Sample Information of PBA-g-PMMA Graft Copolymers

Sample ID[a]	*PMMA*		PBA-g-PMMA[b]		Vol% of PMMA[c]	No.[d]
	M_n (kg/mol)	PDI	M_n (kg/mol)	PDI		
MG-8.4-3.3-8.6	8.4	1.04	294.9	1.99	8.6	3.3
MG-18.1-2.8-18.4	18.1	1.02	260.6	2.00	18.4	2.8
MG-29.3-1.5-9.3	29.3	1.01	432.6	1.69	9.3	1.5
MG-29.3-3.0-33.8	29.3	1.01	245.8	1.25	33.8	3.0

[a]Sample identification MG-M_n (PMMA)-No. of branch points-vol% of PMMA. [b]Number-average molecular weight M_n and PDI were measured in THF at 40 ^oC using the Polymer Laboratories PL-120 SEC system, with *dn/dc* estimated by $wt\%(PMMA)\times0.085 + wt\%(PBA)\times0.067$ where 0.085 mL/g is *dn/dc* the for PMMA and 0.067 is the *dn/dc* for PBA, and the wt% of PMMA and PBA was obtained from ^1H NMR spectra. [c]vol% was calculated based on the density of 1.159 g/mL for PMMA and 1.080 g/mL for PBA. [d]No. of branch points was calculated based on $\mathrm{M_n(PBA-g-PMMA)\times wt\%(PMMA)/M_n(PMMA)}$.

4.3.3 Thermal Properties of PBA-g-PMMA Graft Copolymers

The great difference on glass transition temperatures (T_gs) and thermodynamic mismatch give rise to the microphase separation behavior of TPE. Thermal properties of the PBA-g-PMMA copolymers were investigated using DSC to determine the glass transition temperatures (T_gs). In the differential scanning calorimetry (DSC) thermograph (**Figure 4-5**) of the graft copolymer synthesized, both T_gs at -46 ^oC and 118 ^oC were observed, which corresponded to the those of PBA and PMMA. The observation of typical T_gs of each domain also gives the circumstantial indication of the phase separation behavior in the graft copolymer.

4.3.4 Microphase Separation Behaviors of PBA-g-PMMA Graft Copolymers

Microphase separation behavior of the PBA-g-PMMA samples was further investigated using atomic force microscopy (AFM) and small angle X-ray scattering (SAXS). In the case of AFM images, the bright regions of the phase image represent the stiff domain, i.e. PMMA, due to the increase of phase angle of the probe oscillation. The dark zones refer to the soft domains, i.e. PBA.[19] Different morphologies were observed with different branch size and the volume ratio of PMMA, as shown in **Figure 4-6**. With the increase of the chain length of PMMA, the microphase separation behavior was improved. This observation agrees with simulated results by the combination of self-consistent field theory (SCF) and molecular dynamics (MD) simulation proposed by Bates et al., which indicated that the increase of chain length *N* can promote the phase separation behavior.[20] For

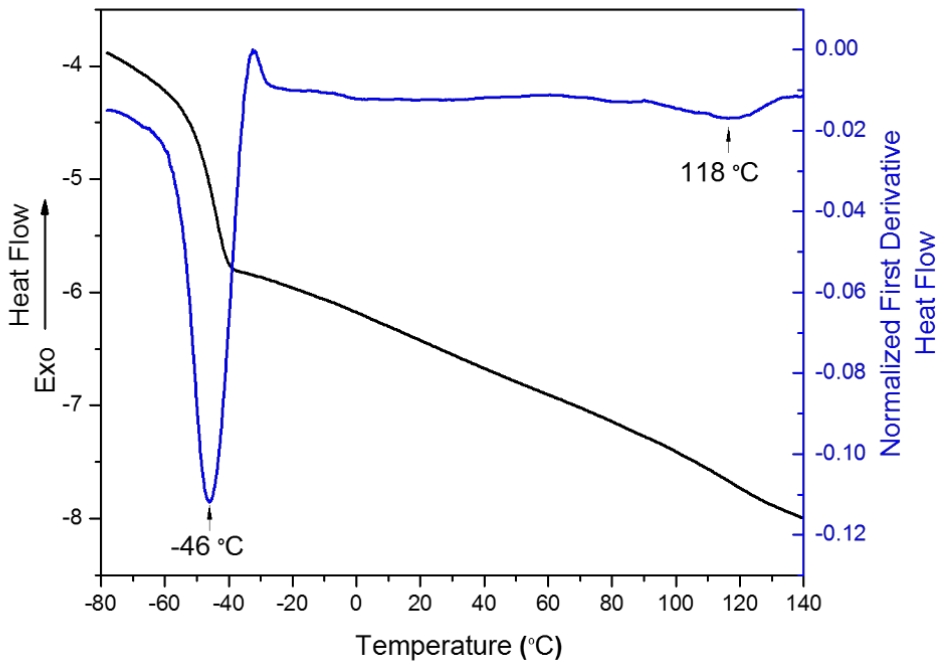

Figure 4-5 DSC thermograph of MG-18.1-2.8-18.4 and its normalized first derivative. Two transitions correspond to each of the acrylic domains were observed. The difference of the intensity of each transition is caused by the proportion diversity between PMMA and PBA components.

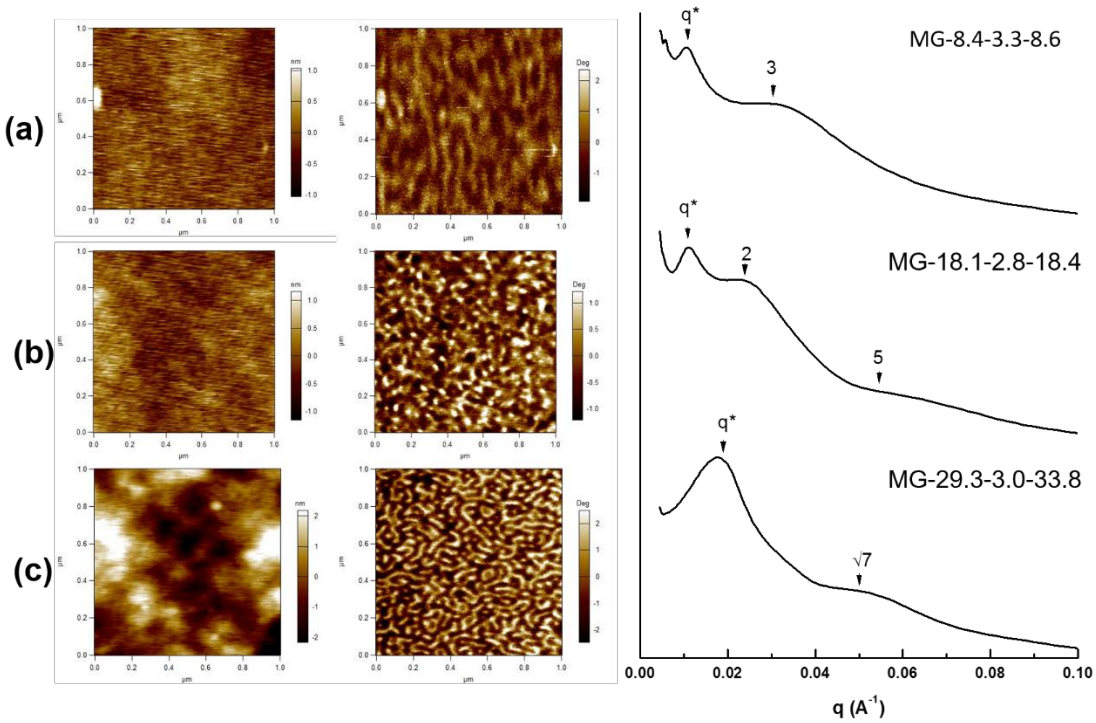

Figure 4-6. AFM height images (left) and phase images (mid), and SAXS profiles (right) of PBA-g-PMMA. From top to bottom correspond to: (a) MG-8.4-3.3-8.6; (b) MG-18.1-2.8-18.4; (c) MG-29.3-3.0-33.8

this study, longer PMMA chains lead to more entanglements between hard domains. Thus higher degree of phase separation can be achieved. SAXS profiles also exhibited the distinctive peaks, as the indication of microphase separation behavior. The broad polydispersity indices contributed to the poor long order distribution of the morphologies. However, the relative positions of these peaks roughly consist with the AFM images. With the increase of both the chain length and volume ratio of PMMA, the morphologies changed from sphere-like (**Figure 4-6(a)**), hexagonal-like (**Figure 4-6(b)**) to worm-like (**Figure 4-6(c)**) shapes.

4.3.5 Mechanical Properties of PBA-g-PMMA Graft Copolymers

The mechanical properties of PBA-g-PMMA graft copolymers were characterized through dynamic mechanical analysis (DMA) and uniaxial tensile tests. As shown in **Figure 4-7**, the storage modulus, loss modulus, and tan δ over a temperature range from -60 ^{o}C to 140 ^{o}C were investigated. At low temperature relaxation process was observed at -43 ^{o}C, corresponding to the glass-to-rubber transition of PBA phase indicated by a stepwise decrease in storage modulus (G'(T)). Further heating lead to another drop of G'(T) when the temperature approached 95 ^{o}C, corresponding to the glass-to-rubber transition of PMMA hard phase. Similar to the results from DSC, this two-step transition indicates the existence of microphase separation behavior of the graft copolymer.

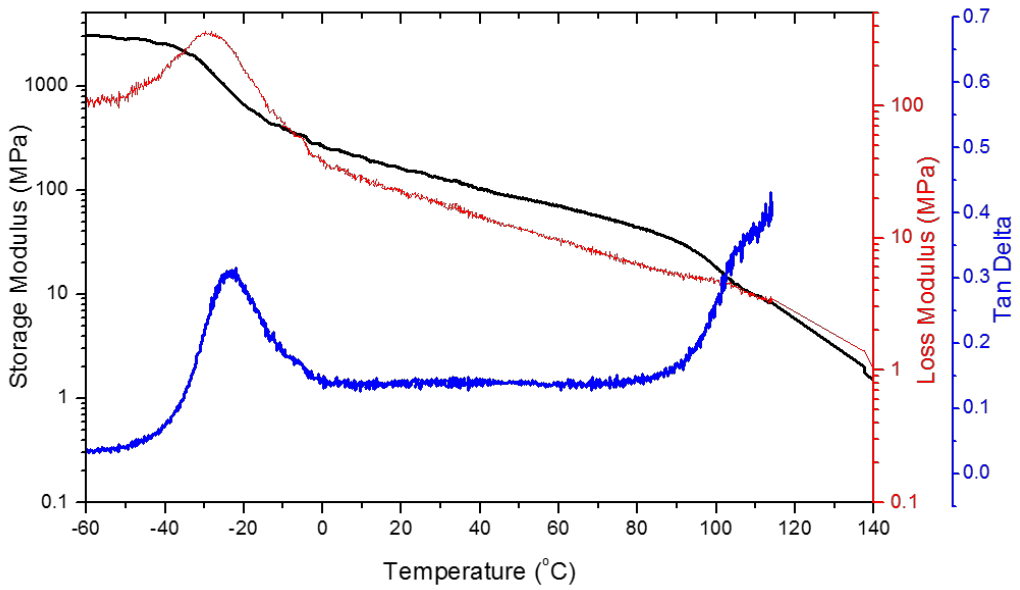

Figure 4-7. Storage modulus, loss modulus, and tan δ of MG-18.1-2.8-18.4

As shown in **Figure 4-8** and summarized in **Table 4-3**, the typical stress to strain relation exhibits the exceptional mechanical property of these all acrylic multigraft copolymers. It was reported that the volume fraction can affect the mechanical behavior of polyacrylates based graft copolymer.[10] Herein, the distinct influence of polymer molecular weight is demonstrated.

Several interesting results were found from this uniaxial tensile tensile tests, including: (1) With the increase of the volume ratio of PMMA, the mechanical strength could be adjusted in a wide range from 1.9 MPa (vol% of PMMA ~10 %) to 10.8 MPa (vol% of PMMA ~34%). Meanwhile, the elongation of the material was sacrificed. (2) Interestingly, as compared to the previously study, MG-8.4-3.3-8.6 exhibits much higher stress and elongation at break as compared to the previously reported work with the same structure and similar molecular weight (MG 11.7-5.3-22.2 in the work by Goodwin, A. at al. with ϵ_B around 450% and σ_B around 0.6 MPa). Even though fewer branch points exist in the polymer, which has been demonstrated another key factor that can influence the mechanical performance.[21] This distinct improvement can be explained by the average molecular weight between chain entanglements, M_e. With M_e(PBA) as 28 kg/mol, the increase of Mn(PBA) can bring more chain entanglements, which in return, helps to improve the total modulus.[2] (3) The M_e difference between PBA and Polyisoprene (M_e: 6.1 kg/mol) or polybutadiene (M_e: 1.7 kg/mol) leads to the “disappointing observation” of polyacrylates based TPEs’ mechanical performance as compared to styrenic

Table 4-3. Mechanical Property Parameters of PBA-g-PMMA Graft Copolymers

Sample ID	E (MPa)	σ_B (MPa)	ε_B (%)
MG-8.4-3.3-8.6	0.2	1.9	1881
MG-18.1-2.8-18.4	1.3	4.3	856
MG-29.3-3.0-33.8	21.9	10.8	497
MG-29.3-1.5-9.3	0.2	2.0	1712

*E: Young's modulus, σ_B: stress at breaking point, ε_B: elongation at break

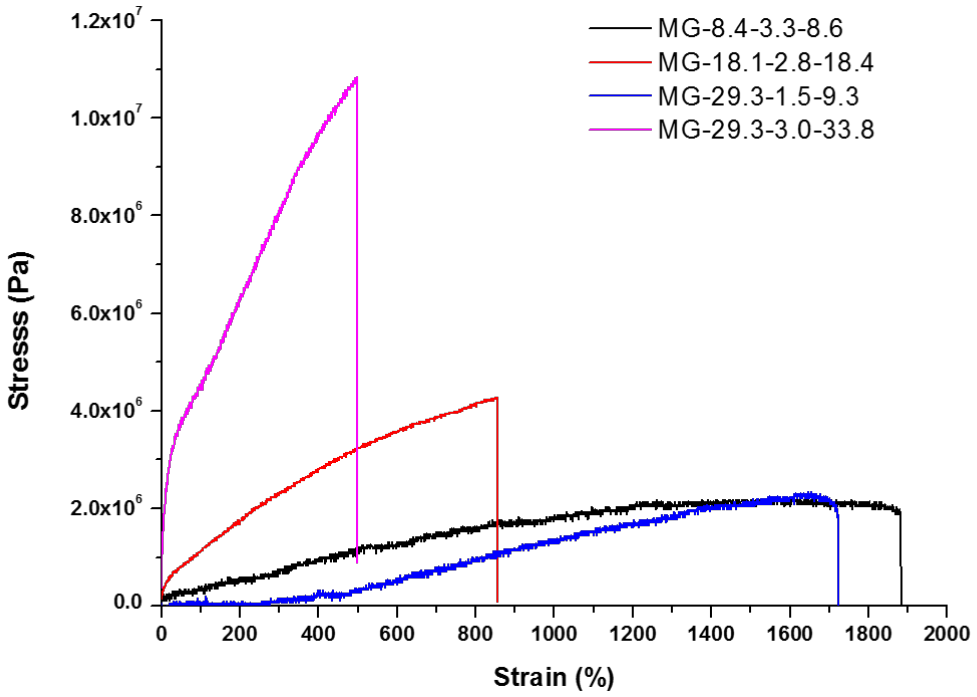

Figure 4-8. Stress-strain behaviors of PBA-g-PMMA graft copolymers

TPE.[22] However, surprisingly, the combination of high molecular weight and the graft architecture give the supreme elongation and stress of the polymers synthesized. All the polymer samples showed exceptional elongation other than the PMMA-b-PBA-b-PMMA triblock copolymers with similar volume ratio of PMMA, e.g. MG-18.1-2.8-18.4 showed the elongation of 856%, similar triblock copolymers with the vol%(PMMA) of 22% only exhibited elongation of 545%.[23] Even with the vol%(PMMA) of 33.8%, the elongation can still be around 500%. (4) MG-29.3-1.5-9.3 exhibits stress of 2.0 MPa with the final strain reaches 1712%, which is far beyond the performance of commercial PMMA-b-PBA-b-PMMA triblock copolymers like Arkema's Nanostrength® and with stress lower than 1 MPa and elongation only around 500%.[24] Moreover, its elongation is even superior to that of commericial Styrenic TPEs like Kraton® at 1080%, and comparable with the double tailed PI-g-PS multigraft copolymers at around 1600%.[7] By this means, all acrylic superelastomers were produced.

Another key standard for the superelastomer is its exceptional recovery behavior. As reported by Mays et al., the PI-g-PS with tetrafunctional branch points showed its superior recovery with only 40% strain loss after stretched to 1400%.[21] The hysteresis of the PBA-g-PMMA graft copolymer was simply examined by the stretching of the dog-bone specimen, as shown in **Figure 4-9**. With the initial cross-head length around 16 mm, the sample was stretched to 200 mm. The specimen returned to its original shape, with less than 2 mm strain loss (<15%). Thus, the

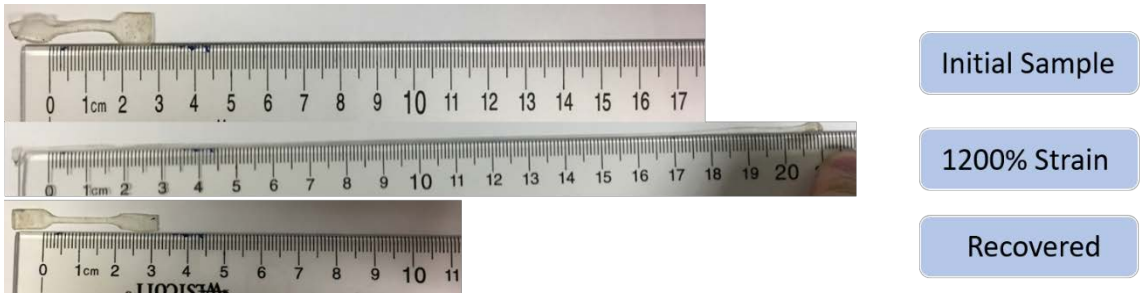

Figure 4-9 Photographs on the hysteresis test of MG-29.3-1.5-9.3. From top to bottom are: Initial sample with the cross head length of 16 mm; sample stretched to 200 mm with around 1200% strain; recovered sample with the cross head length of around 18 mm.

great recovery performance of the graft copolymer was thus demonstrated.

4.4 Conclusion

In conclusion, a new method to synthesize the graft copolymer of poly(butyl acryalate)-g-poly(methyl methacrylate) (PBA-g-PMMA) using graft through methodology was reported. The initiation system of *sec*-BuLi/PVBA makes it possible to synthesize the PMMA macromonomer within one batch of anionic polymerization, with quantitative conversion and short reaction time, as compared to other conventional routes. The resulting graft copolymers exhibited great microphase separation behaviors. For the first time, the combination of the architecture of graft copolymers and enhanced molecular weight make the polymers synthesized exhibit extraordinary mechanical strength and superelastomeric properties: strain at break can far exceed that of conventional triblock copolymer polyacrylates based TPEs. In addition, their great strain recovery behavior was demonstrated that make the material superior to the traditional linear type TPEs. These distinctive mechanical properties impart the potential to expand the application range of all-acrylic thermoplastic elastomers (TPEs) as the possible substitution for current styrenic TPEs.

References

(1) Oshita, S.; Chapman, B.; Hirata, K. Acrylic Block Copolymer for Adhesive Application. *PSTC Tape Summit 2012* **2012**.

(2) Tong, J. D.; Jerôme, R. Synthesis of poly(methyl methacrylate)-b-poly(n-butyl acrylate)-b-poly(methyl methacrylate) triblocks and their potential as thermoplastic elastomers. *Polymer* **2000**, *41*, 2499-2510.

(3) Pochan, D. J.; Gido, S. P.; Pispas, S.; Mays, J. W.; Ryan, A. J.; Fairclough, J. P. A.; Hamley, I. W.; Terrill, N. J. Morphologies of microphase-separated A2B simple graft copolymers. *Macromolecules* **1996**, *29*, 5091-5098.

(4) Mays, J. W.; Uhrig, D.; Gido, S.; Zhu, Y.; Weidisch, R.; Iatrou, H.; Hadjichristidis, N.; Hong, K.; Beyer, F.; Lach, R.; Buschnakowski, M. Synthesis and Structure – Property Relationships for Regular Multigraft Copolymers. *Macromolecular Symposia* **2004**, *215*, 111-126.

(5) Mijović, J.; Sun, M.; Pejanović, S.; Mays, J. W. Effect of Molecular Architecture on Dynamics of Multigraft Copolymers: Combs, Centipedes, and Barbwires. *Macromolecules* **2003**, *36*, 7640-7651.

(6) Uhrig, D.; Schlegel, R.; Weidisch, R.; Mays, J. Multigraft copolymer superelastomers: Synthesis morphology, and properties. *European Polymer Journal* **2011**, *47*, 560-568.

(7) Zhu, Y.; Burgaz, E.; Gido, S. P.; Staudinger, U.; Weidisch, R.; Uhrig, D.; Mays, J. W. Morphology and Tensile Properties of Multigraft Copolymers with

Regularly Spaced Tri-, Tetra-, and Hexafunctional Junction Points. *Macromolecules* **2006**, *39*, 4428-4436.

(8) Uhrig, D.; Mays, J. Synthesis of well-defined multigraft copolymers. *Polymer Chemistry* **2011**, *2*, 69-76.

(9) Ito, S.; Goseki, R.; Ishizone, T.; Hirao, A. Synthesis of well-controlled graft polymers by living anionic polymerization towards exact graft polymers. *Polymer Chemistry* **2014**, *5*, 5523-5534.

(10) Goodwin, A.; Wang, W.; Kang, N.-G.; Wang, Y.; Hong, K.; Mays, J. All-Acrylic Multigraft Copolymers: Effect of Side Chain Molecular Weight and Volume Fraction on Mechanical Behavior. *Industrial & Engineering Chemistry Research* **2015**, *54*, 9566-9576.

(11) Wang, W.; Wang, W.; Lu, X.; Bobade, S.; Chen, J.; Kang, N.-G.; Zhang, Q.; Mays, J. Synthesis and Characterization of Comb and Centipede Multigraft Copolymers PnBA-g-PS with High Molecular Weight Using Miniemulsion Polymerization. *Macromolecules* **2014**, *47*, 7284-7295.

(12) Zeng, F.; Shen, Y.; Zhu, S. Synthesis of Styrenic-Terminated Methacrylate Macromonomers by Nitroanion-Initiated Living Anionic Polymerization. *Macromolecular Rapid Communications* **2001**, *22*, 1399-1404.

(13) Hadjichristidis, N.; Iatrou, H.; Pispas, S.; Pitsikalis, M. Anionic polymerization: High vacuum techniques. *Journal of Polymer Science Part A: Polymer Chemistry* **2000**, *38*, 3211-3234.

(14) Uhrig, D.; Mays, J. W. Experimental techniques in high-vacuum anionic polymerization. *Journal of Polymer Science Part A: Polymer Chemistry* **2005**, *43*, 6179-6222.

(15) Lai, J. T.; Filla, D.; Shea, R. Functional polymers from novel carboxyl-terminated trithiocarbonates as highly efficient RAFT agents. *Macromolecules* **2002**, *35*, 6754-6756.

(16) Seki, A.; Ishiwata, F.; Takizawa, Y.; Asami, M. Crossed aldol reaction using cross-linked polymer-bound lithium dialkylamide. *Tetrahedron* **2004**, *60*, 5001-5011.

(17) Gilman, H.; Haubein, A. H.; Hartzfeld, H. THE CLEAVAGE OF SOME ETHERS BY ORGANOLITHIUM COMPOUNDS. *The Journal of Organic Chemistry* **1954**, *19*, 1034-1040.

(18) Fayt, R.; Forte, R.; Jacobs, C.; Jerome, R.; Ouhadi, T.; Teyssie, P.; Varshney, S. K. New initiator system for the living anionic polymerization of tert-alkyl acrylates. *Macromolecules* **1987**, *20*, 1442-1444.

(19) Magonov, S. N.; Elings, V.; Whangbo, M. H. Phase imaging and stiffness in tapping-mode atomic force microscopy. *Surface Science* **1997**, *375*, L385-L391.

(20) Bates, F. S.; Fredrickson, G. H. Block copolymer thermodynamics: theory and experiment. *Annual Review of Physical Chemistry* **1990**, *41*, 525-557.

(21) Staudinger, U.; Weidisch, R.; Zhu, Y.; Gido, S.; Uhrig, D.; Mays, J.; Iatrou, H.; Hadjichristidis, N. In *Tilte*2006; Wiley Online Library.

(22) Tong, J.-D.; Jerôme, R. Dependence of the Ultimate Tensile Strength of Thermoplastic Elastomers of the Triblock Type on the Molecular Weight between Chain Entanglements of the Central Block. *Macromolecules* **2000**, *33*, 1479-1481.

(23) Moineau, C.; Minet, M.; Teyssié, P.; Jérôme, R. Synthesis and Characterization of Poly(methyl methacrylate)-block-poly(n-butyl acrylate)-block-poly(methyl methacrylate) Copolymers by Two-Step Controlled Radical Polymerization (ATRP) Catalyzed by NiBr2(PPh3)2, 1. *Macromolecules* **1999**, *32*, 8277-8282.

(24) Jean-Marc Boutillier, J.-P. D., Mickael Havel, Raber Inoubli, Stephanie Magnet, Christian Laurichesse, and Daniel Lebouvier. Self-Assembling Acrylic Block Copolymers for Enhanced Adhesives Properties. *ASI Adhesives & Sealants Industry,* May 1 2013, 2013.

CHAPTER 5 CONCLUSIONS, FUTURE WORK, AND PERSPECTIVE

5.1 Conclusions

Overall, this dissertation was aimed at developing all acrylic thermoplastic elastomers (TPEs) with improved mechanical performance:

The first approach we attempted was the introduction of poly(1-adamantyl acrylate) (PAdA)-- a kind of acrylic polymer with high glass transition temperature to enhance the upper service temperature of the modulus of all acrylic based TPE. To obtain a well-rounded understanding of this polymer, we successfully synthesized the PAdA via anionic polymerization for the first time using diphenylmethyl potassium (DPMK) as an initiator, with a large excess of diethyl zinc (Et_2Zn) in THF at -78 ^{o}C. The resulting polymer exhibited predicted molecular weights, polydispersity indices of around 1.10, great living character of its chain end anoin, and a low level of isotactic content. The PAdA homopolymers exhibit a very high glass transition temperature (133 ^{o}C) and outstanding thermal stability (T_d: 376 ^{o}C), which are both much superior to other polyacrylates. The solution behavior and the unperturbed dimensions of PAdA were further studied using different techniques and theories. The polymer chain exhibits a comparable persistence length, and diameter per bead to those of poly(methyl methacrylate) (PMMA) and polystyrene (PS), and a characteristic ratio (C_∞) of 10.4, which is larger than that of PMMA. In addition, among various solvents investigated, tetrahydrofuran (THF) was demonstrated as the thermodynamically moderate solvent for PAdA. All these merits, both in bulk and solution states, make PAdA a

promising candidate for acrylic based thermoplastic elastomers with higher upper service temperature and enhanced mechanical strength.

The outstanding properties of PAdA were utilized by the cooperation with poly(tetrahydrofurfuryl acrylate) (PTHFA) to make the PAdA-b-PTHF-b-PAdA (ATA) triblock copolymers. This type of all acrylic TPE was synthesized through reversible addition fragmentation chain transfer (RAFT) polymerization. The resulting polymer showed distinct microphase separation behaviors with different morphologies by the change of the molar ratio of PAdA. Through the dynamic mechanical analysis (DMA), the upper service temperature of this material was investigated with the value of 123 ^{o}C, which is higher than that of both conventional styrenic TPEs and acrylic TPEs. The ATA triblock copolymers with the wt% of PAdA of 18.7% exhibited a stress at break of 1.1 MPa and elongation of 803%. This mechanical performance was also superior to the commercial all acrylic based thermoplastic elastomers like Arkema's Nanostrength® and with stress lower than 1 MPa and elongation only around 500%.[1]

In another work, the inherent defects of acrylic based TPEs due to the relatively large entanglement molecular weight (M_e) was overcome by the build of multigraft architecture. As compared to the conventional methods, the PMMA macromonomer was synthesized within one batch via anionic polymerization using sec-butyl lithium/N-isopropyl-4-vinylbenzylamine (sec-BuLi/PVBA) initiation system, with advantages including quantitative yield, quick reaction time, and

simple operation. The final poly(butyl acrylate)-g-poly(methyl methacrylate) (PBA-g-PMMA) graft copolymers were produced using graft-through methodology by RAFT polymerization. By the combination of enhanced molecular weight and complex architecture, the resulting polymer showed exceptional microphase separation behavior, which was demonstrated by various characterization methods, including differential scanning calorimetry (DSC), dynamic mechanical analysis (DMA), atomic force microscopy (AFM) and small angle X-ray scattering (SAXS). Moreover, the PBA-g-PMMA graft copolymer exhibited extraordinary mechanical strength (from 34.5 MPA to 62.1 MPa) and superelastomer characteristics with greatly improved elongation (around 1700%) than the linear type triblock copolymers and exceptional recovery behavior (less than 15% strain loss after stretched to 1200% strain). These distinct mechanical properties greatly expand the potential application range of all-acrylic TPEs as the possible substitution for current styrenic TPEs.

5.2 Future Work and Perspectives

Two different approaches have been successfully employed in our work on the design and development of all acrylic thermoplastic elastomers with high performance. The resulting polymers exhibited great enhancement of the mechanical properties and made them comparable or even superior to styrenic thermoplastic elastomers. However, there are still many potential approaches to

make further improvement. In addition, the merits of the methodologies and chemicals also have the potential use for other applications.

5.2.1 Driving Forces-- Extensive Influence on the Improvement of the Performance of TPEs

As discussed in **Section 1.3.4**, the introduction of extra driving forces for the association of hard domains can help to increase the microphase separation and physical crosslinking behaviors of TPEs. Thus the mechanical properties of TPEs are expected to be improved. Possible driving forces that can be used include ionic bond,[2] hydrogen bonding,[3] coordination bond,[4] or other intermolecular interactions. However, one has to be cautious during the selection of these tools and the functionalization degree of the target materials. For instance, even a very small degree of sulfonation was reported to destroy the elastomeric property of SEBS, which may not be an ideal approach for the modification of TPEs.[2]

Inspired by the previous work on the modification of poly(*tert*-butyl methacrylate)-b-poly(butadiene)-b-poly(*tert*-butyl methacrylate),[4] we attempted to introduce the hydrogen bonding to all acrylic based TPE as a combination to the multigraft architecture. The macromonomer of poly(*tert*-butyl methacrylate) (PtBMA) was synthesized via anionic polymerization in THF at -78 ^{o}C using the *sec*-BuLi/PVBA initiation system, followed by the RAFT copolymerization of the butyl acrylate monomer with the PtBMA macronomer. The procedures were similar

to those introduced in **Section 4.2**. The molecular information of the resulting PBA-g-PtBMA graft copolymer is as shown in **Table 5-1**. The composition of each domain was calculated based on the ratio of integrated areas between the peaks at around 1.3-1.5 ppm (-C(CH_3)$_3$ of PtBMA and O-C-C-CH_2-C of PBA) and 4.0 ppm (-O-CH_2- of PBA) in ^{1}H NMR spectra. (**Figure 5-1**) The typical SEC curves of PMMA macromonomer and resulting PBA-g-PtBMA are shown in **Figure 5-2**.

The PtBMA block in the resulting graft copolymer was hydrolyzed using 12X of HCl following the procedure as previously reported.[5] Different reaction time was used and resulted in the graft copolymers with the hydrolysis degrees of 42% and 54%.

From our preliminary results, the hydrolysis greatly improved the microphase separation behavior of the graft copolymers, as the AFM images shown in **Figure 5-3**.

The stress-strain curves of the graft copolymers are shown in **Figure 5-4**. Similar to the mechanical performances of PBA-g-PMMA graft copolymers, the PBA-g-PtBMA graft copolymer exhibited stress higher than 1 MPa, which is higher than that of commercial acrylic based TPEs. Moreover, the elongation at break was not observed even when the stretching reached the limit of the instrument (elongation of 3592%, with the stress of 1.4 MPa). This exceptional strain may be contributed to the great increase in the number of branch points to 5.7 compared to the PBA-g-PMMA, for which the number of branch points was only around 3.

Table 5-1. Sample Information of PBA-g-PtBMA Graft Copolymer

Sample ID[a]	*PtBMA*		PBA-g-PMMA[b]		Vol% of PtBMA[c]	No.[d]
	M_n (kg/mol)	PDI	M_n (kg/mol)	PDI		
MG-13.1-5.7-26.0	13.1	1.01	300.5	1.39	26.0	5.7

[a]Sample identification MG-M_n (PtBMA)-No. of branch points-vol% of PtBMA. [b]Number-average molecular weight M_n and PDI were measured in THF at 40 ^oC using the Polymer Laboratories PL-120 SEC system, with *dn/dc* estimated by $wt\%(PtBMA)\times 0.085 + wt\%(PBA)\times 0.067$ where 0.085 mL/g is *dn/dc* the for PtBMA and 0.067 is the *dn/dc* for PBA, and the wt% of PtBMA and PBA was obtained from ^1H NMR spectra. [c]vol% was calculated based on the density of 1.023 g/mL for PtBMA and 1.080 g/mL for PBA. [d]No. of branch points was calculated based on $\mathrm{M_n(PBA-g-PtBMA)\times wt\%(PtBMA)/M_n(PtBMA)}$

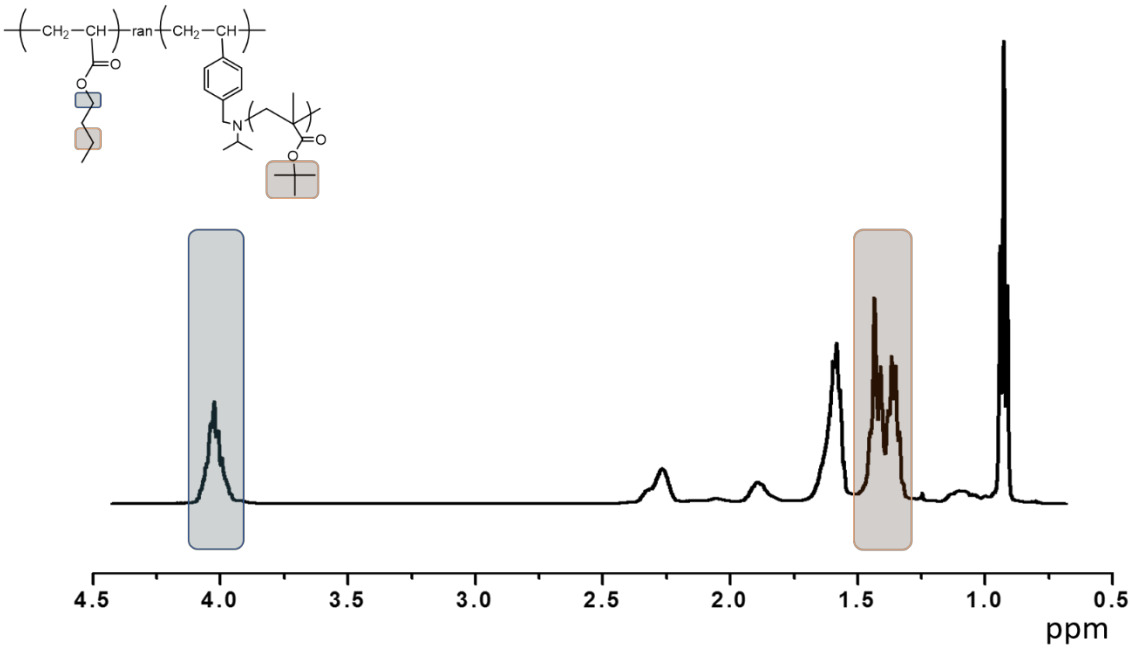

Figure 5-1. ^{1}H NMR spectra of PBA-g-PtBMA graft copolymer.

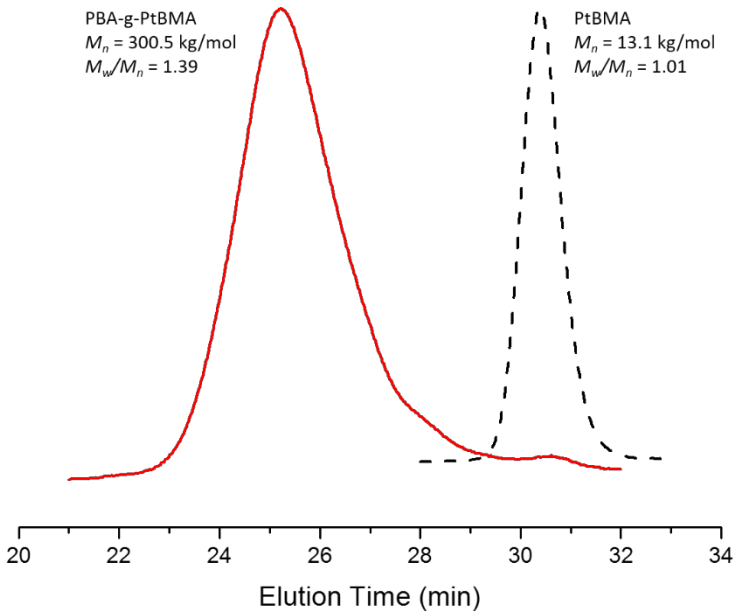

Figure 5-2. SEC profiles of PBA-g-PtBMA and PtBMA macronomer.

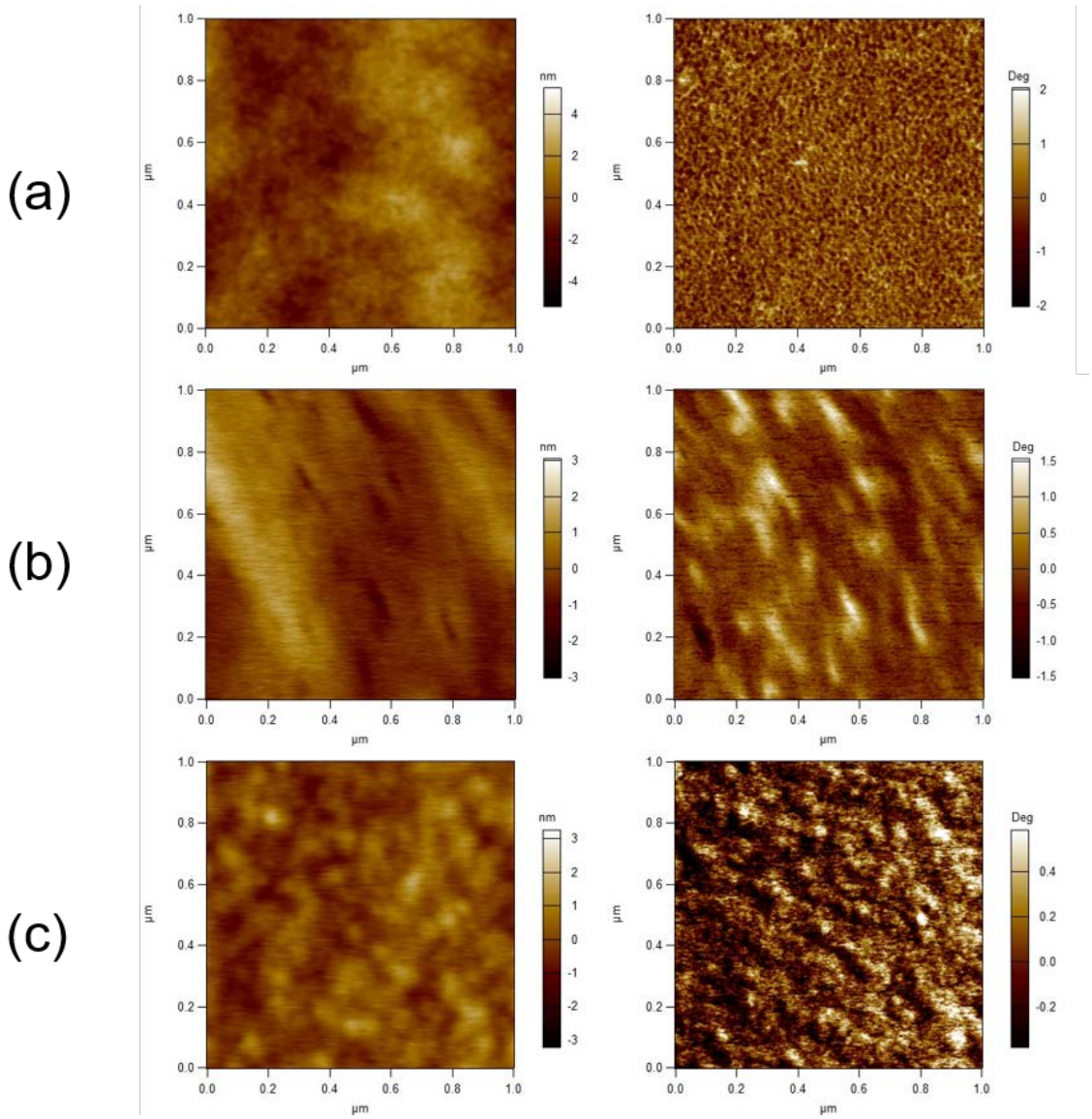

Figure 5-3. AFM height images (left) and phase images (right) of PBA-g-PtBMA with the hydrolysis degress of (a) 0%; (b) 42%; (c) 54%.

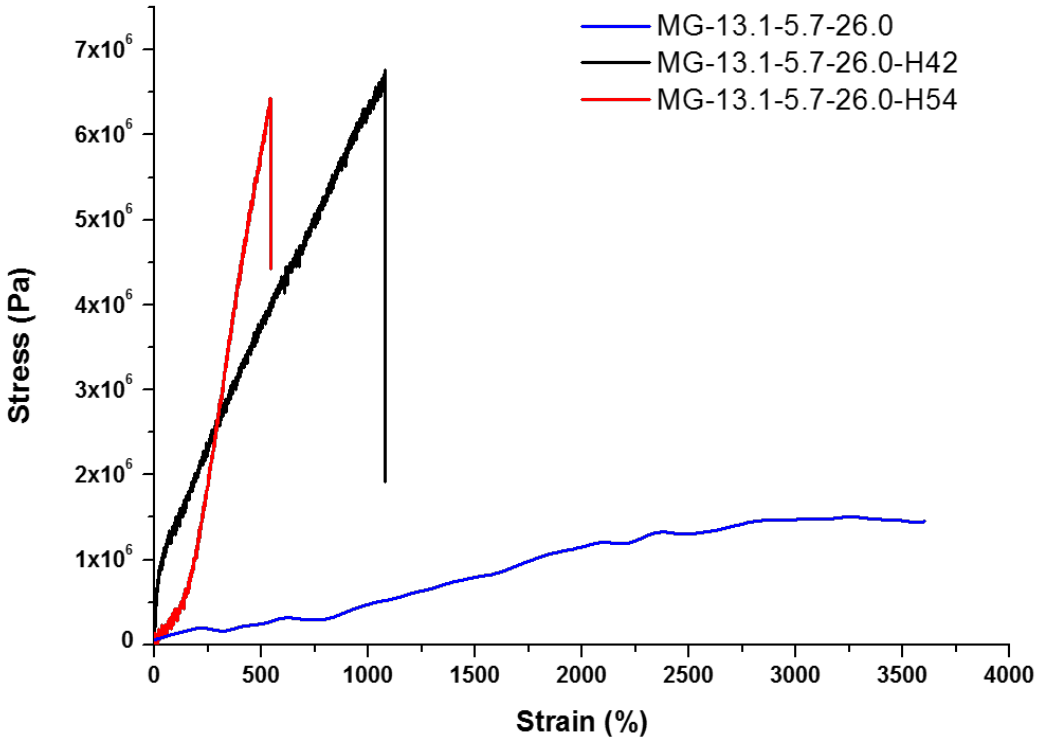

Figure 5-4. Stress-strain curves of PBA-g-PtBMA graft copolymers with different hydrolysis degrees

The hydrolysis greatly enhanced the mechanical strength of the material. With the hydrolysis degrees of 42%, the stress at 1000% strain increased to 6.3 MPa, which was around 12.6 times higher than the unmodified polymer with the stress at 1000% of 0.5 MPa. Although the elongation was greatly decreased, the strain at break of 1080% was still much higher than conventional all acrylic TPEs. The further increase of hydrolysis degree from 42% to 54% extensively affected the elongation behavior of the material, with the strain at break of 543% and ultimate mechanical strength of 6.4 MPa.

All these exceptional improvements demonstrated the great influence of hydrogen bonding on the mechanical strength of the TPE. Further study will be performed to further adjust the hydrolysis degree to obtain the optimized combination of improved strength and high elongation behavior.

Furthermore, the hydrolyzed graft copolymers will be treated with NaOH to ionized the carboxyl group, so that the ionic bond can be introduced for further improvement of the mechanical property. Cations with large size and multiple charges such as Zn^{2+} or Ca^{2+} will be added to the system and form the coordination bond with the anionic charges. Which has been reported greatly enhanced the mechanical strength.[4] The resulting TPE is also expected to be imparted with the self-healing property due to the strong coordination interactions.[6]

The mechanical property of triblock copolymer of PAdA-b-PTHFA-b-PAdA (ATA) may also be enhanced, taking advantages of the strong host-guest

interactions between adamantane and β-cyclodextrin (β-CD).[7] One possible approach is proposed as shown **in Scheme 5-1**, for which the physical crosslinking junctions can be reinforced by the host-guest interactions between adamantyl groups and β-CD.

5.2.2 The Combination of High Upper Service Temperature and Complex Architecture

Both the use of hard segments with high T_gs and the build of multigraft architecture have been demonstrated useful for the improvement of the mechanical performance. As a versatile initiation system, *sec*-BuLi/PVBA can be used for the anionic polymerization of various type of poly(meth)acrylates.[8,9] The macromonomer of poly(meth)acrylates with high T_gs, such as PAdA (T_g: 133 ^oC)[10] and poly(1-adamantyl methacrylate) (PAdMA, T_g: higher than 202 ^oC),[11] can be synthesized, followed by the radical copolymerization with BA to produce the graft copolymers. The resulting graft copolymers are expected to possess an improved upper service temperature. Moreover, the rigidity of the hard segment and the great microphase separation behavior due to the multigraft architecture may lead to a kind of superelastomer with ultra-high mechanical performance.

In addition, the graft through methodology makes it possible to combine different macromonomers during the copolymerization. The anionic polymerization characteristic also has the ability to make block or random copolymeris with the combination of different monomers. PtBMA can be introduced to the system by

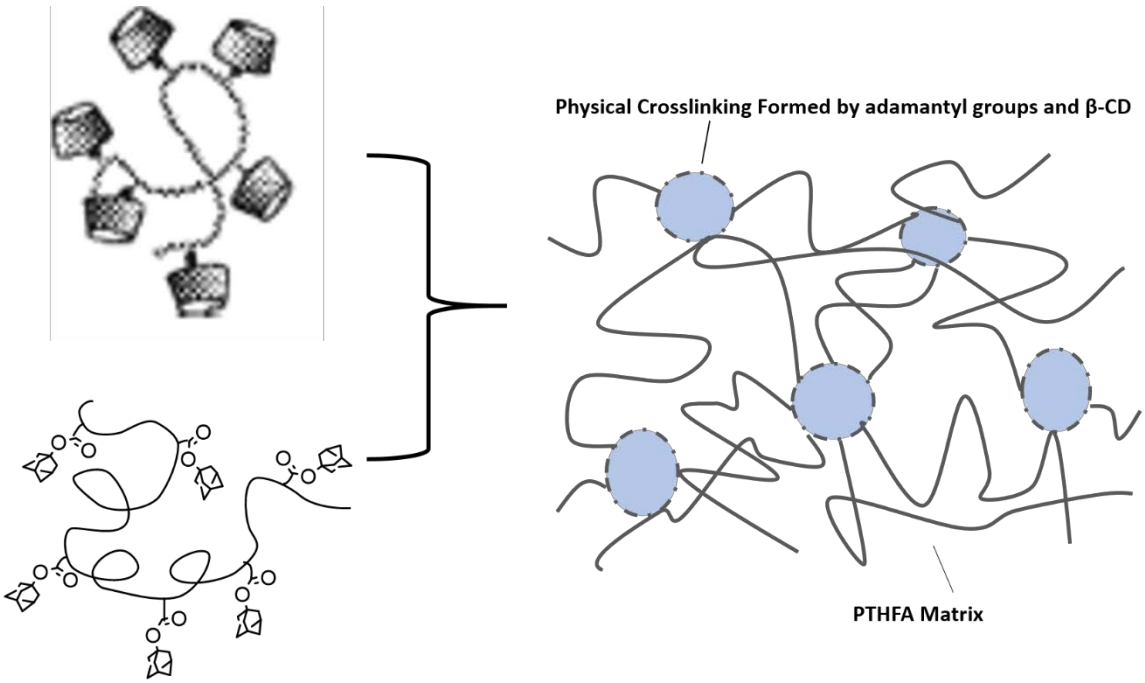

Scheme 5-1. Proposed on the approach to enhance the mechanical property of ATA triblock copolymers.

either copolymerization with the other monomer with high T_g during the anionic polymerization to make the macromonomer, or copolymerization of its macromonomer with the other macromonomer with high T_g. Thus, further modification can introduce other driving forces such as hydrogen bonding, ionic bonds, or coordination interactions to the system to further enhance the mechanical strength.

5.2.3 PVBA-Powerful Tool to Build Complex Architectures

The initiation system of *sec*-BuLi/PVBA provides a powerful and efficient approach for synthesizing the macromonomer with 100% yield, quick reaction and simple operations. In addition to the random copolymerization to make graft copolymers, it also has the potential to build complex architectures. For this purpose, high purity of the macromonomer is essential to meet the requirement for anionic polymerization. We have attained this requirement by stirring the macromonomer solution in benzene over CaH_2, filtering through the filter, and freezing dry three times before ampulizing and dilution in THF. The concentration of the ampulized solution can be determined by comparing the integrated areas between the peaks of the polymer and THF in ^{1}H NMR spectra.

The preliminary attempt was performed to make PS-PMMA-PMMA miktoarm stars. As shown in **Figure 5-5**, a large excess of LiCl was added to the living PS solution in THF at -78 ^{o}C in order to avoid the attack of the living chain ends to the carbonyl groups in PMMA macromonomer. The color change from

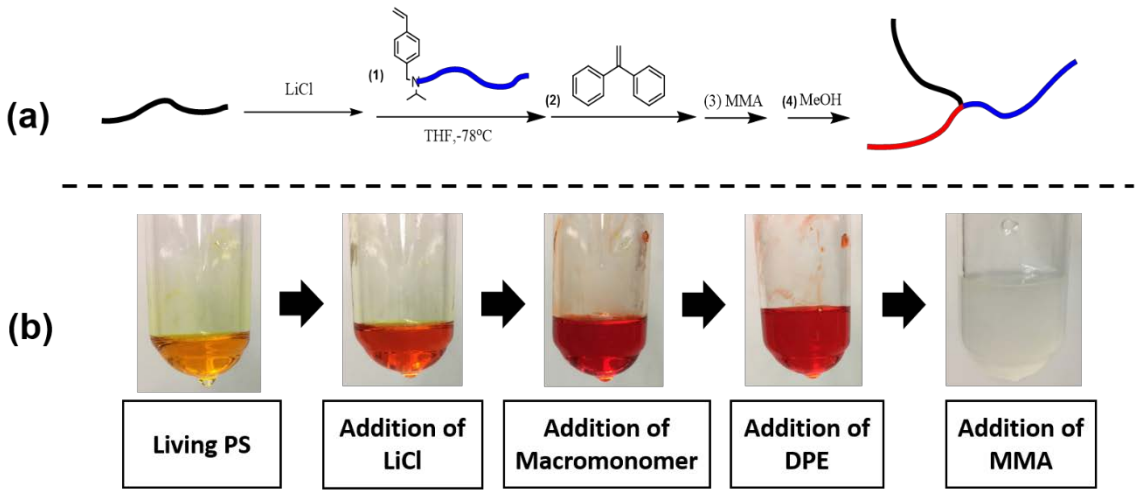

Figure 5-5. (a) Illustrate scheme on the synthesis of PS-PMMA-PMMA miktoarm star; (b) photographs of the reaction solutions.

orange to light red indicated the formation of a complex between the living chain ends with the salt. After the addition of PMMA macromonomer, the color changed to deep red, indicating the successful coupling reaction between living PS and the vinyl group of the macromonomer. After the addition of diphenylethylene to decrease the activity of the living chain ends, MMA monomer was charged to the reaction solution, with the observation of the disappearance of color, which is a common phenomenon for living PMMA solutions. The polymerization was quenched with degassed methanol and precipitated in a large excess of hexane.

The SEC profiles are shown in **Figure 5-6**. The broad distribution of the peaks for PS and PS-PMMA may be caused by the side reactions of the aliquots when hot sealed and taken off from the reaction system. The SEC trace of the final polymer showed a tail of the remaining PS-b-PMMA deblock copolymers with the content of around 25%. However, the remaining peaks of PS or PMMA macrnomomer were not observed, indicating the complete coupling reaction with no deactivation of living PS. Meanwhile, the high purity of the macromonomer was also demonstrated.

The complete coupling reactions between living PS and PMMA macromonomer make it possible to synthesize the multigraft copolymers with tetrafunctional branch points, which have the potential to be the next generation superealstomers with high performance. As illustrated in **Scheme 5-2**, after the coupling reaction, acryloyl chloride can be used to end cap the living chain ends

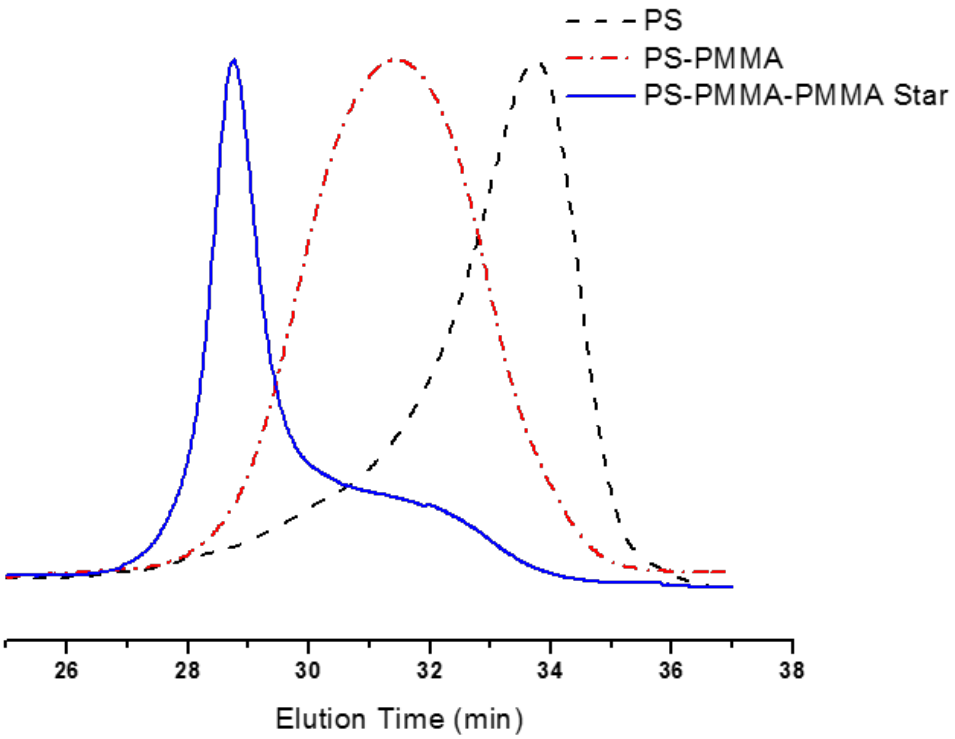

Figure 5-6. SEC traces of PS, PS-PMMA, and PS-PMMA-PMMA miktoarm star.

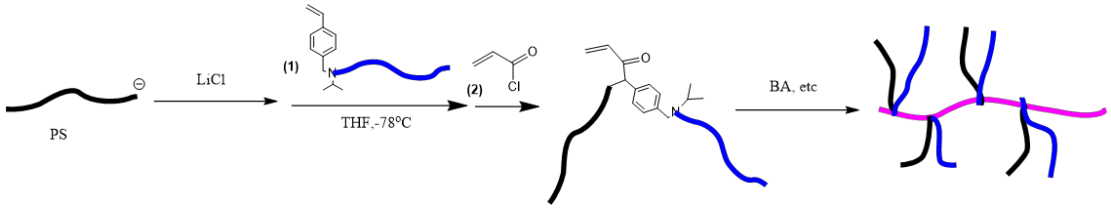

Scheme 5-2. Illustration on the approach to make multigraft copolymer superelastomers with tetrafunctional branch points.

and produce the double tailed macromonomer, followed by the radical copolymerization with butyl acrylate to make the final multigraft copolymer superelastomers.

Moreover, by using potassium naphthalenide rather than *sec*-BuLi as the difunctional initiator, more types of architectures including tetra-arm stars and H-shaped copolymers can be synthesized (**Scheme 5-3**).

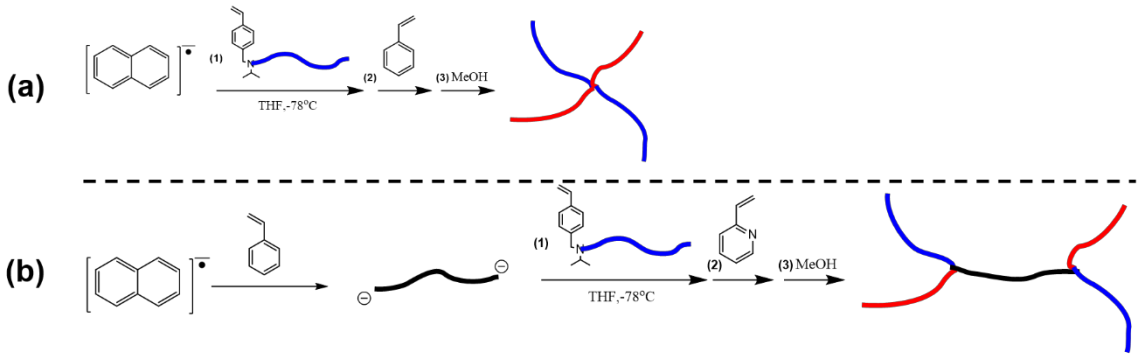

Scheme 5-3. Illustration of the approach for the synthesis of (a) PS_2PMMA_2 star; (b)$PSPMMA_2P_2VP_2$ H-shape copolymer.

References

(1) Jean-Marc Boutillier, J.-P. D., Mickael Havel, Raber Inoubli, Stephanie Magnet, Christian Laurichesse, and Daniel Lebouvier. Self-Assembling Acrylic Block Copolymers for Enhanced Adhesives Properties. *ASI Adhesives & Sealants Industry,* May 1 2013, 2013.

(2) Barra, G. M. O.; Jacques, L. B.; Oréfice, R. L.; Carneiro, J. R. G. Processing, characterization and properties of conducting polyaniline-sulfonated SEBS block copolymers. *European Polymer Journal* **2004**, *40*, 2017-2023.

(3) Söntjens, S. H. M.; Renken, R. A. E.; van Gemert, G. M. L.; Engels, T. A. P.; Bosman, A. W.; Janssen, H. M.; Govaert, L. E.; Baaijens, F. P. T. Thermoplastic Elastomers Based on Strong and Well-Defined Hydrogen-Bonding Interactions. *Macromolecules* **2008**, *41*, 5703-5708.

(4) Tobolsky, A. V.; Lyons, P.; Hata, N. Ionic clusters in high-strength carboxylic rubbers. *Macromolecules* **1968**, *1*, 515-519.

(5) Giebeler, E.; Stadler, R. ABC triblock polyampholytes containing a neutral hydrophobic block, a polyacid and a polybase. *Macromolecular Chemistry and Physics* **1997**, *198*, 3815-3825.

(6) Burnworth, M.; Tang, L.; Kumpfer, J. R.; Duncan, A. J.; Beyer, F. L.; Fiore, G. L.; Rowan, S. J.; Weder, C. Optically healable supramolecular polymers. *Nature* **2011**, *472*, 334-337.

(7) Li, L.; Guo, X.; Wang, J.; Liu, P.; Prud'homme, R. K.; May, B. L.; Lincoln, S. F. Polymer Networks Assembled by Host−Guest Inclusion between Adamantyl and β-Cyclodextrin Substituents on Poly(acrylic acid) in Aqueous Solution. *Macromolecules* **2008**, *41*, 8677-8681.

(8) Liu, F.; Eisenberg, A. Synthesis of Poly(tert-butyl acrylate)-block-Polystyrene-block-Poly(4-vinylpyridine) by Living Anionic Polymerization. *Angewandte Chemie International Edition* **2003**, *42*, 1404-1407.

(9) Zeng, F.; Shen, Y.; Zhu, S. Synthesis of Styrenic-Terminated Methacrylate Macromonomers by Nitroanion-Initiated Living Anionic Polymerization. *Macromolecular Rapid Communications* **2001**, *22*, 1399-1404.

(10) Lu, W.; Huang, C.; Hong, K.; Kang, N.-G.; Mays, J. W. Poly(1-adamantyl acrylate): Living Anionic Polymerization, Block Copolymerization, and Thermal Properties. *Macromolecules* **2016**, *49*, 9406-9414.

(11) Ishizone, T.; Tajima, H.; Torimae, H.; Nakahama, S. Anionic Polymerizations of 1-Adamantyl Methacrylate and 3-Methacryloyloxy-1,1′-biadamantane. *Macromolecular Chemistry and Physics* **2002**, *203*, 2375-2384.

VITA

Wei Lu was born in Jiangsu China. He obtained the Bachelor of Science Degree in Chemistry in July 2012 from Jilin University, joined Jimmy Mays' research group in November 2012, and graduated in May 2017 with a PhD. Degree in Polymer Chemistry focused on developing all acrylic based thermoplastic elastomers with improved mechanical performance.

During his five years' study and research in the University of Tennessee, he worked on various projects, including water purification membranes, anion conducting polymer membranes, polymer membranes for carbon dioxide separations, all acrylic based thermoplastic elastomers, study and formulation on RTV silicone adhesives, and the study of dipolar effects in inhomogeneous polymeric media. He published five first-authored papers and contributed to one book chapter about the thermoplastic elastomers. He presented his research on many occasions including 2 ACS National Meetings, 2 FWP meetings of Oak Ridge National Lab, APTEC annual meeting and the department seminar. He has been honored with the Graduate Senate Travel Award (2015) from the University of Tennessee and won the Best Poster Award at Board of Visitors Annual Meeting in the Chemistry Department, the University of Tennessee.